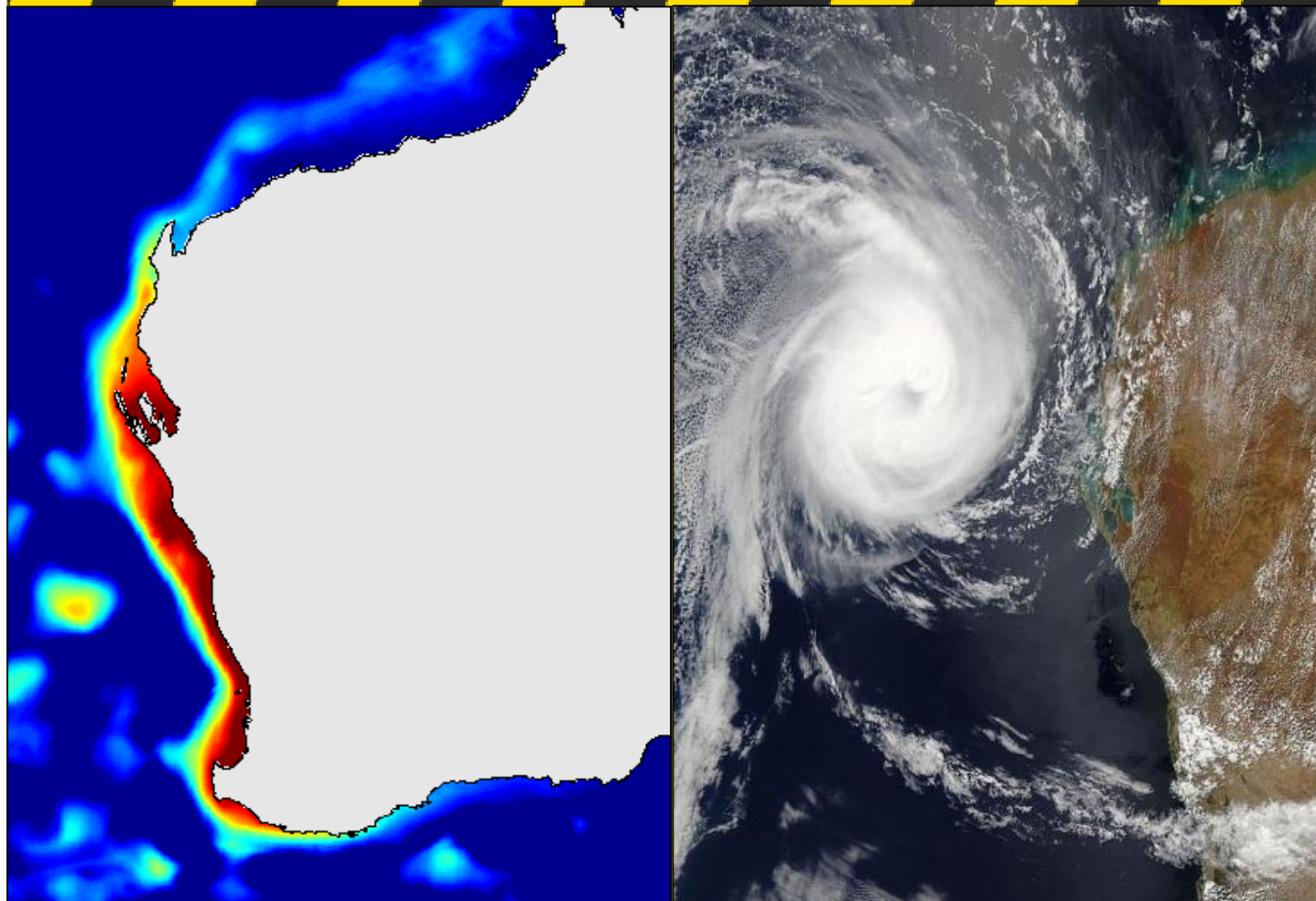


bnhcrc.com.au

PREDICTING CONTINENTAL SHELF WAVES IN AUSTRALIA

C Pattiaratchi, E.M.S Wijeratne, Y Hetzel, I Janekovic

University of Western Australia
Bushfire and Natural Hazards CRC





Version	Release history	Date
1.0	Initial release of document	22/02/2016



Australian Government
Department of Industry,
Innovation and Science

Business
Cooperative Research
Centres Programme

This work is licensed under a Creative Commons Attribution-Non Commercial 4.0 International Licence.



Disclaimer:

University of Western Australia and the Bushfire and Natural Hazards CRC advise that the information contained in this publication comprises general statements based on scientific research. The reader is advised and needs to be aware that such information may be incomplete or unable to be used in any specific situation. No reliance or actions must therefore be made on that information without seeking prior expert professional, scientific and technical advice. To the extent permitted by law, University of Western Australia and the Bushfire and Natural Hazards CRC (including its employees and consultants) exclude all liability to any person for any consequences, including but not limited to all losses, damages, costs, expenses and any other compensation, arising directly or indirectly from using this publication (in part or in whole) and any information or material contained in it.

Publisher:

Bushfire and Natural Hazards CRC

February 2016

Citation: Pattiaratchi C, Wijeratne E, Hetzel Y, Janekovic I (2016) Predicting continental shelf waves in Australia, Bushfire and Natural Hazards CRC



TABLE OF CONTENTS

SUMMARY	3
INTRODUCTION	5
BACKGROUND	7
Evidence for CSWs around Australia	7
CSW generation by tropical cyclones	7
CYCLONE FORWARD SPEED	7
CYCLONE PATH	8
CYCLONE INTENSITY AND WIND FORCING	8
CSW propagation	8
METHODS	9
Site description	9
TROPICAL CYCLONES IN WESTERN AUSTRALIA	9
CONTINENTAL SHELF BATHYMETRY OF NORTHWEST AUSTRALIA	9
ROMS model description	11
NWS IDEALISED MODEL SETUP	11
AUSTRALIA-WIDE MODEL	15
WA cyclone and tide gauge data 2011	17
Data analysis	18
RESULTS	20
NWS idealised model	20
COASTLINE PARALLEL CYCLONES NEAR SHELF EDGE TRAVELLING ACROSS THE WHOLE MODEL DOMAIN WITH DIFFERENT FORWARD SPEEDS	20
COASTLINE PARALLEL CYCLONES NEAR SHELF EDGE TRAVELLING A QUARTER OF THE MODEL DOMAIN WITH DIFFERENT SPEEDS	23
COASTLINE PARALLEL CYCLONES TRAVELLING OVER 25% OF THE MODEL DOMAIN AT 3.5 MS ⁻¹ AT VARIOUS DISTANCES FROM THE COASTLINE	25
COASTLINE PARALLEL CYCLONES NEAR SHELF EDGE TRAVELLING A QUARTER OF THE MODEL DOMAIN WITH DIFFERENT INTENSITIES	27
45° CYCLONES WITH DIFFERENT SPEEDS	27
PERPENDICULAR CYCLONES WITH DIFFERENT SPEEDS	30
Regional scale modelling of CSWs	33
TROPICAL CYCLONE BIANCA	33
TROPICAL CYCLONE CARLOS	40
DISCUSSION AND CONCLUSIONS	46



Influence of cyclone incident parameters	46
PERPENDICULAR CYCLONES	46
PARALLEL CYCLONES	47
45° CYCLONES	49
<hr/>	
Regional scale modelling of CSWs	50
CYCLONE PATH	50
CONTINENTAL SHELF BATHYMETRY.....	51
<hr/>	
CONCLUSIONS	53
REFERENCES.....	55
APPENDIX A - TROPICAL CYCLONE BIANCA DETAILED DESCRIPTION	65
APPENDIX B - TROPICAL CYCLONE CARLOS DETAILED DESCRIPTION	66



SUMMARY

A range of processes can cause extreme water levels that endanger human life and cause property damage. Storm surges caused by tropical cyclones are well known to pose a risk for coastal inhabitants. However, a lesser-known effect of landfalling cyclones is the generation of coastally trapped waves that can propagate along the coast and influence water levels thousands of kilometres away. Examples of such waves include continental shelf waves (CSWs) that travel to the left along the coastline in the southern hemisphere and are common along the Australian coastline (Church et al., 1986; Eliot and Pattiaratchi, 2010).

This study investigated the generation and propagation characteristics of continental shelf waves (CSWs) in Western Australia, a hotspot of continental shelf wave activity in Australia, utilising the Regional Ocean Modelling System (ROMS). An idealised model of the North West Shelf (NWS) with ~ 4 km spatial resolution and 30 vertical sigma layers was forced by simulated tropical cyclones that varied in speed, direction (parallel, perpendicular or at 45° to the coastline) and category. Realistic cyclone simulations were performed for Tropical Cyclone Bianca in 2011 using an Australia-wide model and comparisons made to observations.

Results from the idealised numerical model showed that a cyclone's path, speed and category affect continental shelf wave generation and propagation. Greater cyclone category resulted in higher amplitude continental shelf waves. Cyclones that travelled parallel to the coastline generated continental shelf waves that were faster than the cyclone forward speed and produced higher amplitude waves than those generated by different trajectories. Increased parallel cyclone forward speed corresponded to an increase in the continental shelf wave height. If the parallel cyclone forward speed was too fast (i.e. greater than 14 ms⁻¹), the continental shelf wave height decreased. Parallel moving cyclones travelling near to the continental shelf break with a forward speed of ~ 7.5 ms⁻¹ generated the highest amplitude waves. If the cyclone discontinued travelling parallel, the continental shelf wave gained similar properties to continental shelf waves generated by perpendicular or 45° travelling cyclones. These type of cyclones generated continental shelf waves that had a lower wave height, which were even lower for faster moving cyclones. The propagation speed of these waves scaled to the Coriolis parameter and characteristic length scale of the continental shelf. The lower wave height of these waves can be explained by the continental shelf wave travelling as a "free wave".

Propagation characteristics of continental shelf waves generated by Cyclone Bianca and Carlos from realistic cyclone simulations showed cyclone path and continental shelf bathymetry had an influence on CSW height and propagation speed. The calculated approximate travel speed from lag correlation analysis was 5.8 ms⁻¹ for both continental shelf waves. Tropical Cyclone Bianca travelled parallel to the Western Australian coastline which reinforced the continental shelf wave height. Tropical Cyclone Carlos continued offshore from Exmouth so the continental shelf wave had little energy to propagate around the curved coastline in the Capes Region. Both continental shelf waves



decreased in propagation speed between Exmouth and Carnarvon where the continental shelf width decreased rapidly. The continental shelf wave generated by Tropical Cyclone Bianca rapidly decreased at Albany which may be explained by the curvature of the coastline which resulted in wave scattering.

Results from this study demonstrate how particular cyclone properties influence the generation of continental shelf waves and through this improves our ability to predict the influence of CSWs on extreme water levels along the Australian coast. . It is recommended that design criteria, modelling studies and inundation risk assessments for coastal regions in Western Australia need to consider the effects of continental shelf waves.



INTRODUCTION

Winds that cause water levels to increase at the coast have the potential to generate coastally trapped waves that travel parallel to the coast with amplitude decreasing offshore (Gill and Schumann, 1974) (Figure 1). Examples of such waves include continental shelf waves (CSWs) that travel to the left along the coastline in the southern hemisphere and are common along the Australian coastline (Church et al., 1986; Eliot and Pattiaratchi, 2010). In Western Australia CSWs are commonly generated by the passage of tropical cyclones in the northern part of the state and propagate for thousands of kilometres influencing water levels and circulation (Eliot and Pattiaratchi, 2010).

Continental shelf wave (CSWs) have been identified worldwide and are recognised as significant and integral components of the physical and biological marine environment (Mysak 1980; Schulz, Mied & Snow 2012). They are unidirectional long waves that have a large wavelength compared to the depth of the water and are trapped along the coastline. They propagate parallel to the coast, along continental slopes and shelves with their maximum amplitude occurring at the coast and decreasing offshore (Eliot & Pattiaratchi 2010). They have periods ranging from a few days to a few weeks and speeds in the range of 2 - 20 ms⁻¹ (Brink 1991; Eliot & Pattiaratchi 2010; Schumann & Brink 1990). CSWs can travel long distances, influencing water levels and ocean dynamics far away from their generating region (Mysak 1980). These waves are defined under the broader category of a coastal-trapped wave (CTW) which also include edge waves and Kelvin waves.

One type of generating mechanism for CSWs is a tropical cyclone. Tropical cyclones (also named hurricanes or typhoons) bring strong winds, storm surge, torrential rain and waves that can have a damaging impact on industry, coastal environments and communities (Nott 2006). For example, tropical cyclones such as the 1970 Tropical Cyclone Bhola in Bangladesh and India, the 1974 Tropical Cyclone Tracy in Australia and the 2005 Hurricane Katrina in the United States have resulted in many deaths and high damage costs (Emanuel 2005). In addition to this, tropical cyclones are likely to pose an even greater threat to coastal communities and the marine environment. Tropical cyclones are expected to increase in intensity as a result of climate change (Walsh & Ryan 2000). Damage costs associated with tropical cyclones can exceed billions of dollars if the population and industry continue to intensify in coastal areas (Pielke & Lardsea 1998). Quantifying the response of the ocean to tropical cyclones is critical to mitigating their impact on local communities, infrastructure, industry and the environment. While the ocean responds to cyclones in many complex ways, one of the most significant effects of a tropical cyclone occurring on a regional scale is the CSW. The alongshore component of wind stress from tropical cyclones and the water circulation patterns can input enough energy to generate CSWs and other forms of CTWs (Baines, Boyer & Xie 2004; Brink 1991; Eliot & Pattiaratchi 2010).

The north-western region of Western Australia (WA), Australia, is a region that experiences intense tropical cyclone activity. The North West Shelf (NWS) of WA alone receives approximately 10 % of the global total of tropical cyclones per year, occurring predominantly in the austral-summer from November through to April (Hosseini & Willis 2009). These tropical cyclones can generate CSWs, which propagate southward along the WA coastline, trapped on the continental shelf to conserve potential vorticity (Brink 1991; Grimshaw 1988;

Tang & Grimshaw 1995). CSWs have been identified in water level data more than 2000 km south at Fremantle, WA and as far away as Tasmania (Eliot & Pattiaratchi 2010). The environmental influence of CSWs in WA has been mentioned in the research by Cresswell *et al.* (1989) and O'Callaghan, Pattiaratchi & Hamilton (2007). CSW trough to crest wave heights of 0.63 m has been observed in southern WA which is a significant increase to water levels for this micro-tidal region (Eliot & Pattiaratchi 2010). CSWs have also been identified to pose significant risk of dune scarping and erosion for WA beaches if they are coupled with waves and wind set-up (Pearman 1988; Bryant 1990). This implies it is important to factor in CSW forcing into design criteria along the coastline and risk assessments on inundation.

Unfortunately, there remains a general paucity of research data on CSWs in WA. Consequently, an evaluation of the role played by CSWs in the WA marine environment needs further investigation if our knowledge of the little known dynamics of the Indian Ocean marine environment is to be advanced. An improved capability to predict CSWs in WA is also required. One of Australia's largest oil and gas industries is located on the NWS and is exposed to tropical cyclones and CSWs. High population density towns, cities and infrastructure occur along the coastline of WA, which can all be affected by CSWs although they may be far from the tropical cyclone prone areas. Understanding CSWs in WA is essential so that risks can be managed and damages associated with increased water levels by CSWs mitigated.

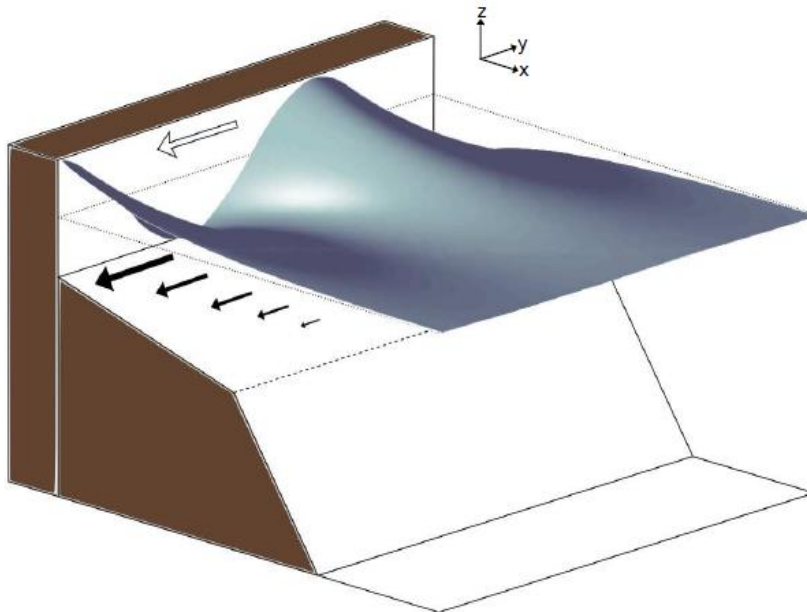


FIGURE 1 – AN EXAMPLE OF A SHELF WAVE IN THE NORTHERN HEMISPHERE BY PEARCE (2011), RECREATED FROM CUTCHIN & SMITH (1973). THE PHASE PROPAGATION OF THE WAVE IS SHOWN BY THE WHITE ARROW. THE WATER VELOCITY UNDER THE CREST OF THE WAVE IS SHOWN BY THE BLACK ARROWS. THE DISPLACEMENT OF THE SEA SURFACE IS LARGER IN THE FIGURE AS CSW AMPLITUDES RANGE IN THE ORDER OF CENTIMETRES.



BACKGROUND

Evidence for CSWs around Australia

CSWs were first discovered on the east coast of Australia by Hamon (1962, 1966) when the local meteorological changes could not explain spatial lags in the tidal data. CTWs have also been observed extensively around Australia and are common along the Australian coastline (Eliot & Pattiaratchi 2010). Measurements made in the most southerly extent of the Great Barrier Reef have shown the existence of CTWs occurring behind a large continental shelf island (Griffin & Middleton 1986). The intensive observational study, the Australian Coastal Experiment collected data on the dynamic aspects of CSWs in southern and eastern Australia (Church *et al.* 1986; Church, Freeland & Smith 1986; Freeland *et al.* 1986; Merrifield & Middleton 1994). The CSWs along the south and east coasts are generated by the alongshore component of wind stress, primarily from mid-latitude cyclones (Church & Freeland 1987; Griffin & Middleton 1991). The investigations of CSWs in Australia have shown that they propagate anti-clockwise along the Australia continent at 5 – 7 ms⁻¹ over 4000 km (Church & Freeland 1987; Provis & Radok 1979).

Southward propagating CSWs in WA have also been identified. The generating mechanism of these waves are via tropical cyclones or the passage of frontal systems (Eliot & Pattiaratchi 2010; Fandry & Steedman 1994; Fandry, Leslie & Steedman 1985; Tang, Holloway & Grimshaw 1997; Webster 1985). CSWs are the dominant CTWs present in WA due to the time and space scale of tropical cyclones which make this possible (Tang 1994).


Speeds of the CSWs in WA are consistent with other studies and other locations around the world. Fandry, Leslie & Steedman's (1984) study of three CSWs from three tropical cyclones in WA had propagation speeds of 4.6 ms⁻¹ to 7 ms⁻¹ with amplitude peaks of up to 2 m. The propagation speeds of CSWs in WA identified by Fandry, Leslie & Steedman (1984) are similar to those found by Provis & Radok (1979) and Church & Freeland (1987) for CSWs occurring in the east and south-eastern coast of Australia, which are generated by mid-latitude cyclones. The CSWs generated by tropical cyclones in WA in the work by Eliot & Pattiaratchi (2010) are also consistent with previous studies as the CSWs were shown to have propagation speeds between 5 ms⁻¹ to 6 ms⁻¹. North West Gulf of Mexico (Pearce 2011). Although similar in some regards, the propagation characteristics of CSWs in WA are still relatively unclear.

CSW generation by tropical cyclones

The amplitude and area affected by continental shelf waves depends upon a range of factors related to the cyclone and how it interacts with the continental shelf region. An introduction to the various factors investigated in this study is presented below.

Cyclone forward speed

Cyclone forward speed has been identified as an important factor in CSW and other CTW generation. Dukhovskoy, Morey & O'Brien (2009) mention how amplitude and frequency of the oscillations excited in the ocean are due to cyclone forward speed. Dukhovskoy, Morey & O'Brien (2009) conclude that hurricanes with different forward speeds can force stronger or weaker upslope and downslope motions of water particles on the continental shelf.



Fandry, Leslie & Steedman (1984) used tide gauge data available around Australia to analyse three different tropical cyclones that occurred in WA during the 1970s and found that higher surges with longer duration were related to slower moving cyclones in the region. Tropical cyclone forward speed in WA was further investigated by Fandry & Steedman's (1994) modelling study of the barotropic response on the NWS to tropical cyclones. They found that one component of the magnitude of the ocean's response was due to storm intensity which includes the component of cyclones forward speed.

Cyclone path

The path of a tropical cyclone has also been identified in studies to have a strong influence on CSW generation and dynamics. Eliot & Pattiaratchi (2010) analysed tropical cyclone paths and related them to CSW presence along the WA coastline. They classified the amplitude of the CSWs generated based on six different types of cyclone paths. Their research indicated that storm surge from a tropical cyclone was strongly affected by the cyclones path. As a consequence, tropical cyclones which travelled parallel to the coastline showed CSWs with the highest wave amplitudes because of resonance and the presence of the tropical cyclone. Eliot & Pattiaratchi's (2010) research is also confirmed in the work by Tang & Grimshaw (1995). They found that the most effective tropical cyclone to generate CSWs are the cyclones that travel parallel to the coastline in the direction of the CSW.

Cyclone intensity and wind forcing

Fandry & Steedman (1994) cited cyclone intensity as one of the major factors affecting the magnitude of the oceans response to tropical cyclones in a modelling study of the Australia NWS, which is also one of the foci of this research. They concluded that the cyclone's intensity described by radius to maximum winds, ambient to central pressure different and cyclone speed all affect the magnitude of the oceans response to cyclones.

CSW propagation

Once generated, CSWs have the potential to travel over thousands of kilometres, significantly affecting water levels. Certain factors identified in literature are known to affect the amplitudes, energy, modes and wave propagation speeds as they travel. For example, latitude (via the coriolis parameter) can affect CSW propagation (Dorr & Grimshaw 1986; Schulz, Mied & Snow 2012). Strong stratification through the water column can increase wave damping (Brink 2006) but it has also been shown to have little effect on CTW velocity and phase speeds for lower order modes (Battisti & Hickey 1984; Ding, Bao & Shi 2012). Other factors include shelf width, bathymetry, coastline (e.g. curvature, islands, irregularities) and currents. These factors have been identified as particularly relevant for this study since the shelf width changes significantly in some locations and the Leeuwin Current system dominates coastal waters of WA.

While shelf width can affect the propagation of CSWs and CTWs, bathymetry (including bottom friction) of the continental shelf has also been found to influence these waves. A major cause of decay of CSWs and CTWs is bottom friction which corresponds to bathymetry (Brink 1991, 2006; Csanady 1987; Church & Freeland 1987; Schulz, Mied & Snow 2012; Webster 1985).



METHODS

Two main approaches to simulating CSW generation and propagation along the coastline of WA were adopted in this study. These were: (1) The numerical simulation of CSW generation on an idealised Northwest shelf by various synthetic tropical cyclone wind fields to investigate the dynamics of CSW generation and propagation; (2) Realistic model simulation of the CSW generated by Tropical Cyclones Bianca in 2011 and comparison with measured data.

Site description

Tropical cyclones in Western Australia

The northwest shelf (NWS) of Western Australia is subject to, on average, five tropical cyclones in the months of November to April (Eliot & Pattiaratchi 2010). This region is the most common source region for CSWs and for this reason it was chosen for this study. Intense tropical cyclones can cause extensive damage with economic consequences to industry and townships along the coastline of WA (McBride 2012) and can also generate continental shelf waves that can propagate for thousands of kilometres along the coastline (Eliot & Pattiaratchi 2010).. Typical cyclones on the NWS have a uniform central core of radius 20 to 30 km with maximum wind speeds ($\sim 50 \text{ ms}^{-1}$) occurring at the outer edge of the core (Hearn & Holloway 1990). On average, cyclone forward speeds range between 1.4 ms^{-1} to 5.6 ms^{-1} on the NWS but can also be much faster (Bureau of Meteorology 2013a). For this study we investigated the effects of an idealised Category 5 cyclone with winds speeds up to 70 m s^{-1}

Continental shelf bathymetry of northwest Australia

The NWS region stretches 2400 km along the northwest coastline of WA. It consists of a wide, shallow, continental shelf, marginal terraces and platforms (Wilson 2013). There are four physiographic regions on the NWS: (1) The inner shelf ($\sim 0 \text{ m} - 30 \text{ m}$); (2) The middle shelf ($\sim 30 - 200 \text{ m}$), consisting of more than 40 % of the region, characterised by a gentle slope; (3) The outer shelf/slope ($\sim 200 \text{ m}$ to base of slope), characterised mainly by a steep slope; and (4) The abyssal plain/deep ocean floor which has a flat, gentle slope at depths greater than $\sim 4000 \text{ m}$ (Baker *et al.* 2008). The bathymetry of the NWS is shown in Figure 2.

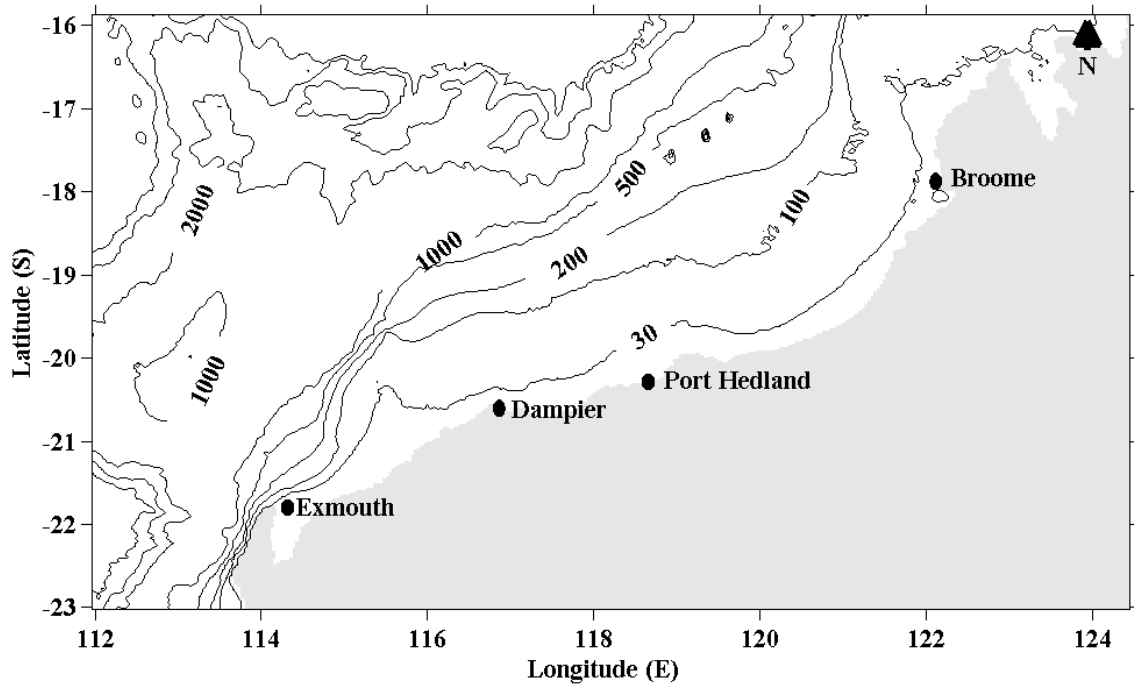


FIGURE 2 – THE NWS OF WA. THE WATER DEPTHS AND TOWNS ARE SHOWN. DAMPIER AND PORT HEDLAND ARE MAJOR INDUSTRIAL TOWNS IN WA. DEPTH CONTOURS ARE IN METERS.

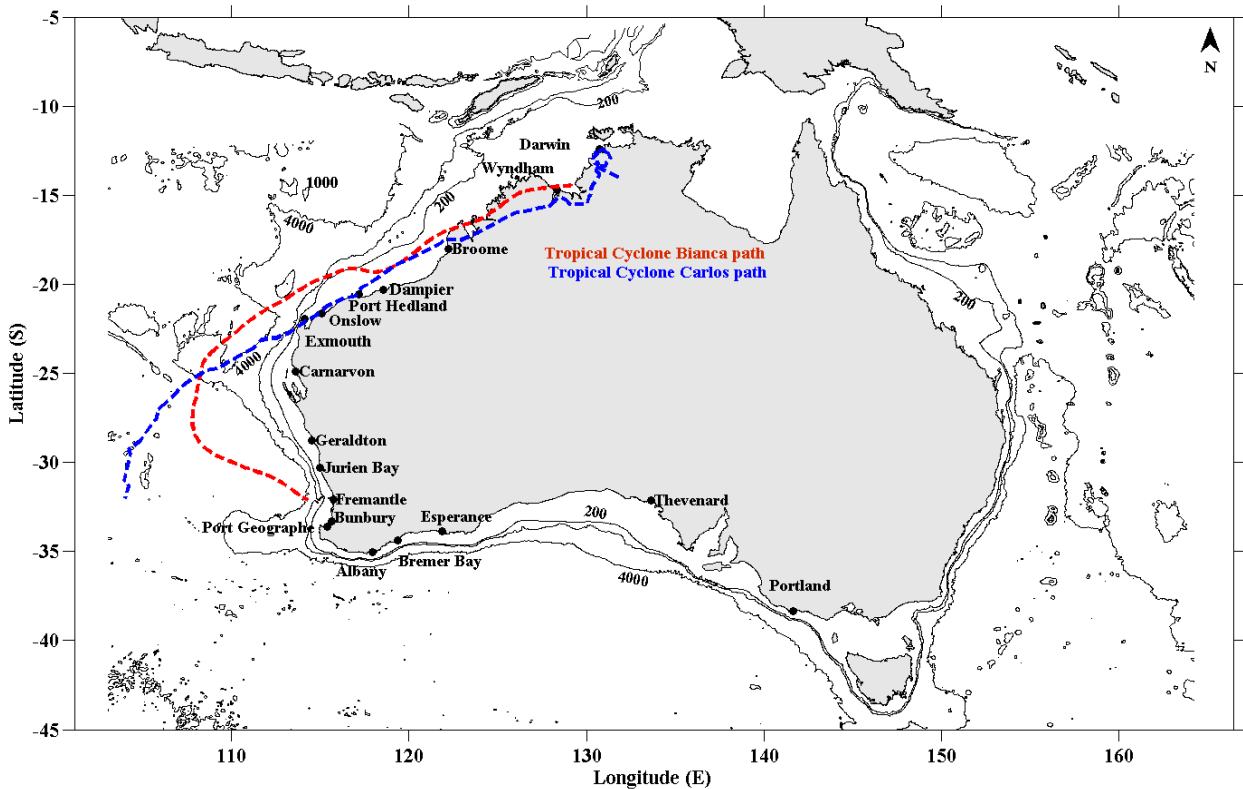


FIGURE 3 – BATHYMETRY OF WA, INCLUDING THE SOUTHERN AND NORTHERN COASTS OF AUSTRALIA.

water in the range of 34 – 35 due to the influence of the Indonesian Throughflow waters (Pearce *et al.* 2003; Wilson 2013).



ROMS model description

The Regional Ocean Modeling System (ROMS) is a free-surface, hydrostatic, primitive equation ocean model. ROMS has been widely used in a variety of contexts to simulate at local to regional levels the ocean environment and has been successfully applied to study the circulation and hydrodynamics of Western Australia (e.g. Macdonald *et al.* 2012), internal tides (e.g. Rayson *et al.* 2011; Van Gastel *et al.* 2009; Xu *et al.* 2013). Tropical cyclone studies and the oceans response have also been performed using ROMS, however there has been a very limited number of these studies (e.g. Li *et al.* 2006; Patricola *et al.* 2012; Zed 2007).

The ROMS model uses stretched, free surface, terrain following, sigma-coordinates in the vertical which provides increased resolution in areas such as the continental slope or thermocline. The sigma-coordinate system captures better the interactions between bathymetry and ocean dynamics than z-coordinates, hence the s-coordinate system is essential for modelling CSWs and ocean processes on continental shelves and continental slopes (Dukhovskoy, Morey & O'Brien 2009; Maiwa, Masumoto & Yamagata 2010).

In the horizontal, ROMS uses orthogonal curvilinear coordinates (Arakawa C grid) where model variables such as sea surface height and pressure are defined in the centre of the grid cells whereas the velocity is defined along the edge of the grid cell (Arakawa & Lamb 1977). The model can be forced at the boundaries by tides and ocean currents and meteorological inputs from observations of atmospheric model (winds, pressure, heat fluxes).

NWS idealised model setup

The NWS idealised model was created to determine the extent of influence that cyclone properties had on the characteristics of CSWs (propagation speed and wave height) and the generation of these waves. The model simulations performed are forced by synthetic tropical cyclones that vary in speed, direction and category. The NWS idealised model is a three-dimensional model with constant salinity and temperature. The idealised NWS model setup is discussed below along with a description of the model simulations performed and methods used to analyse the simulation results.

The domain of the model included the whole of the NWS, extending from 10°S to 25°S and 115°E to 130°E, covering a rectangular ocean basin. The curvilinear orthogonal grid had a spatial resolution of ~ 4 km both in the latitude and longitudinal directions. The idealised model had 400 by 400 grid cells (Figure 4). There were 30 sigma layers in the vertical water column (Figure 5).

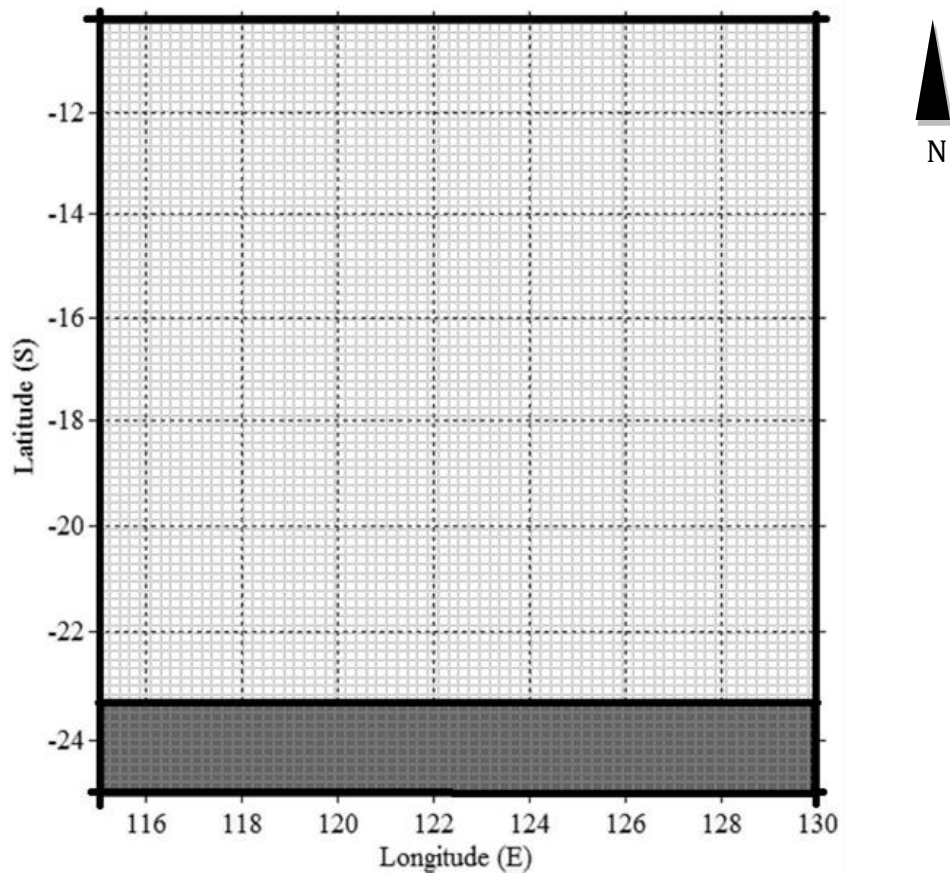


FIGURE 4 – NWS IDEALISED MODEL GRID GENERATED USING SEAGRID. EACH SMALL SQUARE REPRESENTS A GRID CELL. THE DARK GREY SECTION IS MASKED AS LAND.

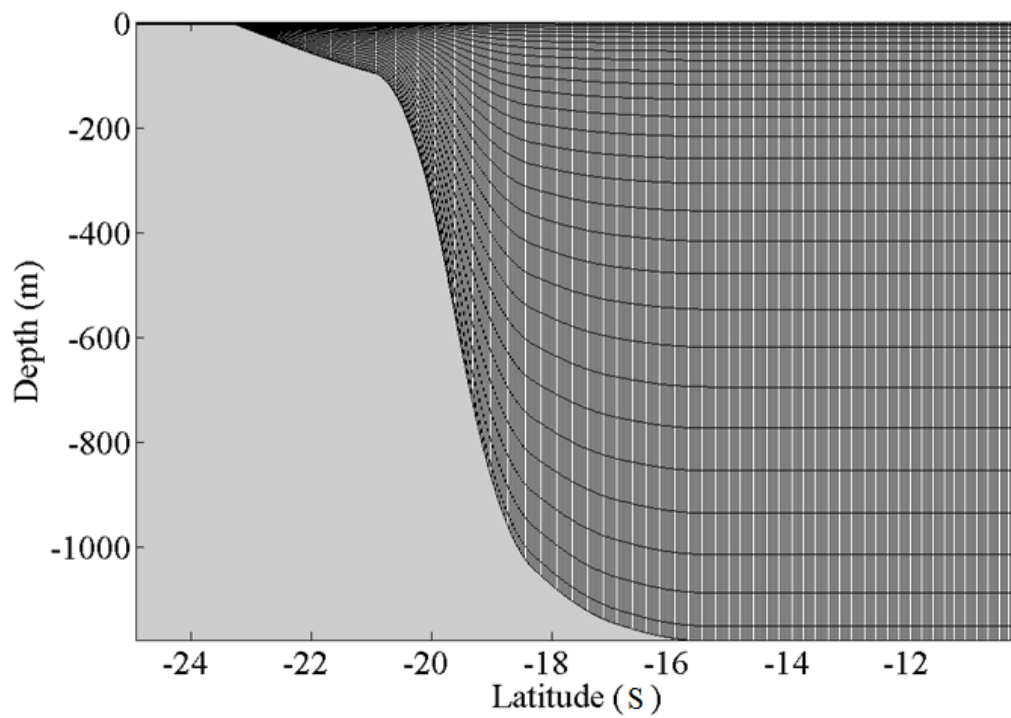


FIGURE 5 – THE 30 VERTICAL SIGMA LAYERS USED IN THE NWS IDEALISED MODEL.

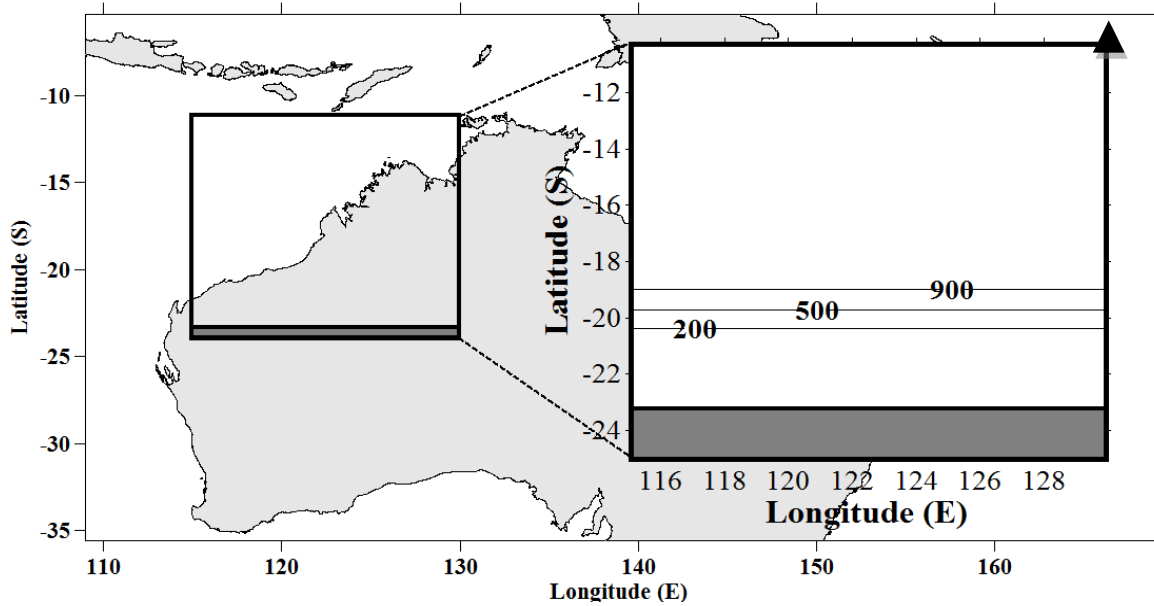


FIGURE 6 – NWS IDEALISED MODEL BATHYMETRY OVERLAYED ONTO THE WA COASTLINE.

The temperature and salinity values in the model remained constant with depth and time and are typical values that occur on the NWS. The parameters such as net shortwave radiation flux, net surface freshwater flux, net surface heat flux and surface net heat flux sensitivity to sea surface temperature (Table 2) are difficult to appropriately assign due to the model being idealised, however, these parameters remained constant for all model simulations thus limiting the impact that these parameters may have on the model simulation results.

TABLE 1 – PARAMETERS IN THE NWS IDEALISED MODEL.

Parameter name	Units	Parameter value in model
Surface u-momentum stress	Nm ⁻²	Varying in domain and time
Surface v-momentum stress	Nm ⁻²	Varying in domain and time
Surface air pressure	mb	Varying in domain and time
Net shortwave radiation flux	Watts m ⁻²	100
Surface net heat flux sensitivity to sea surface temperature	Watts m ⁻² per °C	-30
Net surface heat flux	Watts m ⁻²	100
Net surface freshwater flux	cm day ⁻¹	100
Sea surface salinity	-	35
Sea surface temperature	°C	30

Prior to the passage of the tropical cyclone and after the passage of the tropical cyclone, the surface air pressure remained constant over the whole grid at a value of 1000 mb and the u-velocity wind component was also constant and equal to 5 ms⁻¹ (0.039 Nm⁻² surface u – momentum stress) while

the v – velocity wind component was equal to 0 ms^{-1} . The direction of the wind was westerly, which is the direction that usually occurs on the NWS during the summer months (Pearce *et al.* 2003; Webster 1983). The passage of the tropical cyclone in the model grid occurred after a spin-up period of a few days so that cyclone entered stable ocean conditions.

MATLAB was used to generate a very simple vortex-like cyclone wind and pressure field that allowed for changing the cyclone category, direction and forward speed for the model simulations (see *Appendix C- Idealised cyclone wind forcing MATLAB code* for a description of the MATLAB code). The cyclone wind and pressure field was three hourly, and was interpolated onto the 400×400 grid used in the ROMS model simulations. An example of the cyclone pressure field with velocity vectors is shown in Figure 7.

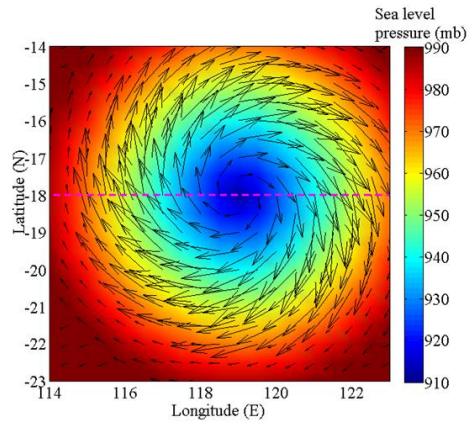


FIGURE 7 – EXAMPLE CYCLONE WIND AND PRESSURE FIELD OF A CATEGORY 5 CYCLONE, USED IN THE NWS IDEALISED MODEL, GENERATED IN MATLAB.

A Category 5 cyclone was the standard cyclone used in the model runs. The standard description of a Category 5 used in the model is presented in Table 2. Simulations of different categories were also performed, based on the classification by the Bureau of Meteorology, but were limited by computer restraints.

TABLE 2 – A DESCRIPTION OF THE STANDARD TROPICAL CYCLONE USED IN THE MODEL SIMULATIONS.

Category 5	
Maximum wind gusts	81.7 ms^{-1}
Maximum mean wind speed	59.7 ms^{-1}
Minimum mean wind speeds	5 ms^{-1}
Minimum pressure	905 mb
Cyclone forward speed	3.5 ms^{-1}
Radius to maximum winds	70 000 m

Over 70 simulations, with run times of approximately two days each for one month simulation on a 20 core computer were performed to test what cyclone factors influence the generation and propagation of CSWs. The model output surface sea levels at half hourly intervals. A summary of the simulations completed are shown in Figure 8. The main division between simulation runs were via path (parallel, perpendicular or 45° angle). Model simulations were also performed with a parallel cyclone moving only a quarter of the model grid

to test behaviour of the CSW generated by a parallel moving cyclone but not affected by the cyclone by making the cyclone traverse only a quarter of the model grid and then disappearing. Cyclone category and distance from the coast was also tested in this instance.

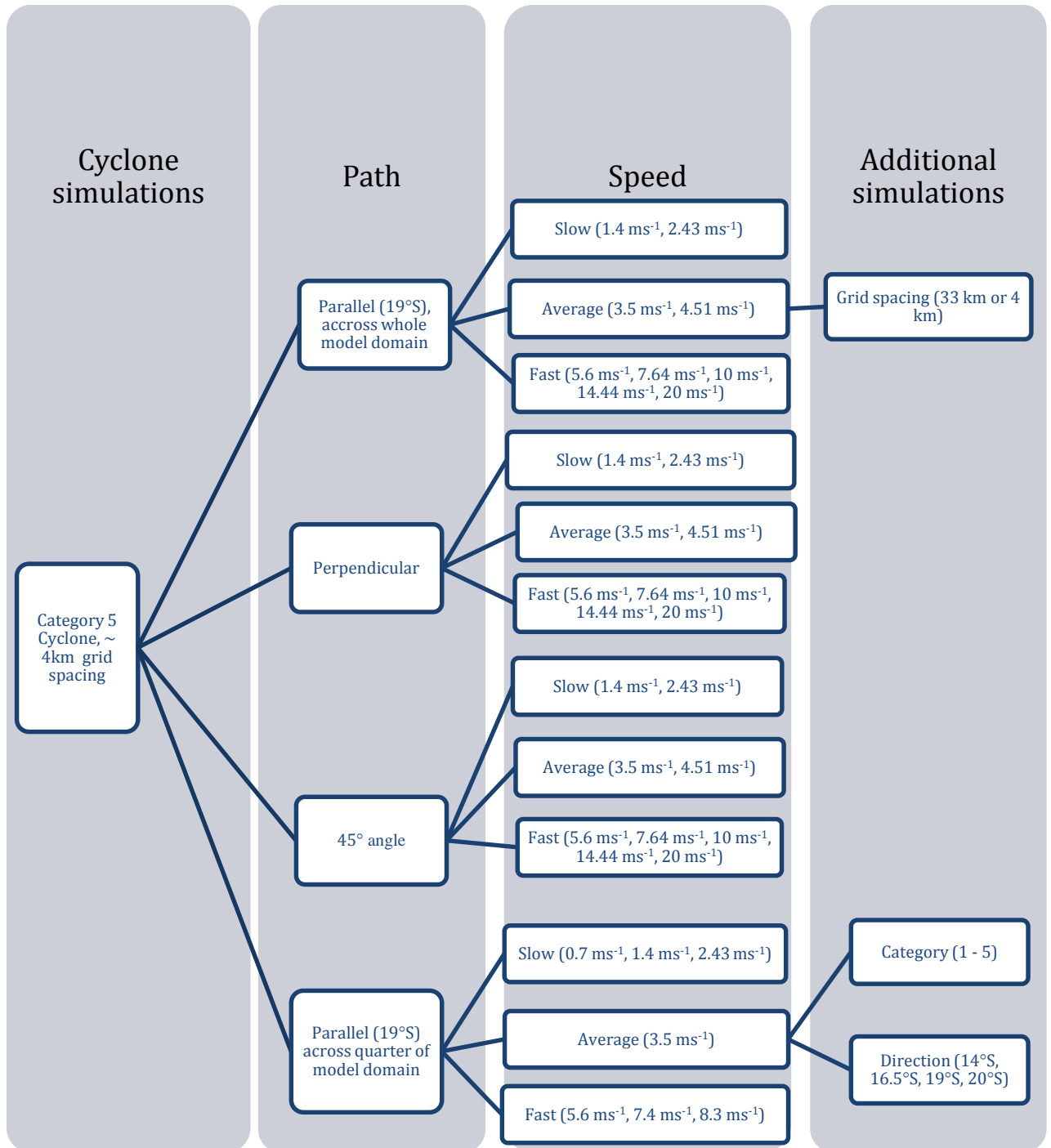


FIGURE 8 – THE VARIOUS MODEL SIMULATIONS PERFORMED ALTERING DIFFERENT PARAMETERS (E.G. FORWARD SPEED AND DIRECTION) RELATING TO THE CATEGORY 5 CYCLONE.

Australia-wide model

A three dimensional continental shelf and slope ROMS model of the whole of Australia (Oz-ROMS), was developed by the University of Western Australia (UWA) to quantify shelf-ocean fluxes of water and carbon over daily to annual



timescales around Australia. Validated with measured data sourced mainly from the Integrated Marine Observing System (IMOS) datasets (e.g. coastal tide gauges, ocean gliders etc), the model can simulate major surface current (e.g. Leeuwin Current), subsurface current systems, eddies, seasonal currents, upwelling, internal waves on the NWS, dense shelf water cascades, inertial oscillations and tidal amplitudes. Present in this model is also CSWs generated by tropical cyclones on the NWS. The selected year for analysing the tropical cyclones and CSWs is during January to April of 2011, selected primarily due to availability of model simulation results and measured data.

The Australia-wide model has a high spatial resolution of ~ 2 – 4 km, covering a curvilinear-orthogonal grid with 1460 x 1460 grid cells and 30 sigma layers in the vertical water column. The model domain extends from 5°S to 45°S and from 100°E to 165°E. The large extent of the model domain ensures that ocean processes are accurately simulated in the model. The model domain is sufficiently large to ensure that the boundaries do not affect the area of interest and that currents and other oceanographic processes are fully considered (Wijeratne 2013, pers. comm., 12 April).

The bathymetry data for the Australia-wide model was obtained from the Geoscience Australia data sets with a 250 m resolution. The model bathymetry and domain of the Australia-wide model is shown in Figure 9. The Australia-wide model high resolution coastline of 1:70 000 scale was sourced from the NOAA National Geophysical Data Centre. The minimum depth cut-off in the Australia-wide model is 15 m (Wijeratne 2013, pers. comm., 12 April).

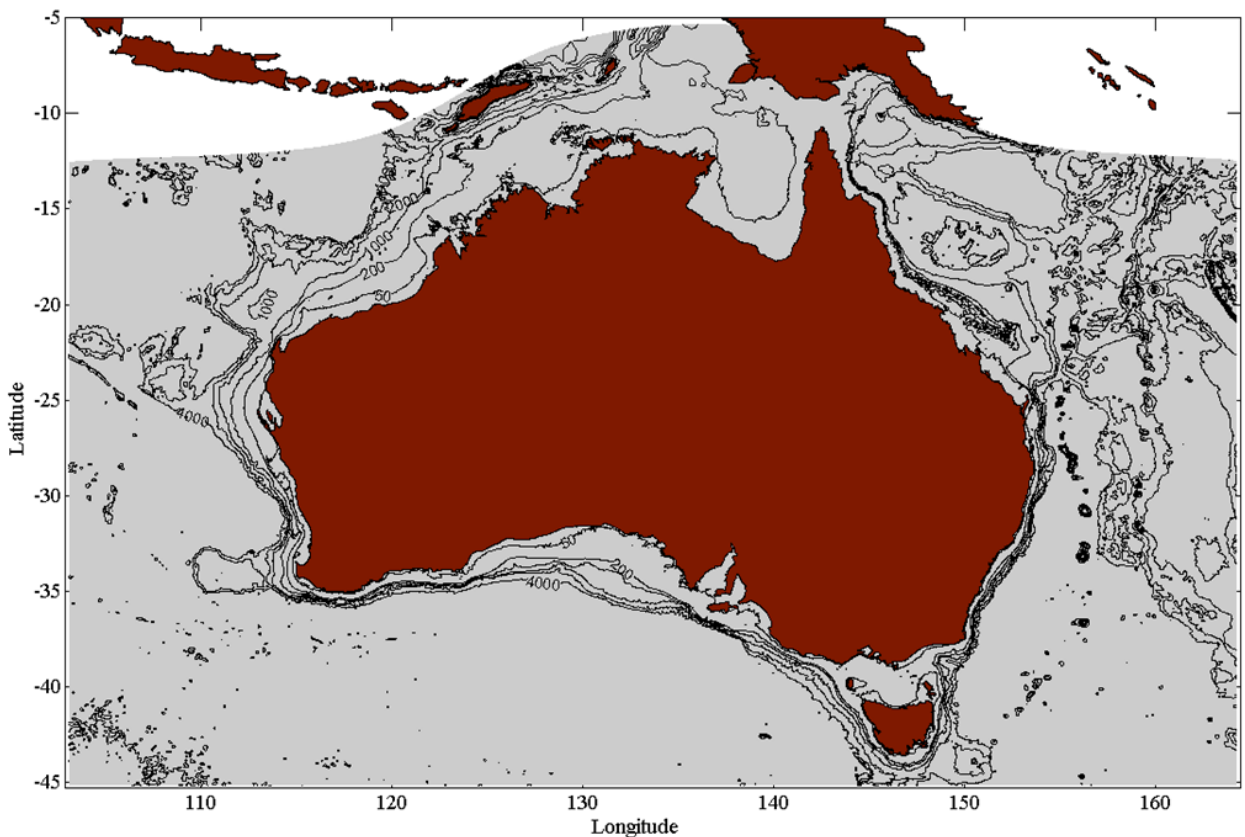


FIGURE 9 - BATHYMETRY AND DOMAIN OF THE AUSTRALIA-WIDE MODEL.

The Australia-wide model is forced using surface winds and atmospheric pressure with 0.25° resolution from the European Centre for Medium-Range Weather Forecasts re-analysis project (ECMWF ERA) interim data. The surface wind stress and sea level pressure forcing changes spatially and temporally every three hours. The ECMWF ERA interim data is used to estimate heat and freshwater fluxes (Wijeratne 2013, pers. comm., 12 April).

The open boundaries in the Australia-wide model occur at all the edges of the model domain. The open boundary forcing in this model is sourced from the HYCOM daily outputs of salinity, temperature, u-velocity and v-velocity components. The tidal forcing boundary conditions in the model were sourced from the OSU TOPEX/Poseidon Global Inverse Solution version 7.2 (TPXO.7.2) (see Egbert, Bennett & Foreman 1994). Boundary conditions in the model include the Chapman, Flather, gradient, nudging and radiation boundary conditions. The model is also forced by monthly climatological mean sea levels derived from the satellite altimeter data from the AVISO database.

Three years of model simulations from 2010 to 2012 have been completed (Wijeratne 2013, pers. Comm., 10 Oct). The model data analysis period for this study was between January and April 2011 which included 5 tropical cyclone events, two of which (Tropical Cyclone Bianca and Carlos) are analysed in this study for understanding CSW generation.

WA cyclone and tide gauge data 2011

The Australia-wide model results for CSWs generated by tropical cyclones in 2011 in WA were compared and statistically analysed with measured data. Firstly, tropical cyclone events in 2011 (January to April) were obtained from the Bureau of Meteorology website, which included details on the cyclone path, category and speed (Bureau of Meteorology 2013b). During January to April, 2011, there were 5 tropical cyclones and two significant tropical lows, that occurred over the north western part of Australia. The paths of these tropical cyclones and tropical lows with their respective dates are shown in Figure 10.

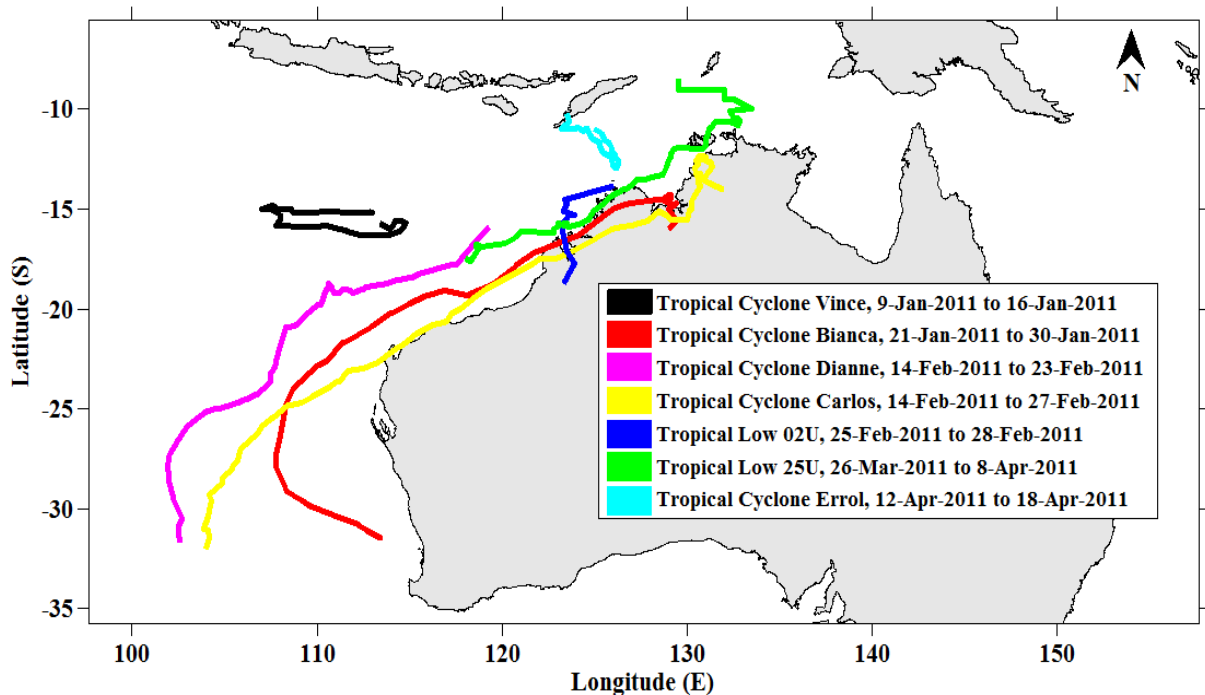


FIGURE 10 – TROPICAL CYCLONES AND LOW DURING JANUARY TO APRIL OF 2011 (BUREAU OF METEOROLOGY 2013B).



The tide gauge water level data used in the analysis was recorded at hourly intervals along the coastline of WA and was obtained from the Department of Transport, which include the stations Port Hedland, Cape Lambert, Onslow, Exmouth, Carnarvon, Geraldton, Jurien Bay, Fremantle, Bunbury, Port Geographe, Albany, Bremer Bay and Esperance. The University of Hawaii Sea Level Centre website was also used to obtain tide gauge sea level data for Broome and Wyndham (WA), Darwin (Northern Territory), Thevenard (South Australia) and Portland (Victoria). The Figure 3 shows the location of these stations along the coastline. Tropical Cyclones Bianca and Carlos were the two cyclones identified in the measured data to have generated CSWs and the focus cyclones in this study.

Data analysis

On completion of the model simulation runs, the water level data from the NWS idealised model, the data were low pass filtered to remove periods less than 48 hours (e.g. Figure 11). This ensured tides were removed so the CSW could be identified in the data. Amplitudes were measured from trough to crest (e.g. Figure 12).

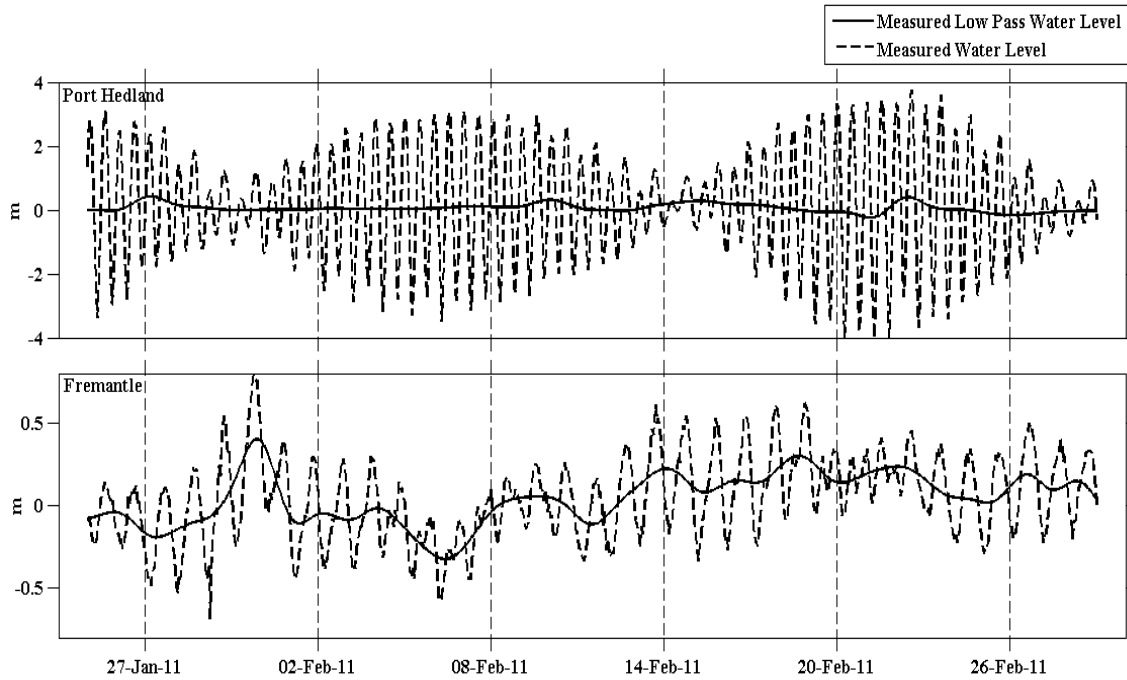




FIGURE 11 – EXAMPLE OF FILTERING MEASURED DATA AT TWO LOCATIONS ALONG THE WA COASTLINE: PORT HEDLAND AND FREMANTLE.

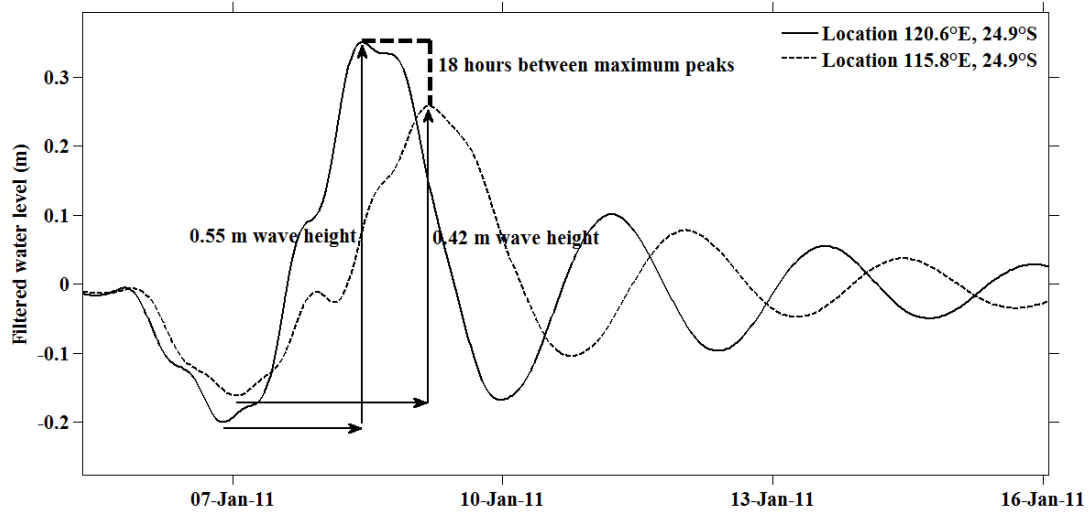


FIGURE 12 – EXAMPLE OF TROUGH TO CREST ANALYSIS OF A CSW AT TWO DIFFERENT LOCATIONS FROM THE NWS IDEALISED MODEL.



RESULTS

Results from the idealised NWS model and the Australia-wide model are presented in this section.

NWS idealised model

Over 70 model simulations of a category 5 synthetic tropical cyclone that varied by path, speed and category were analysed. The results show that changing the various cyclone parameters influenced CSW behaviour.

Coastline parallel cyclones near shelf edge travelling across the whole model domain with different forward speeds

All simulation results showed an initial decrease in water levels as the cyclone entered the model domain. This decrease in water was most significant along the coastline. For parallel cyclones that travelled slow (1.4 ms^{-1}), this decrease in water level was greater by about 0.25 m than for all other faster cyclones simulated ($\geq 2.43 \text{ ms}^{-1}$). This low water represented the minimum amplitude of the CSW. Water levels underneath the cyclone exceeded 0.2 m and rotated clockwise for all simulations. As the tropical cyclone continued to move parallel to the coast, a convergence of high water developed, which travelled as a CSW along the coast. The CSW travelled ahead of the cyclone, to the west (left) of the model grid, when the cyclones had forward speeds less than 5.6 ms^{-1} (Figure 13). The slowest moving cyclone (1.4 ms^{-1}) simulated high water levels ($> 0.2 \text{ m}$) along the coastline of the whole model domain for about 8 days. The duration of high water along the coast reduced with faster moving cyclones but the high water level was also much greater. A cyclone travelling at 5.6 ms^{-1} showed the CSW high water travelling alongside with the cyclone. When the cyclones had faster forward speeds of 7.64 ms^{-1} and 10 ms^{-1} the CSW moved directly parallel, alongside the cyclone. However, the cyclone travelling at 10 ms^{-1} did not generate a CSW that moved directly parallel to the cyclone initially. When the CSW was first generated, it moved much slower than the cyclone, but after the cyclone had travelled 600 kilometres across the model domain, the CSW caught up with the cyclone and moved parallel, alongside it. Cyclones with forward speeds of 14.4 ms^{-1} or 20 ms^{-1} generated a CSW that travelled slower than the cyclone, moving behind the cyclone, rather than in front.

The oceans response after the passage of the parallel cyclone resulted in low and high water level oscillations occurring along the coastline. The number of oscillations and the height of these oscillations reduced as the cyclone forward speed increased. At the 200 m depth contour, where the continental shelf break occurs, long-lasting eddies of low and high water alternated with these high and low water level oscillations that occurred along the coast. The water levels of these oscillations decreased in height and speed over time and moved to the west (left) of the model domain. Surface velocity vectors showed that the low water eddies rotated clockwise and corresponded to the high water occurring at the coast. The high water eddies rotated anticlockwise and corresponded to the low water levels occurring at the coast.

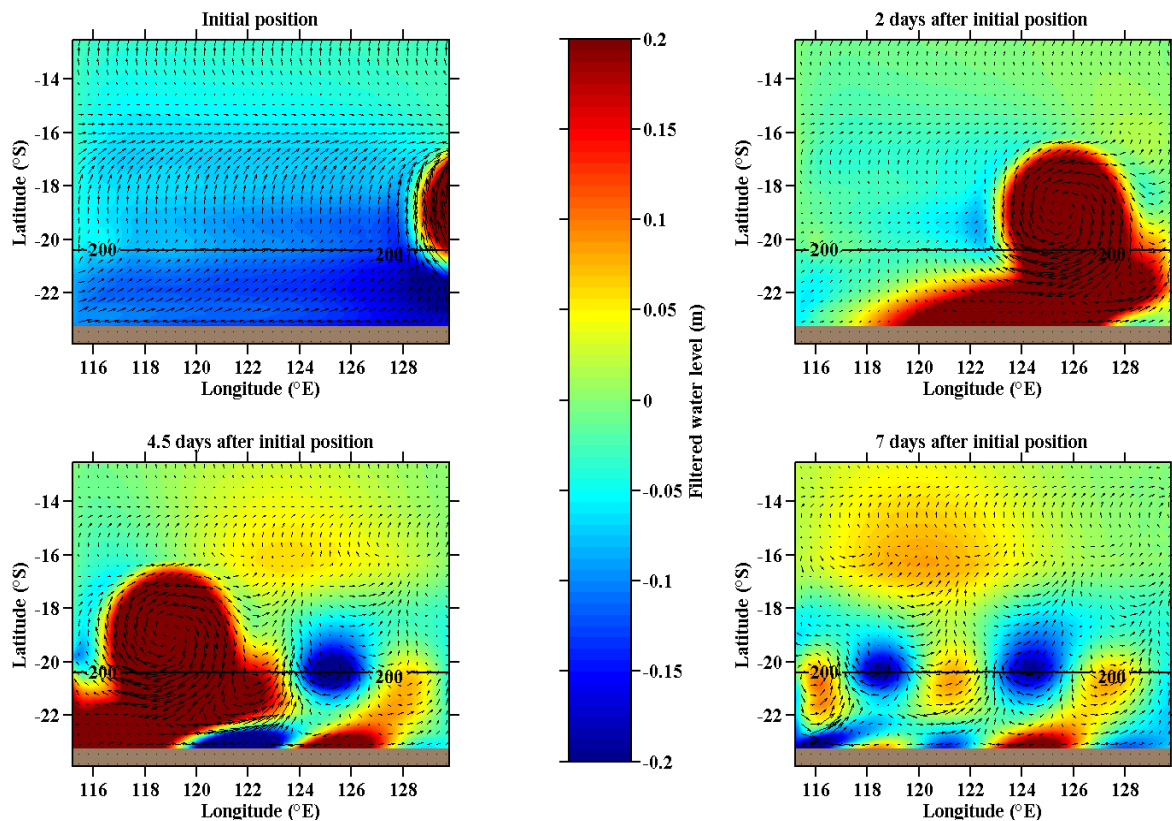


FIGURE 13 - WATER LEVELS DURING THE PASSAGE OF A CYCLONE MOVING PARALLEL TO THE COASTLINE WITH A FORWARD SPEED OF 3.5 MS⁻¹. SURFACE VELOCITY VECTORS ARE ALSO SHOWN.

A comparison of the CSW height and propagation speed, along with CSW minimum and maximum amplitudes for the model simulation runs of a parallel cyclone are shown in Figure 14. The results show that the height of the CSW is dominated more by the high water component (CSW maximum amplitude) than the low water component which occurred ahead of the cyclone (CSW minimum amplitude). Maximum CSW heights attained ranged between 0.5 m and 1.03 m depending on the cyclone forward speed. The maximum CSW height of 1.03 m occurred when the cyclone had a forward speed of 7.64 ms⁻¹. Cyclones that travelled at speeds less than 7.64 ms⁻¹ showed the following general trend: as the cyclone forward speed increased (up to 7.64 ms⁻¹), the CSW height also increased. When the tropical cyclone travelled much faster than 7.64 ms⁻¹, the CSW height decreased with increased cyclone forward speed. The lowest CSW height of 0.5 m for all simulations occurred when the cyclone travelled at 20 ms⁻¹.

CSW propagation speeds ranged between 6 ms⁻¹ and 23.5 ms⁻¹ (Figure 14). The propagation speed of the CSW increased when the cyclone had a faster forward speed except with the fastest cyclone forward speed of 20 ms⁻¹. The CSW in this instance travelled much slower (~ 15 ms⁻¹), which was also slower than the cyclone forward speed of 20 ms⁻¹. All other CSW simulations had propagation speeds (6 ms⁻¹ – 23.5 ms⁻¹) greater than the actual cyclone forward speed (1.4 ms⁻¹ – 14.4 ms⁻¹)

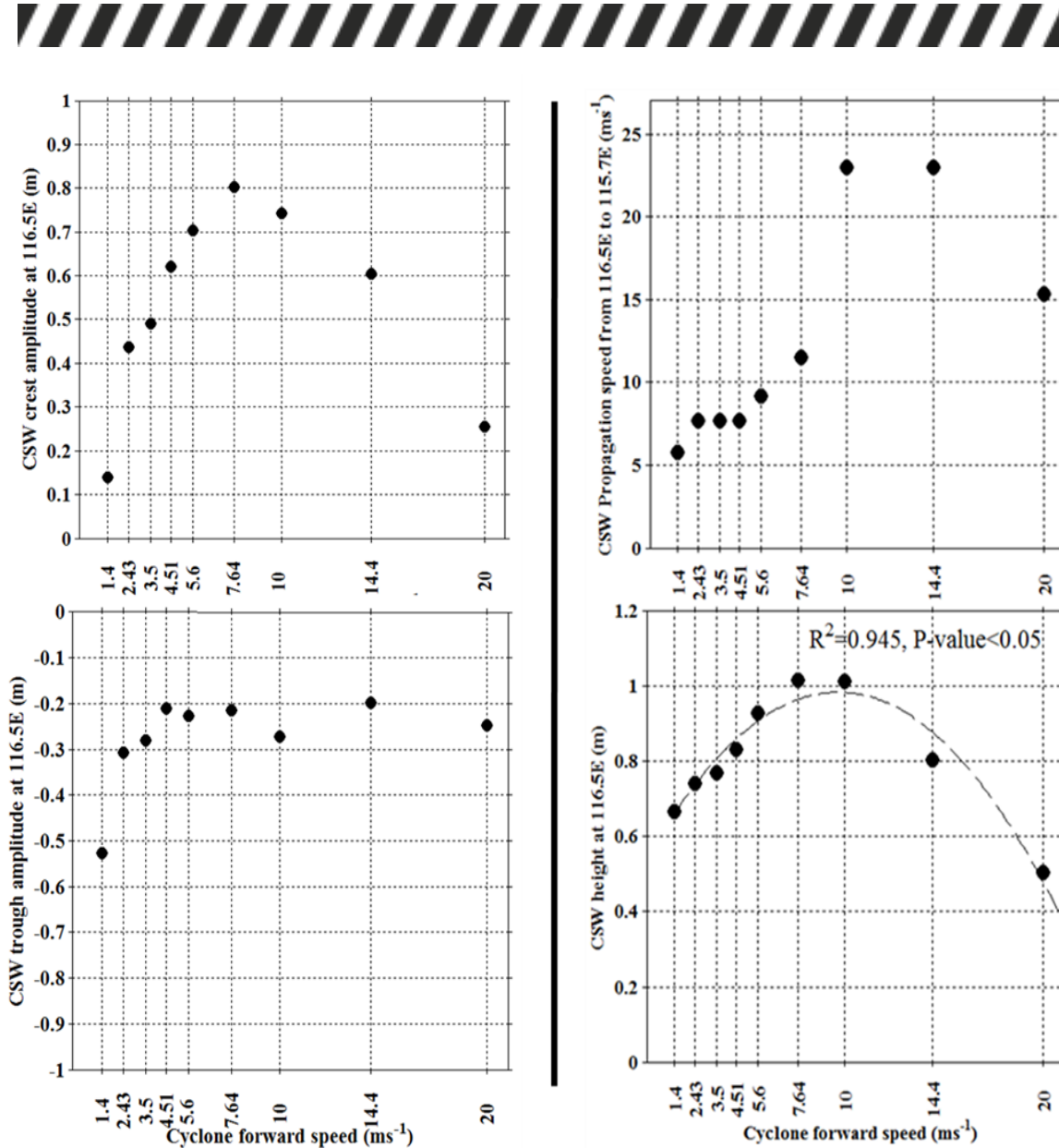


FIGURE 14 – CSW MAXIMUM AMPLITUDE (TOP LEFT), MINIMUM AMPLITUDE (BOTTOM LEFT), PROPAGATION SPEED (TOP RIGHT) AND WAVE HEIGHT (BOTTOM RIGHT) FOR EACH MODEL SIMULATION PERFORMED WITH A PARALLEL CYCLONE TRAVELLING NEAR THE SHELF EDGE, (19°S) ACROSS THE WHOLE MODEL DOMAIN WITH A DIFFERENT FORWARD SPEED.

A parallel moving cyclone near the shelf edge (19°S) travelling over the whole model grid at a speed of 5.6 ms⁻¹ was simulated using a coarser 33 km grid (Figure 15). All forcing and bathymetry data had 33 km grid spacing. This was used to compare grid resolution and the influence this had on CSW height and propagation speed. The results showed that the CSW generated using 33 km spacing estimated the peak surge of the CSW approximately 7 % less than when using the 4 km grid spacing. The crest of the waves that followed after the CSW were estimated at approximately 50 % less in height than the crest of the waves from the 4 km grid spacing. However, the trough water level of the subsequent waves matched well. The propagation speeds of the CSW in both test cases were similar.

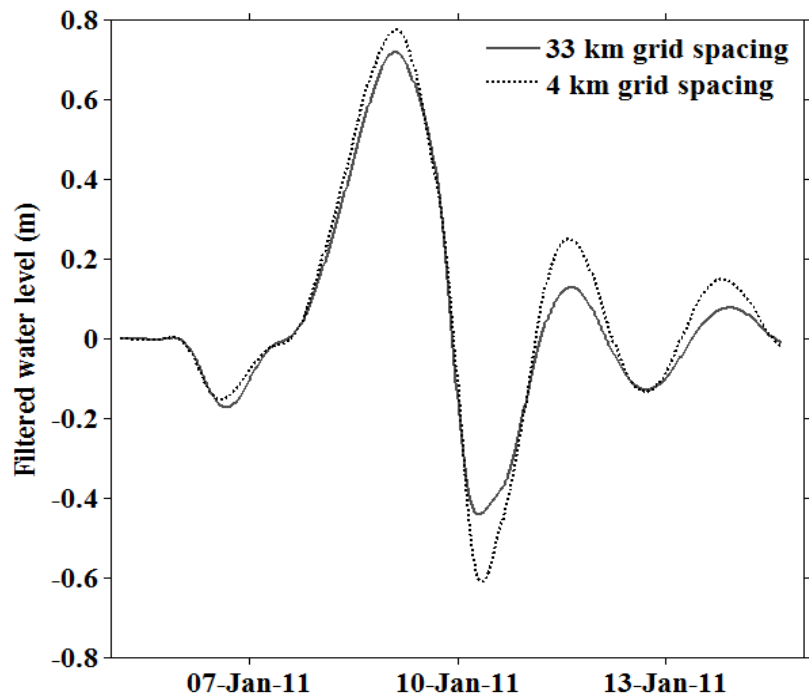


FIGURE 15 - CSW WATER LEVEL AT 116.5°E AT THE COAST FOR TWO DIFFERENT GRID SPACING SIZES. CYCLONE SPEED IS 5.6 MS⁻¹ AND TRAVELS NEAR THE SHELF EDGE (19°S) OVER THE WHOLE MODEL DOMAIN. ALL OTHER PARAMETERS WERE KEPT CONSTANT.

Coastline parallel cyclones near shelf edge travelling a quarter of the model domain with different speeds

Seven simulation runs of a parallel cyclone that travelled near the shelf edge (19°S) across only a quarter of the model domain, each with a different cyclone forward speed, were performed. All other parameters remained the same as the previous setup. The results showed similarities and differences to the CSW generated by the same parallel moving cyclone that travelled over the whole domain at the same latitude. The simulations using a cyclone that travelled only over a quarter of the model domain provided an opportunity to evaluate the properties of the CSW without the presence of the parallel cyclone which travelled over the whole domain.

The results displayed an initial decrease in water level along the coastline as the cyclone entered the grid for all simulations completed (Figure 16). This decrease in water level was greatest for cyclones that travelled the slowest. As the cyclone continued to move parallel, water along the coastline began to build-up and the low water of the CSW, ahead of the cyclone, moved to the west (left) of the domain. When the cyclone disappeared from the model domain, the high water along the coastline continued to move along the coast, as did the CSW. This was followed by low water levels. The CSW heights were greatest for cyclones that travelled slowest (0.7 ms⁻¹, 1.4 ms⁻¹ and 2.4 ms⁻¹). Low water clockwise eddies along the 200 m depth contour also occurred and corresponded to high water along the coastline. High water, anticlockwise eddies along the 200 m depth contour interchanged with the low water eddies in the ocean basin. The high water anticlockwise eddies corresponded to low water along the coastline. However, the oscillations of low and high water levels were much less defined than for simulations of cyclones that travelled parallel across the whole model domain.

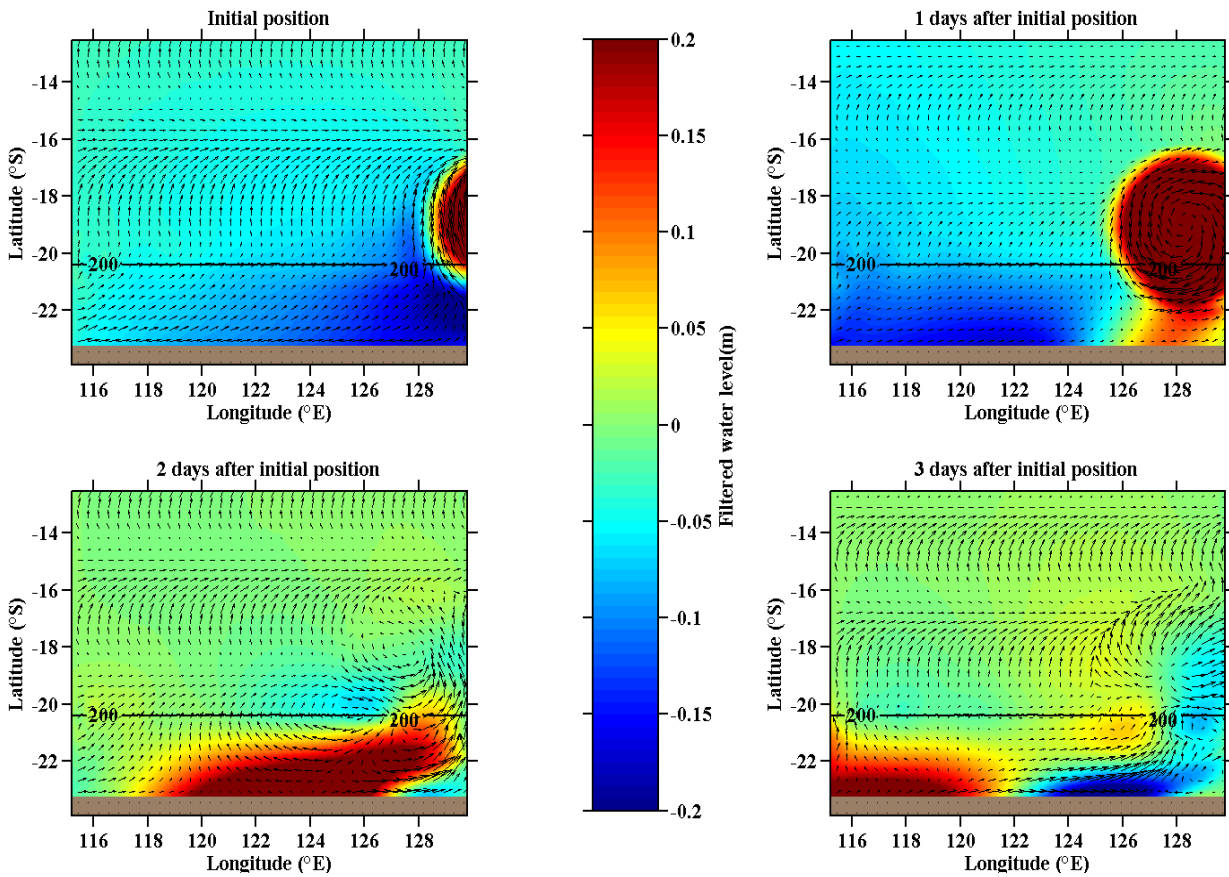


FIGURE 16 - WATER LEVELS DURING THE PASSAGE OF A CYCLONE MOVING PARALLEL TO THE COASTLINE FOR ONLY A QUARTER OF THE DOMAIN WITH A FORWARD SPEED OF 3.5 MS⁻¹. SURFACE VELOCITY VECTORS ARE ALSO SHOWN.

A comparison of the CSW height and propagation speed, along with CSW minimum and maximum amplitudes for the model simulations of a parallel cyclone travelling over a quarter of the model domain are shown in Figure 17. Cyclones that had slower forward speeds of 0.7 ms⁻¹, 1.4 ms⁻¹ and 2.4 ms⁻¹ generated CSWs with the greatest wave height (~ 0.6 m). This is opposite to the CSWs generated by the parallel cyclones that moved across the whole model domain. These had much lower wave heights for slower cyclones, but were still greater in height than the CSWs generated by the same parallel cyclone that moved only a quarter of the way through the model domain. The low water that occurred head of the cyclone (the CSW trough) was greatest for the three slowest cyclones. However, the high water of the CSW dominated the largest component of the CSW height. The three fastest moving cyclones (5.6 ms⁻¹, 7.4 ms⁻¹ and 8.3 ms⁻¹) generated CSWs that had the lowest wave heights (~ 0.31 m). A general trendline showed the CSW height decreases with increased cyclone forward speed (Figure 17). The CSW propagation speed also varied with cyclone forward speed (Figure 17). The two slowest cyclones generated a CSW that had forward speeds of 23.5 ms⁻¹. All other cyclone forward speeds generated a CSW that travelled approximately 15 ms⁻¹.

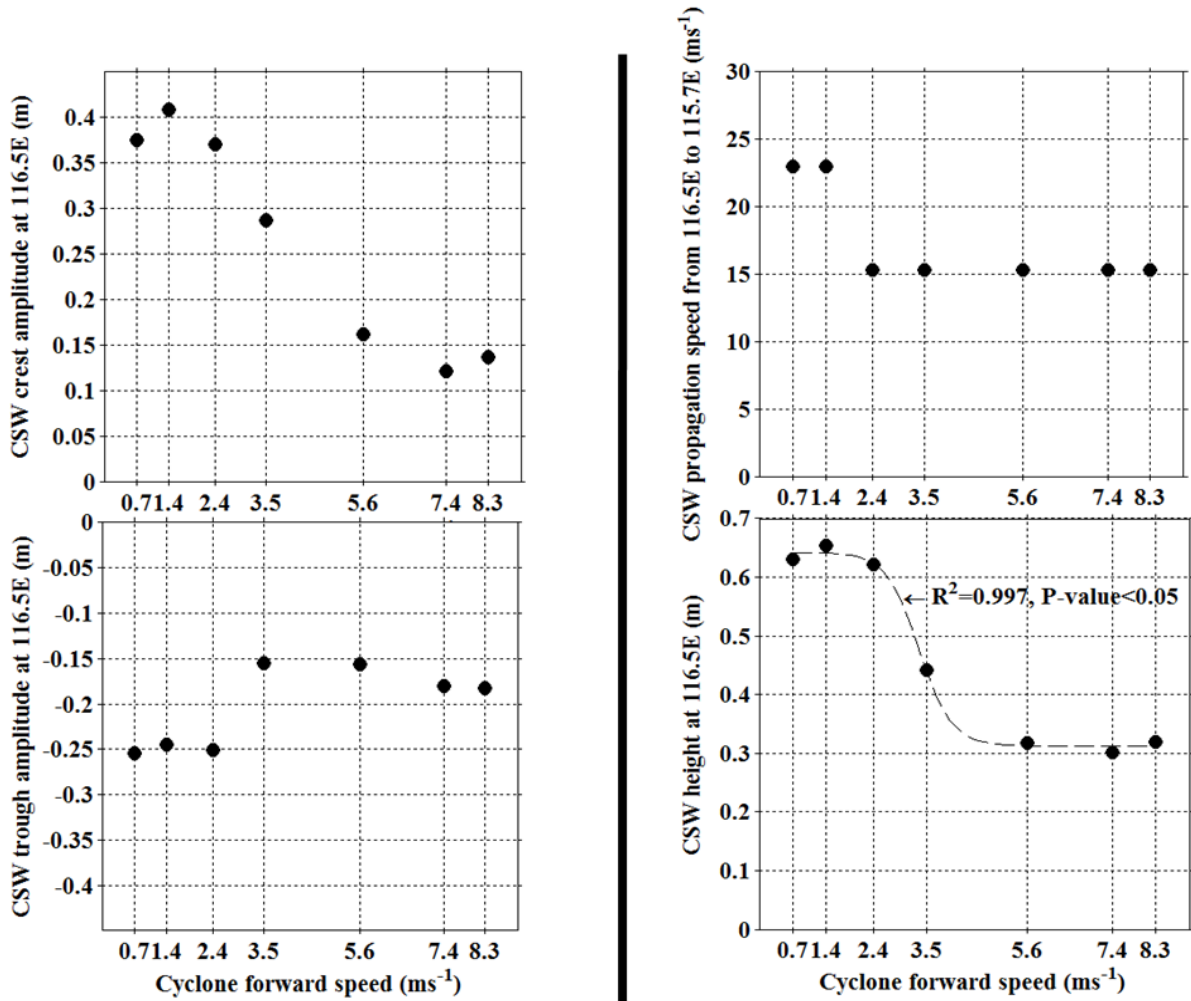


FIGURE 17 - CSW MAXIMUM AMPLITUDE (TOP LEFT), MINIMUM AMPLITUDE (BOTTOM LEFT), PROPAGATION SPEED (TOP RIGHT) AND WAVE HEIGHT (BOTTOM RIGHT) FOR EACH MODEL SIMULATION PERFORMED WITH A PARALLEL CYCLONE TRAVELLING NEAR TO THE SHELF EDGE (19°S) ACROSS A QUARTER OF THE MODEL DOMAIN WITH A DIFFERENT FORWARD SPEED.

Coastline parallel cyclones travelling over 25% of the model domain at 3.5 ms⁻¹ at various distances from the coastline

Cyclones that travelled parallel and offshore (14°S and 16.5°S) were still able to generate a small amplitude CSW. However, this CSW was significantly lower than for the cyclones that travelled near the continental shelf break (19°S) or near the coast (20.5°S and 22°S). The cyclones that travelled at 14°S, 16.5°S, 20.5°S and 22°S displayed similar CSW generation properties discussed in previous sections. First, there was low water ahead of the cyclone, which was followed by the convergence of high water as the CSW. Oscillations of low and high water along the coast did not occur for offshore cyclone simulations (14°S, 16.5°S). The simulation of a cyclone very near to the coastline (22°S) had part of the cyclone over land. This resulted in low water ahead of the cyclone for the duration of the passage of the cyclone over the continental shelf (Figure 18). This low water continued to develop further down the coastline. Once the cyclone departed, the low water moved freely to the west (left) along the coast, followed by high and low water levels. The water level variations along the coast did not extend very far offshore.

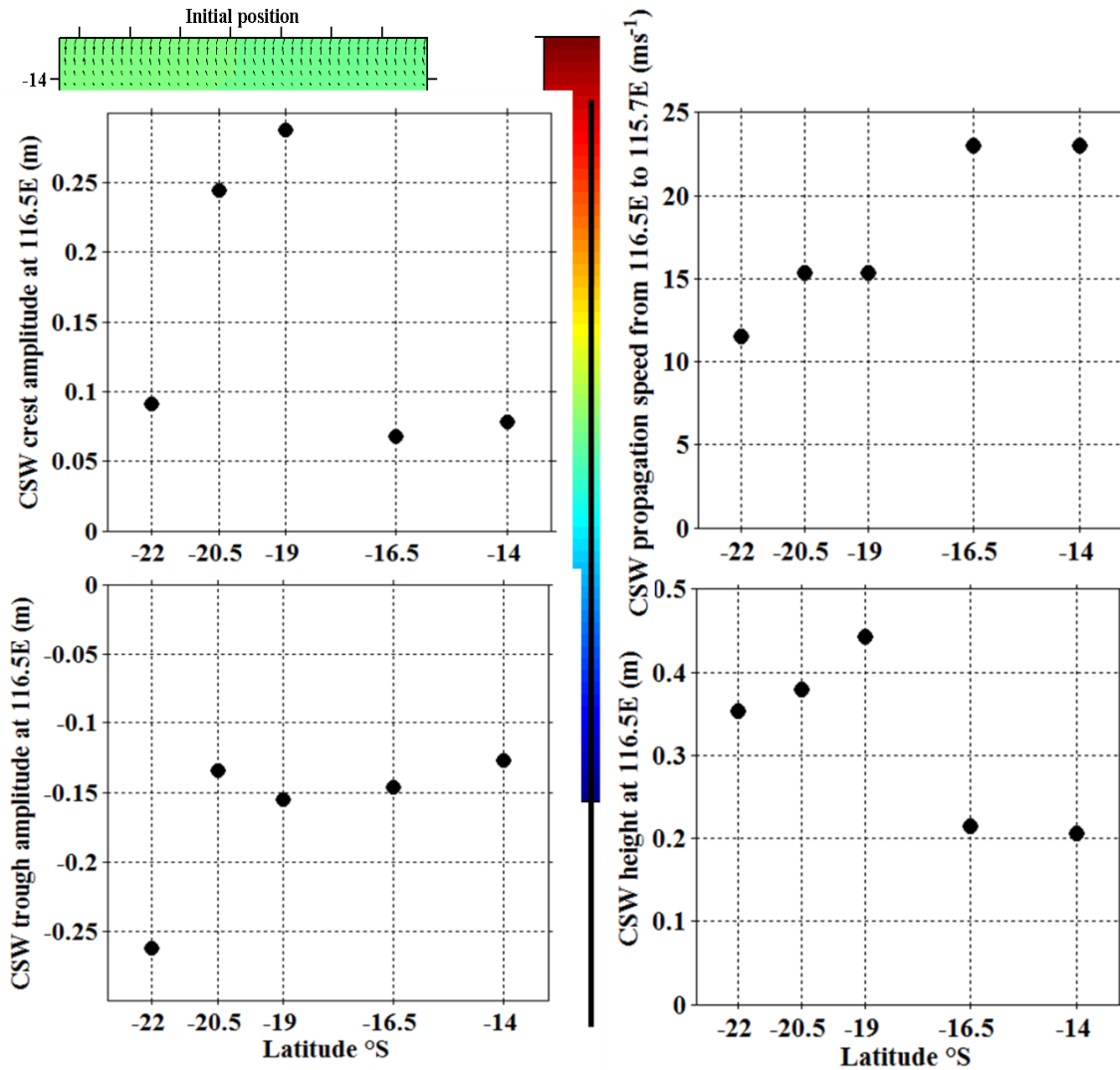


FIGURE 18 - WATER LEVELS DURING THE PASSAGE OF A CYCLONE MOVING PARALLEL TO THE COASTLINE AT A LATITUDE OF 22°S FOR ONLY A QUARTER OF THE DOMAIN WITH A FORWARD SPEED OF 3.5 MS⁻¹. SURFACE VELOCITY VECTORS ARE SHOWN.

A graph comparing CSW amplitudes, height and propagation speed is shown in Figure 19. The results highlight the generation of large volumes of low water by the cyclone that travelled partially over land (22°S). More than 85 % of the CSW height was comprised of this low water. However, in general, the CSW height increased the further the parallel cyclone was from land, up until a certain latitude, where the cyclone was well offshore, distant from the continental shelf. The greatest CSW height of 0.44 m occurred when the tropical cyclone travelled at 19°S, which was near to the continental shelf break. Lowest CSW heights (~ 0.2 m) and fast propagation speeds (23 ms⁻¹) occurred when the tropical cyclones were furthest from the continental shelf. CSW propagation speeds decreased to approximately 15 ms⁻¹ with cyclones that travelled on or near the continental shelf (19°S and 20.5°S). The cyclone that travelled over the continental shelf (22°S) and partly on land had the lowest CSW speed of 11 ms⁻¹.

FIGURE 19 - CSW MAXIMUM AMPLITUDE (TOP LEFT), MINIMUM AMPLITUDE (BOTTOM LEFT), PROPAGATION SPEED (TOP RIGHT) AND WAVE HEIGHT (BOTTOM RIGHT) FOR EACH SIMULATION OF A PARALLEL CYCLONE AT A DIFFERENT DISTANCE FROM THE COAST, ACROSS A QUARTER OF THE MODEL

DOMAIN WITH A SPEED OF 3.5 MS⁻¹. 22°S IS CLOSE TO SHORE.

Coastline parallel cyclones near shelf edge travelling a quarter of the model domain with different intensities

In general more intense cyclones created larger amplitude continental shelf waves. A category 5 cyclone generated a CSW with the greatest wave height (0.45 m). A category 1 cyclone generated a CSW with a wave height of 0.1 m. The propagation speed of the CSW remained at 15.5 ms⁻¹ for all simulations that tested cyclone by category.

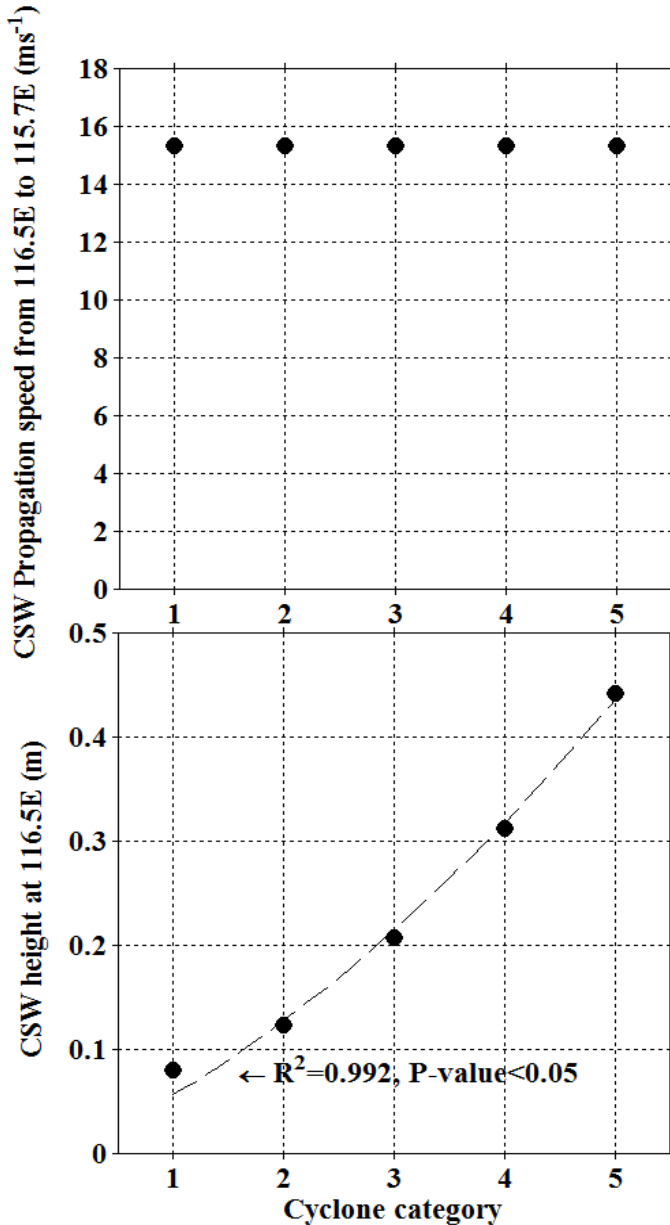


FIGURE 20 - CSW PROPAGATION SPEED AND HEIGHT DEPENDING ON THE CYCLONE'S CATEGORY OF A PARALLEL CYCLONE NEAR THE SHELF EDGE (19°S), THAT TRAVELLED A QUARTER OF THE MODEL GRID ONLY. CYCLONE SPEED IS 3.5 MS⁻¹. ALL OTHER PARAMETERS WERE KEPT CONSTANT.

45° cyclones with different speeds

These nine simulations also displayed an initial decrease in water ahead of the cyclone's path. This low water ahead of the cyclone was most pronounced with the slowest moving cyclone (1.4 ms⁻¹). As the cyclone moved closer to the coastline, a build-up of high water formed. When the cyclone reached the

continental shelf the low water moved along the west (left) of the model domain. Similar to cyclones travelling parallel, the build-up of water along the coastline, for slower moving cyclones, spread further to the west of the model domain along the coast (Figure 21) than the faster cyclones (Figure 22). When the cyclone began to make landfall, the high water ahead of the cyclone separated from the high water that was underneath the actual cyclone due to low water formation between the two high water bodies. After cyclone landfall, low and high water level oscillations along the coastline occurred moving to the west (left) in the model domain. Even after the passage of the tropical cyclone, low water along the tropical cyclone path persisted for a few days when the speed of the cyclone was less than 5.6 ms^{-1} .

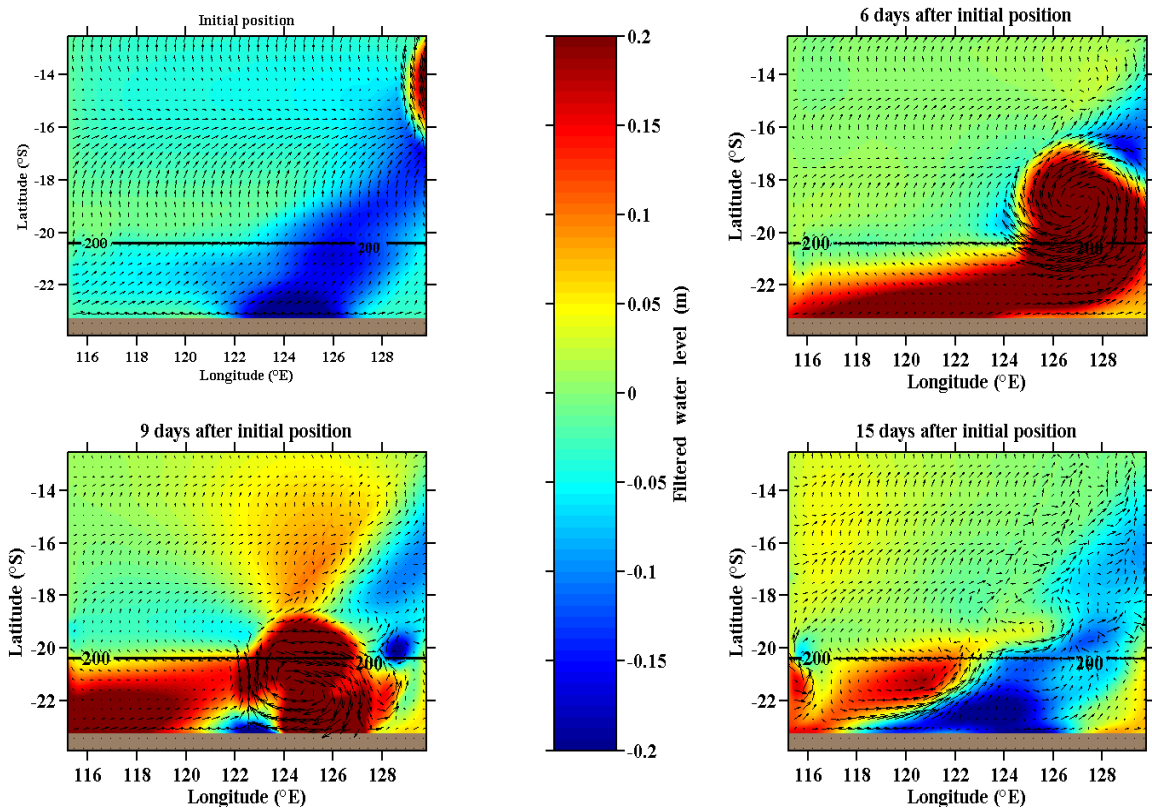


FIGURE 21 - WATER LEVELS DURING THE PASSAGE OF A CYCLONE MOVING AT A 45° TO THE COASTLINE WITH A FORWARD SPEED OF 1.4 MS^{-1} . SURFACE VELOCITY VECTORS ARE ALSO SHOWN.

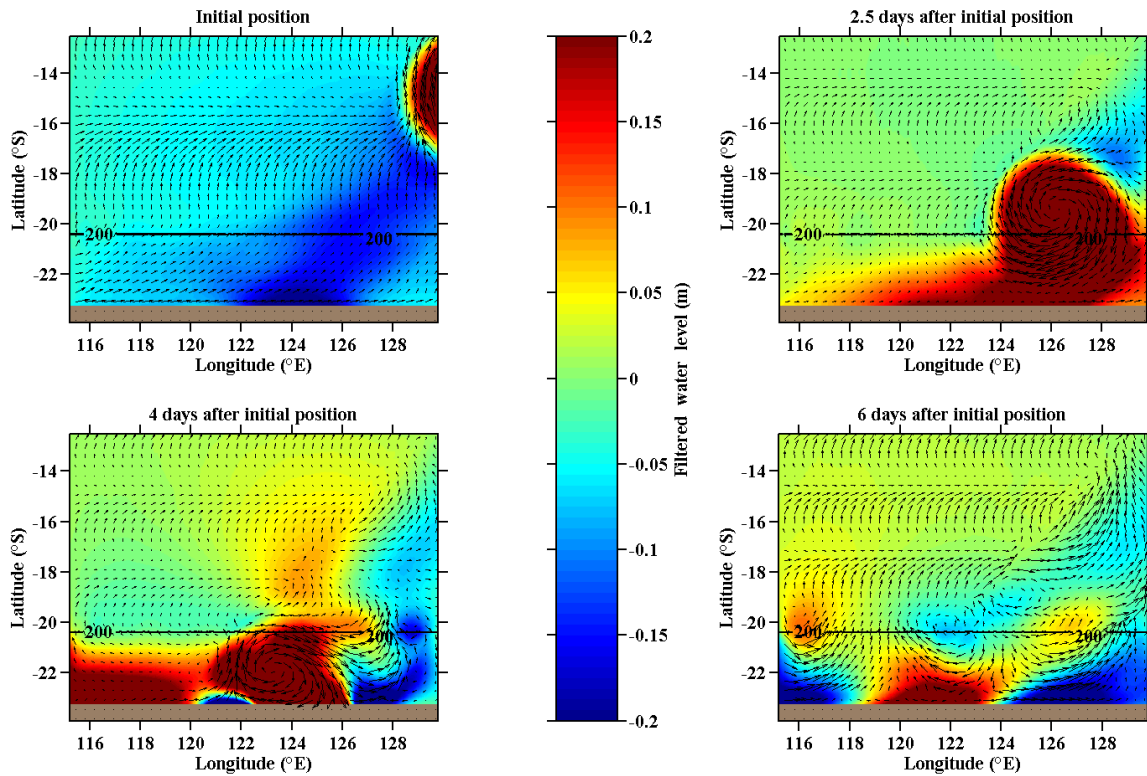


FIGURE 22 - WATER LEVELS DURING THE PASSAGE OF A CYCLONE MOVING AT A 45° TO THE COASTLINE WITH A FORWARD SPEED OF 5.6 MS⁻¹. SURFACE VELOCITY VECTORS ARE ALSO SHOWN.

A comparison of the CSW height and propagation speed, along with CSW minimum and maximum amplitudes for the model simulation runs of 45° cyclones are shown in Figure 23. Once again, the model simulations show that the CSW height is dominated by the high water that is generated from the cyclone, rather than the low water which occurred ahead of the cyclone. The CSW height ranged between 0.68 m and 0.26 m depending on the cyclone forward speed. The height of the CSW generated by 45° cyclones is much less than the CSW heights generated by the tropical cyclones that moved parallel to the coastline at 19°S, across the whole model domain, with the same forward speeds. The two tropical cyclones that travelled the slowest (1.4 ms⁻¹ and 2.43 ms⁻¹) generated the highest CSW height. The CSW height then started to rapidly decline when the cyclone forward speed was 3.5 ms⁻¹, 4.51 ms⁻¹ and 5.6 ms⁻¹. When the cyclone had forward speeds of either 7.64 ms⁻¹, 10 ms⁻¹, 14.4 ms⁻¹ or 20 ms⁻¹ the CSW height was on average, 0.28 m.

The propagation speed of the CSW was slightly more complex, ranging from 11 ms⁻¹ to 23.5 ms⁻¹. The two tropical cyclones that travelled the fastest generated CSWs with propagation speeds of 23.5 ms⁻¹. Cyclones that travelled between 1.4 ms⁻¹ to 10 ms⁻¹ generated CSWs that had propagation speeds of either 11 ms⁻¹ or 15.1 ms⁻¹ unrelated with the cyclone's forward speed.

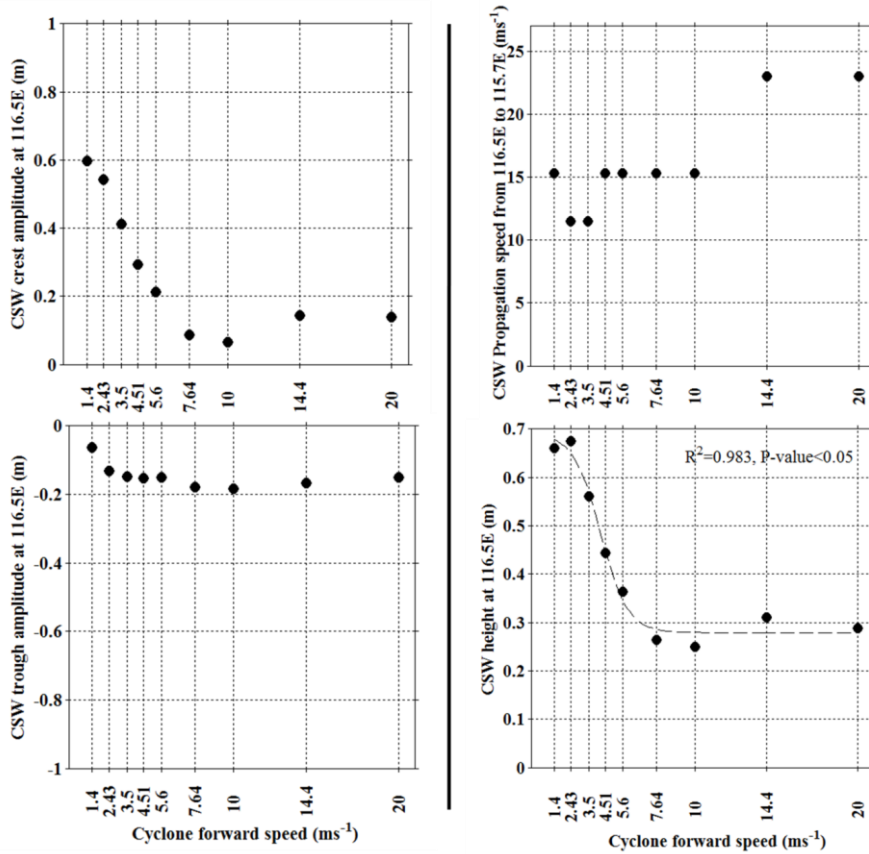


FIGURE 23 - CSW MAXIMUM AMPLITUDE (TOP LEFT), MINIMUM AMPLITUDE (BOTTOM LEFT), PROPAGATION SPEED (TOP RIGHT) AND WAVE HEIGHT (BOTTOM RIGHT) FOR EACH MODEL SIMULATION PERFORMED WITH A 45° CYCLONE TRAVELLING WITH A DIFFERENT FORWARD SPEED.

Perpendicular cyclones with different speeds

Perpendicular cyclones, similar to other simulations, displayed an initial decrease in water level along the cyclone path for all cyclone forward speeds (Figure 24). Low water was most pronounced for the slowest travelling cyclones. As the tropical cyclone moved over the continental shelf, high water increased in magnitude and moved from under the cyclone gyre of high water to the west (left) of the cyclone, and continued moving west. As the perpendicular travelling cyclone made landfall, a zone of low water separated the two high water bodies. The high water from underneath the cyclone moved to the east (right) of the model grid. Water levels show this high water that moved to the east (right) of the model domain, as a small amplitude wave. This wave was most pronounced for cyclones that had fast forward speeds (10 ms⁻¹, 14.4 ms⁻¹ and 20 ms⁻¹). When the cyclone had made landfall, oscillations of low and high water occurred along the coastline, which corresponded to high and low water eddies at the 200 m depth contour. These moved to the west (left) of the model domain and were most defined for the tropical cyclones that travelled slowest (1.4 ms⁻¹ to 7.64 ms⁻¹). These dominated any small amplitude wave travelling in the opposite direction. The eddies and high and low water level oscillations to the west (left) became less dominant when the tropical cyclone travelled fast (10 ms⁻¹, 14.4 ms⁻¹ and 20 ms⁻¹) and the wave travelling in the opposite direction (east, right) was more dominant.

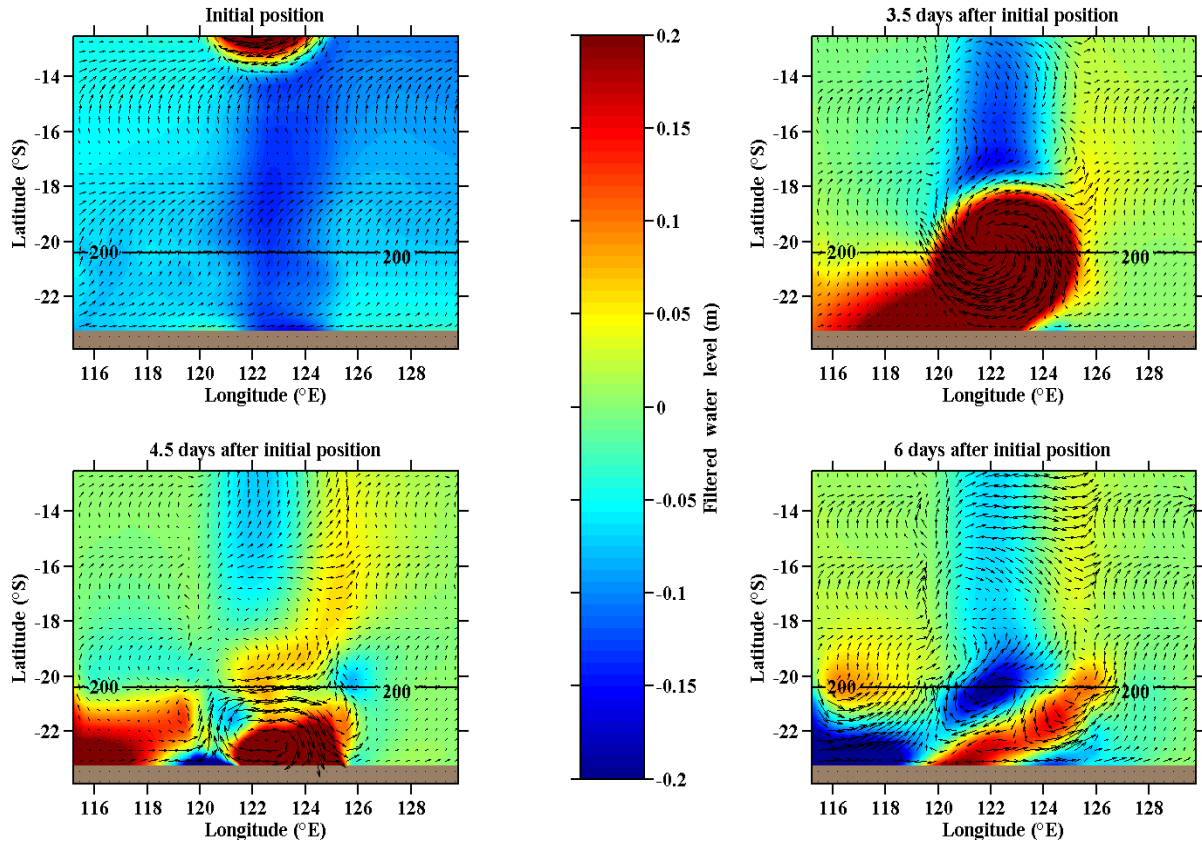


FIGURE 24 - WATER LEVELS DURING THE PASSAGE OF A CYCLONE MOVING PERPENDICULAR TO THE COASTLINE WITH A FORWARD SPEED OF 3.5 MS⁻¹. SURFACE VELOCITY VECTORS ARE ALSO SHOWN.

The high water that moved to the east (right) of the model domain was further investigated for each simulation run by plotting the wave height and propagation speed of this wave (Figure 25). The high water that travelled in the opposite direction to the CSW travelled very fast. When the cyclone forward speed was between 1.4 ms⁻¹ and 5.6 ms⁻¹ the wave had a propagation speed of 23.5 ms⁻¹ and the wave height was very small and less than 0.06 m. When the cyclone forward speed increased and travelled 7.64 ms⁻¹, 10 ms⁻¹, 14.4 ms⁻¹ or 20 ms⁻¹, the propagation speed of the wave was 42 ms⁻¹. The wave height also increased significantly within the range of 0.13 m and 0.16 m when the cyclone had the forward speeds of either 10 ms⁻¹, 14.4 ms⁻¹ or 20 ms⁻¹.

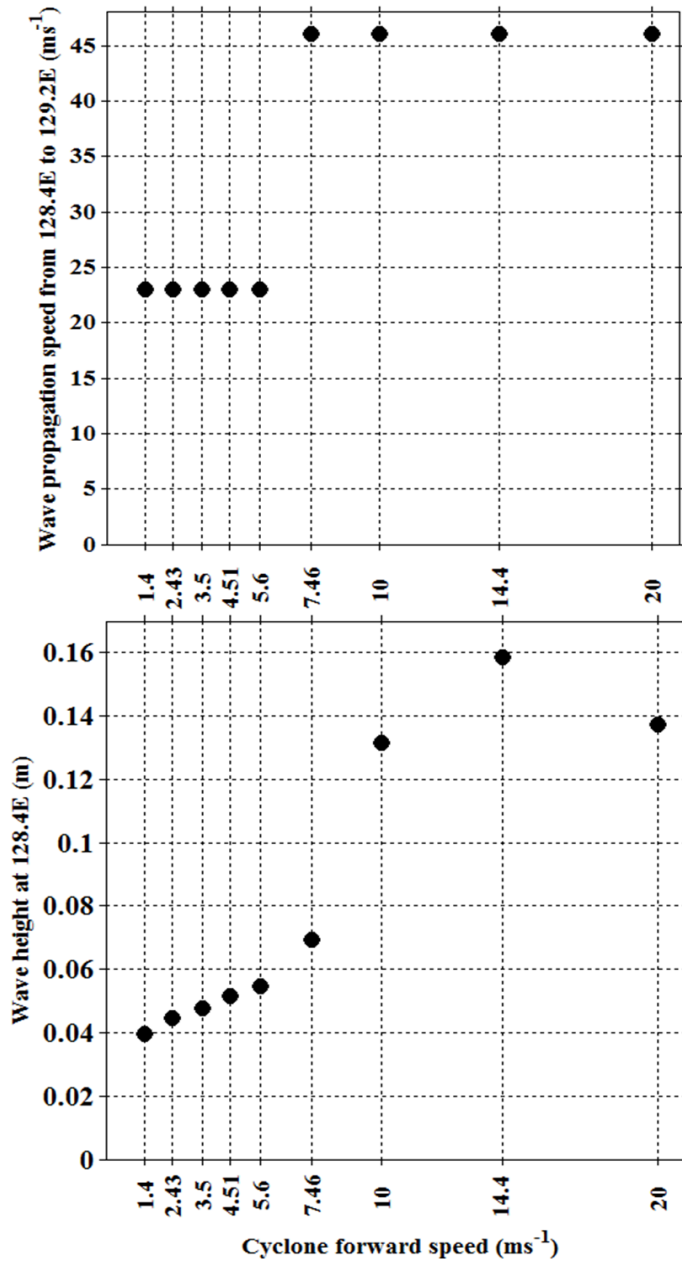


FIGURE 25 - PROPAGATION SPEED AND HEIGHT OF A WAVE THAT TRAVELLED IN AN OPPOSITE DIRECTION TO THE CSW FOR A CYCLONE THAT MADE LANDFALL PERPENDICULAR TO THE COASTLINE. THE CYCLONE FORWARD SPEED VARIED WHILE ALL OTHER PARAMETERS WERE KEPT CONSTANT.

The results show that the high water component of the CSW is the most determining factor of the CSW height (Figure 26). The CSW height ranged between 0.2 m and 0.53 m, which is much less than the CSW heights that have been generated by parallel or perpendicular cyclones. The maximum CSW of ~ 0.5 m occurred when the cyclone travelled at the slowest speeds (i.e. 1.4 ms⁻¹ and 2.43 ms⁻¹). The CSW then rapidly decreased in height when the cyclone forward speed decreased to 3.5 ms⁻¹, 4.51 ms⁻¹ and 5.6 ms⁻¹. When the cyclone had faster forward speeds of 7.64 ms⁻¹, 10 ms⁻¹, 14.4 ms⁻¹ or 20 ms⁻¹ the CSW height was ~ 0.21 m.

Similar to the 45° cyclones, the propagation speed of the CSW was slightly more complex (Figure 26). The propagation speed of the CSW decreased when the tropical cyclone speed increased from 1.4 ms⁻¹ to 4.51 ms⁻¹. The CSW

propagation speed of the wave was 15.5 ms⁻¹ when the cyclone travelled 1.4 ms⁻¹, 5.6 ms⁻¹ or 7.64 ms⁻¹. When the cyclone travelled with the fastest forward speeds (i.e. 10 ms⁻¹, 14.4 ms⁻¹ or 20 ms⁻¹) the CSW propagation speed was a fast 23.5 ms⁻¹.

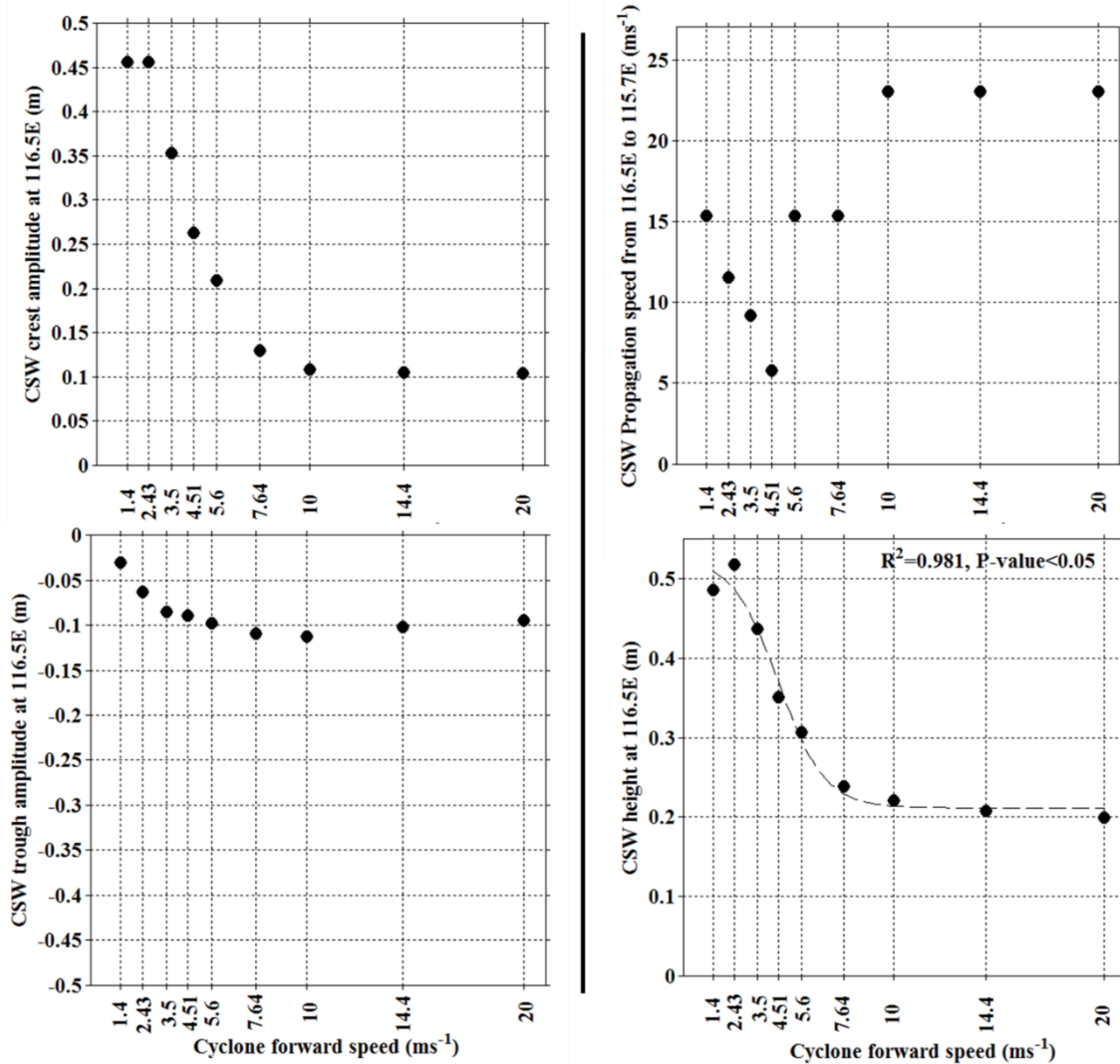


FIGURE 26 - CSW MAXIMUM AMPLITUDE (TOP LEFT), MINIMUM AMPLITUDE (BOTTOM LEFT), PROPAGATION SPEED (TOP RIGHT) AND WAVE HEIGHT (BOTTOM RIGHT) FOR EACH MODEL SIMULATION PERFORMED WITH A PERPENDICULAR CYCLONE TRAVELLING WITH A DIFFERENT FORWARD SPEED.

Regional scale modelling of CSWs

There were five tropical cyclone events that occurred in the summer of 2011. Only two of these events, Tropical Cyclones Bianca and Carlos, showed evidence of a CSW in measured tide gauge data. The CSW heights generated by Tropical Cyclones Bianca and Carlos were determined from the measured tide gauge locations along the WA coastline. The arrival of the CSW for both Tropical Cyclone Bianca and Carlos was first depicted by low water and then high water at the measured data locations. The CSWs shown in the tide gauge data was then compared to the model results.

Tropical Cyclone Bianca

Measured data of a CSW generated by Tropical Cyclone Bianca showed the wave amplitude gradually decrease from its generating region of Port Hedland

right through to Thevenard (Figure 27). Maximum CSW height occurred at Geraldton. The amplitude of the wave significantly decreased between Port Geographe and Albany. The low water level component of the CSW was small at Albany, Bremer Bay, Esperance and Thevenard. High water levels of the CSW at all locations lasted approximately 2 days.

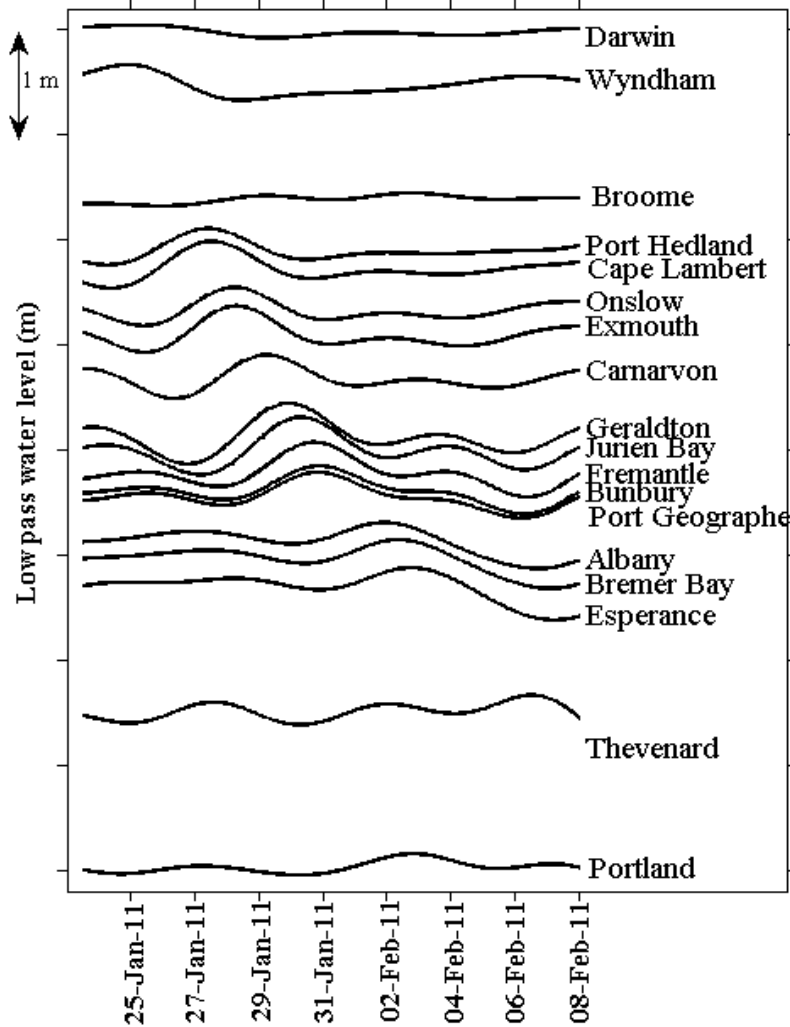


FIGURE 27 - WATER LEVELS ALONG THE WA COASTLINE, INCLUDING THE CSW GENERATED BY TROPICAL CYCLONE BIANCA. THE DIFFERENT SPACING BETWEEN THE LOCATIONS REPRESENT THE DISTANCE BETWEEN THE LOCATIONS.

The measured data compared to the Australia-wide model via skill level analysis showed similarities and differences with the same CSW. From skill level analysis, the arrival of the CSW maximum peak in the model did not occur at the same time as the measured data, thus resulting in low skill levels at Port Hedland, Carnarvon and Albany (Figure 28). The Australia-wide model was not able to define very specifically the low water and then high water of the CSW which was evident in the measured data. The Australia-wide model over predicted the maximum amplitude of the wave at Carnarvon, Geraldton and Fremantle. The CSW minimum amplitude was under predicted at most of the locations except Fremantle and Albany where it over predicted the minimum amplitude of the CSW. In general, the high water of the CSW in the Australia-wide model occurred over a longer time period than in the measured data. However, an important model result is that the CSW was identified as moving down the WA coastline.

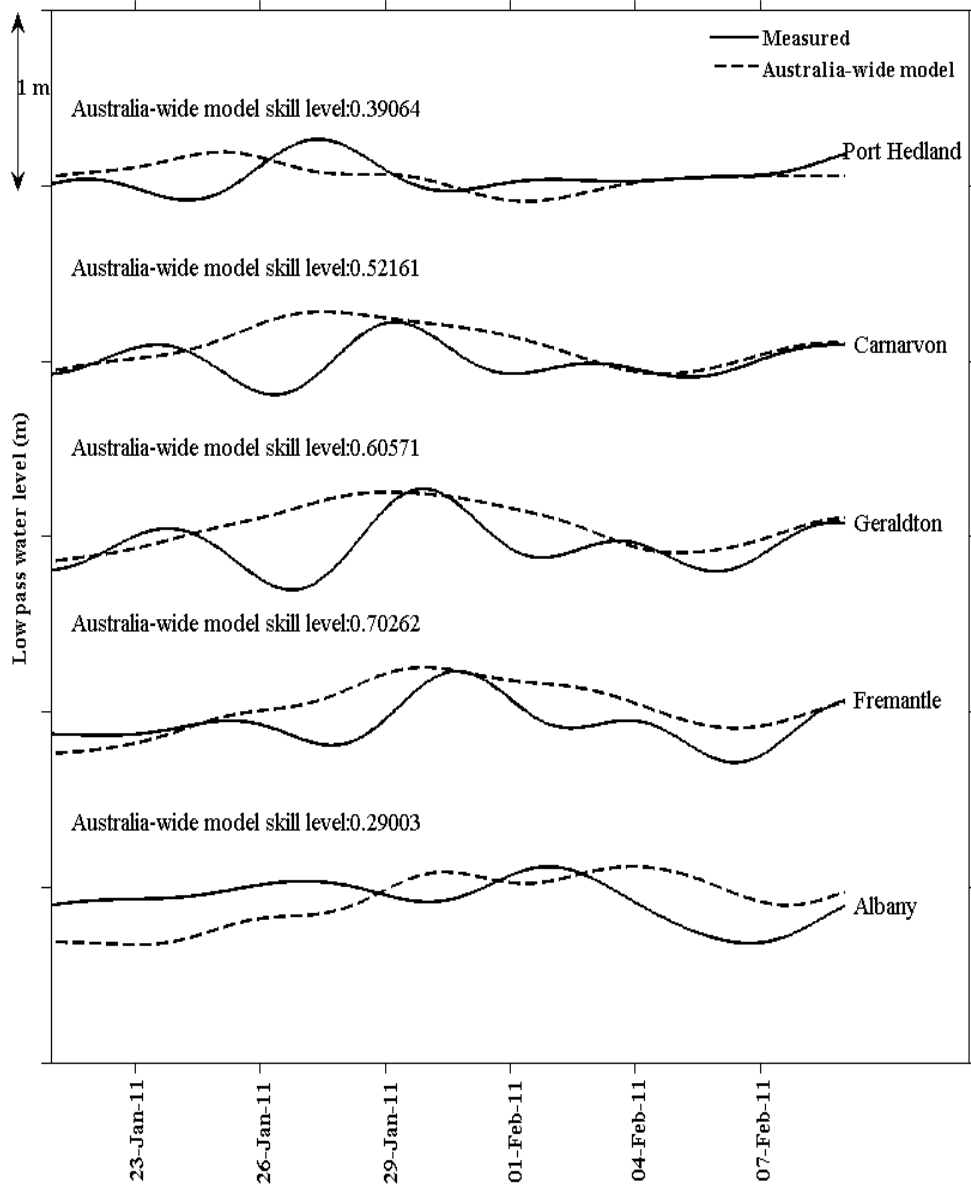


FIGURE 28 - AUSTRALIA-WIDE MODEL AND MEASURED RESULT OF THE CSW GENERATED BY TROPICAL CYCLONE BIANCA.

A comparison of CSW height of the Australia-wide model with the measured data generated by Tropical Cyclone Bianca showed that the model performed well (Figure 29). The calculated trendline comparing the two data sets shows that there is only a small difference, with the modelled data under-predicting at some locations (Figure 29).

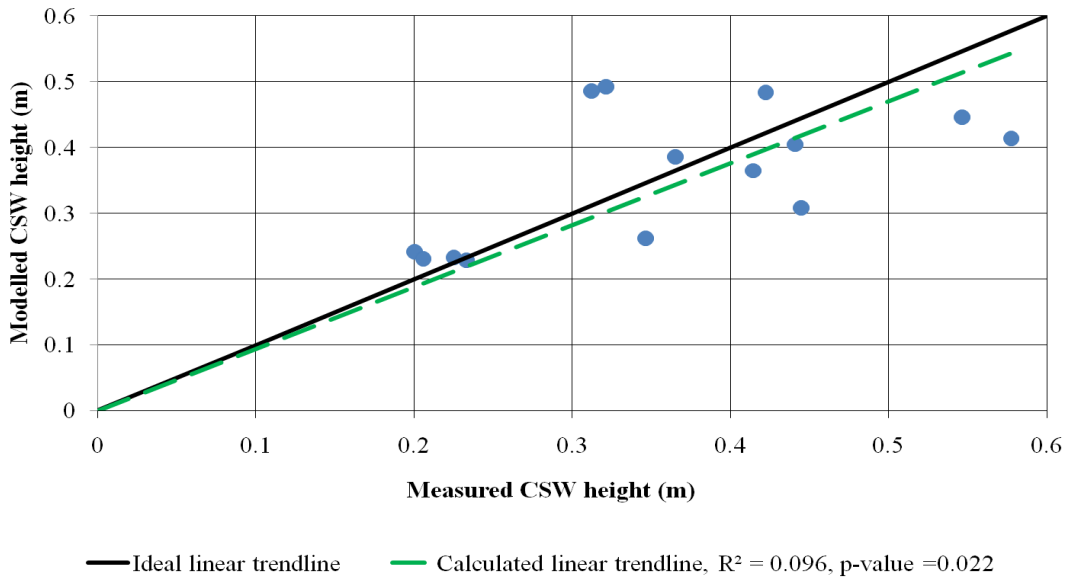


FIGURE 29 - MODELLED CSW HEIGHT AGAINST MEASURED CSW HEIGHT GENERATED BY TROPICAL CYCLONE BIANCA.

Given that the arrival of the CSW in the modelled data did not match up consistently with the arrival of the CSW in the measured data, a comparative analysis of the arrival of the maximum peak of the wave was performed by creating a lag correlation plot for both data sets (Figure 30). The propagation speed of the wave was then compared between the measured and modelled data at selected locations (Table 3). In general, measured and modelled data produced similar results in terms of CSW propagation speed between locations (Figure 30). Both data sets showed a decrease in CSW speed between the locations Exmouth to

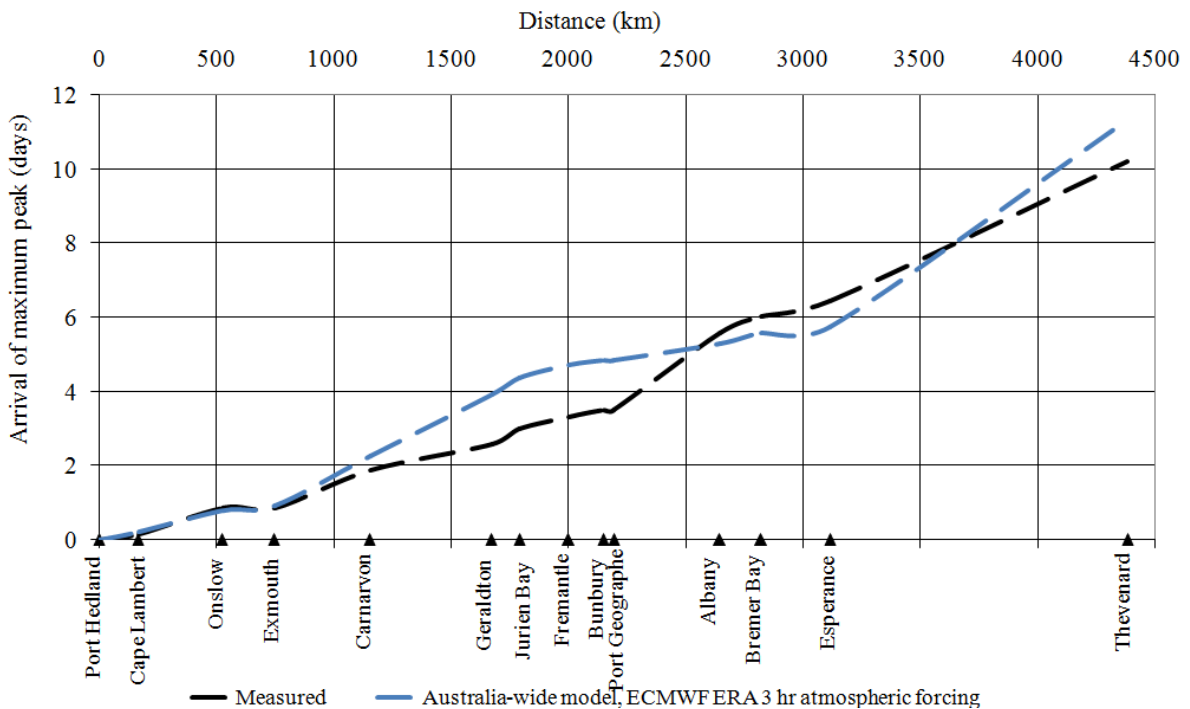


FIGURE 30 - LAG CORRELATION PLOT OF THE ARRIVAL OF THE MAXIMUM PEAK OF THE CSW GENERATED BY TROPICAL CYCLONE BIANCA.



Carnarvon and Port Geographe to Albany. The speed of the CSW increased between Carnarvon to Geraldton and Esperance to Thevenard, but only in the measured data. Between Geraldton and Port Geographe, the modelled and measured CSWs travelled at the same speed (6.6 ms⁻¹). A linear trendline using the lag correlation plot, of the CSW distance with arrival of maximum peak was calculated to determine the CSW average speed. The CSW generated by the tropical cyclone had on average, a speed of 5.8 ms⁻¹ (p-value < 0.01).

TABLE 3 - AVERAGE PROPAGATION SPEEDS BETWEEN SELECTED LOCATIONS OF THE CSW GENERATED BY TROPICAL CYCLONE BIANCA.

Locations	Measured speed (ms ⁻¹)	Australia wide model speed (ms ⁻¹)
Port Hedland to Onslow	7	7.7
Exmouth to Carnarvon	4.71	3.5
Carnarvon to Geraldton	8.5	3.6
Geraldton and Port Geographe	6.6	6.6
Port Geographe to Albany	2.5	5.2
Esperance to Thevenard	3.9	2.6

The measured data and modelled data also depicted changes to the CSW height as it propagated down the coastline of WA (Figure 31). In the measured data, the wave height peaked at Cape Lambert, Exmouth and reached a maximum of 0.58 m at Geraldton. The CSW height decreased at Onslow and Carnarvon, with a significant decrease in wave height occurring between Jurien Bay and Albany. At Fremantle, the CSW height was 0.42 m. The CSW maintained a steady wave height between 0.20 m - 0.23 m when travelling from Albany and Thevenard.

In the modelled data, the results showed an increase in the CSW between Port Hedland to Exmouth, before the wave height decreased to a minimum at Carnarvon (Figure 31). A maximum peak wave height of 0.49 m occurred at Bunbury, and not at Geraldton, where the maximum peak occurred in the measured data. At Fremantle, the model estimated the CSW height as 0.48 m. The wave height then rapidly decreased to 0.24 m at Albany. Between Albany and Thevenard, the CSW's height hovered around a steady 0.23 m.

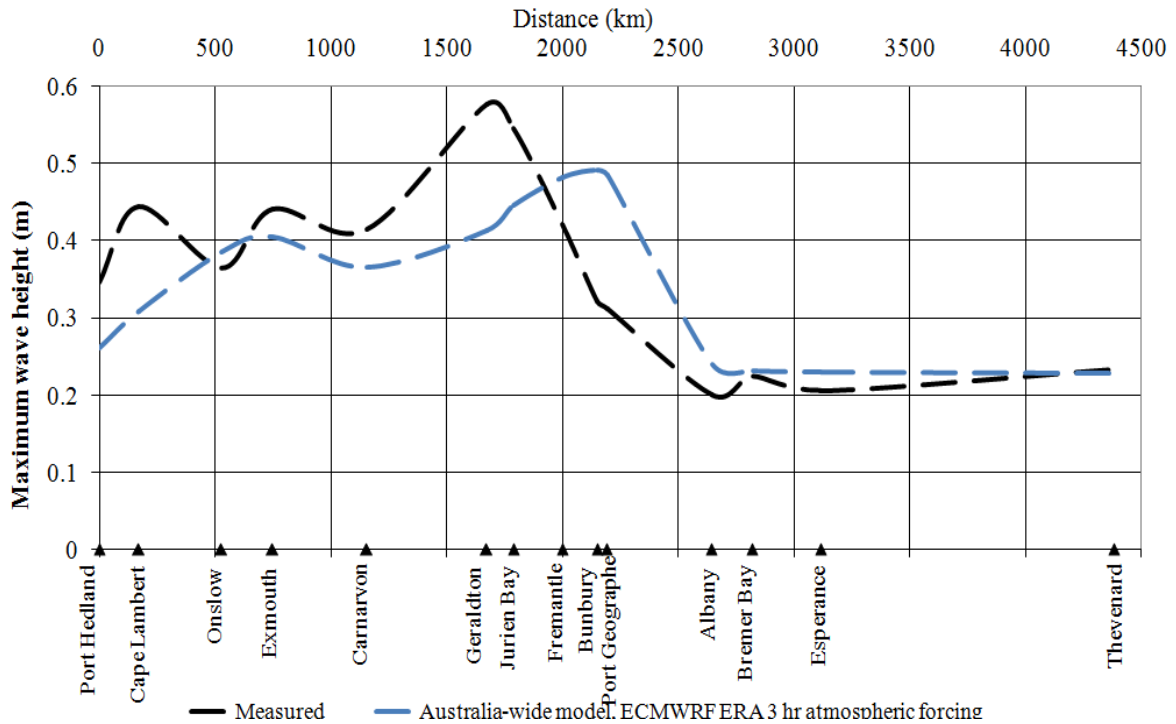


FIGURE 31 - MAXIMUM CSW HEIGHT GENERATED BY TROPICAL CYCLONE BIANCA IN 2011.

Spatial plots over both 20 days and individual days of the CSW generated by Tropical Cyclone Bianca depicts the CSW trapped along the coastline, up to the 200 m depth contour (Figure 32 and Figure 33). Initially, the water levels along the coastline, below latitude 22°S, experienced a decrease in water level greater than 0.05 m. WA and southern WA coastal waters below 30°S experienced a decrease in water level between 0.2 m - 0.3 m. This low water was relative up to the 200 m depth contour. High water then formed along the NWS, up to about the 200 m depth contour. This high water extended along the NWS as a CSW which then travelled southwards along the coast. In the Exmouth Gulf, the water became trapped but moved southwards after a few days. The CSW then moved around Exmouth Gulf moving over a very narrow continental shelf. The CSW did not exceed past the 200 m depth contour and continued moving southwards, increasing the water levels in Shark Bay (~ 25° S). Both the Exmouth Gulf and Shark Bay experienced the greatest increase in water levels by at least 0.3 m. The CSW then continued to move south, hugging the coastline. The CSW curved around the coastline at 34°S (Capes Region) with some of the water moving offshore. The wave then continued travelling east along the coast to Thevenard. CSW amplitudes remained about 0.2 m above mean surface water levels all the way to Thevenard.

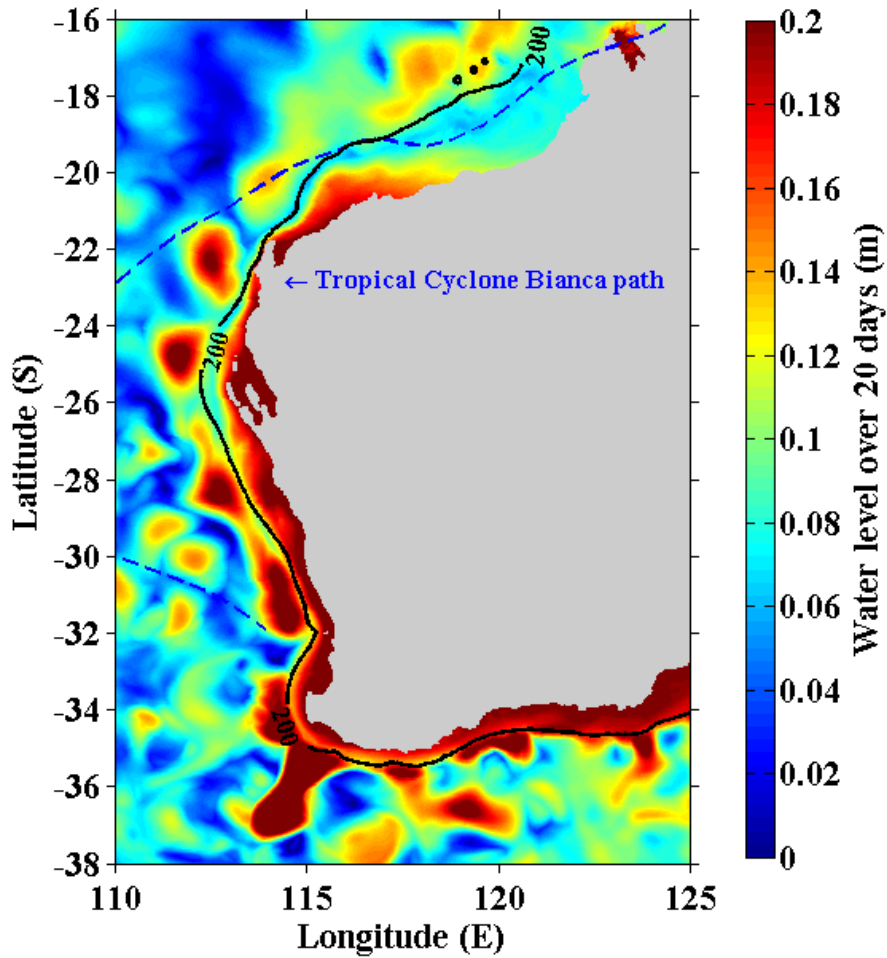


FIGURE 32 - SPATIAL PLOT OVER 20 DAYS OF THE MAXIMUM WATER LEVELS FROM THE AUSTRALIA-WIDE MODEL. THE FIGURE SHOWS THE CSW GENERATED BY TROPICAL BIANCA, WHICH TRAVELS INSIDE THE 200 M DEPTH CONTOUR.

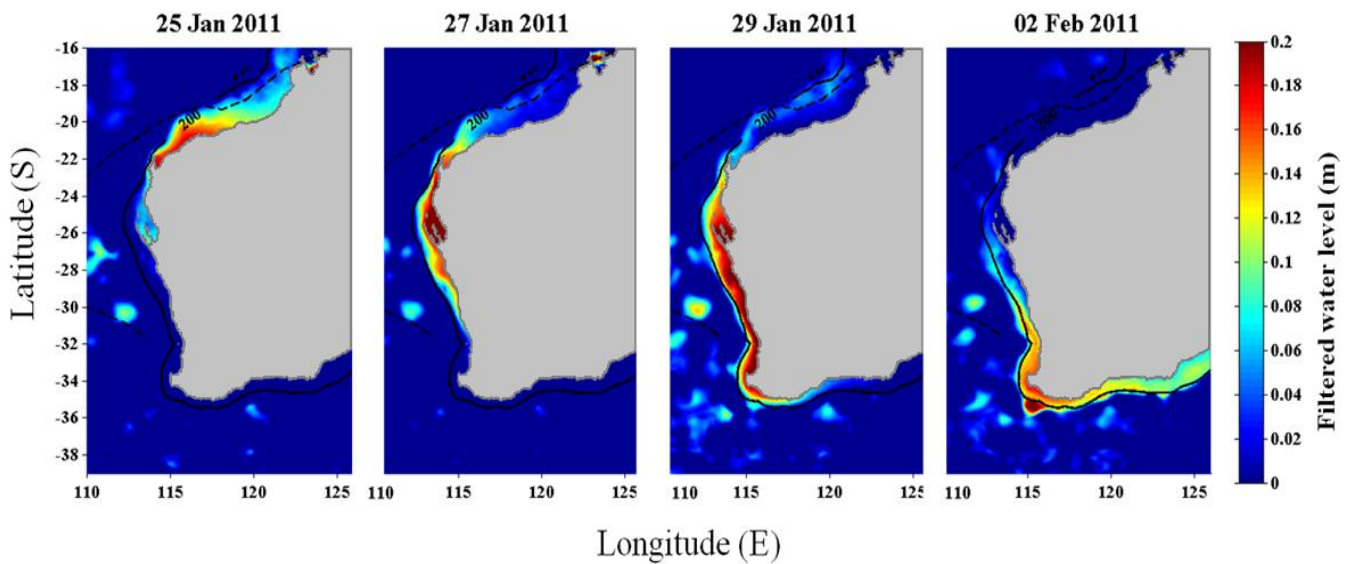


FIGURE 33 - SPATIAL PLOT OF THE CSW GENERATED BY TROPICAL CYCLONE BIANCA OVER FOUR DIFFERENT DAYS.

Tropical Cyclone Carlos

The measured tide gauge data shows the CSW generated by Tropical Cyclone Carlos (Figure 34). The amplitude of the wave gradually decreased from its generating region of Port Hedland right through to Port Geographe. CSW heights were recorded as approximately 0.3 m, before peaking at Onslow and then decreasing at Jurien Bay. The amplitude of the CSW increased further south at Fremantle, Bunbury and Port Geographe.

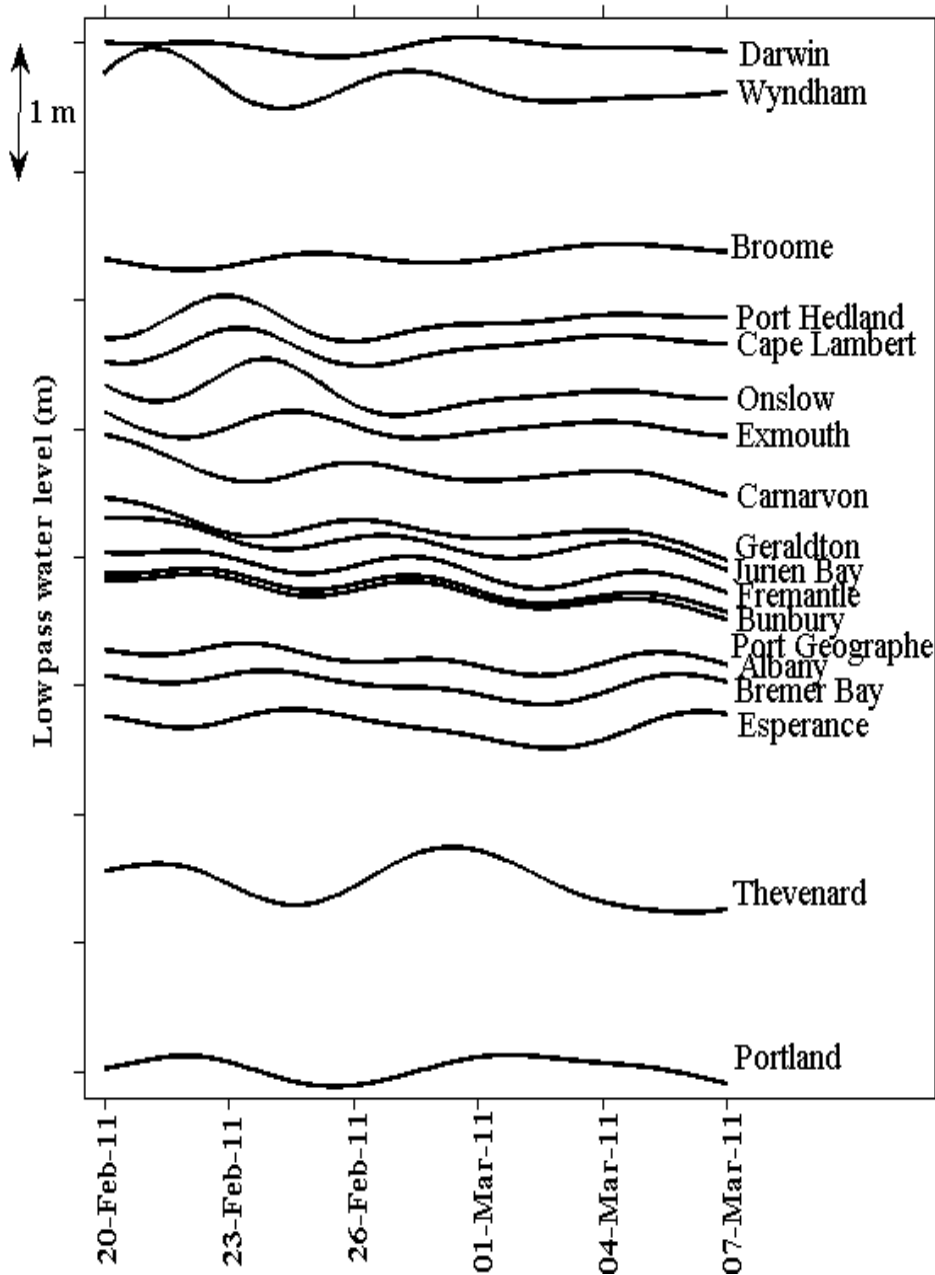


FIGURE 34 - WATER LEVELS ALONG THE WA COASTLINE, INCLUDING THE CSW GENERATED BY TROPICAL CYCLONE CARLOS.

Further analysis of the CSW generated by Tropical Cyclone Carlos was conducted with the Australia-wide model simulation results and comparisons made to the measured data via skill analysis (Figure 35). Results show that the arrival of the CSW in the model occurred after the arrival of the CSW in the measured data, which explains the low model skill. The Australia-wide model over predicted the CSW at Exmouth and Carnarvon. In general, the CSW in the modelled data showed the CSW maintaining a steady wave height. This is quite different to the measured data which showed a decrease in water levels followed by an increase in water level over a much shorter time period of a few days. However, the Australia-wide model results showed the CSW moving southwards, along the WA coastline.

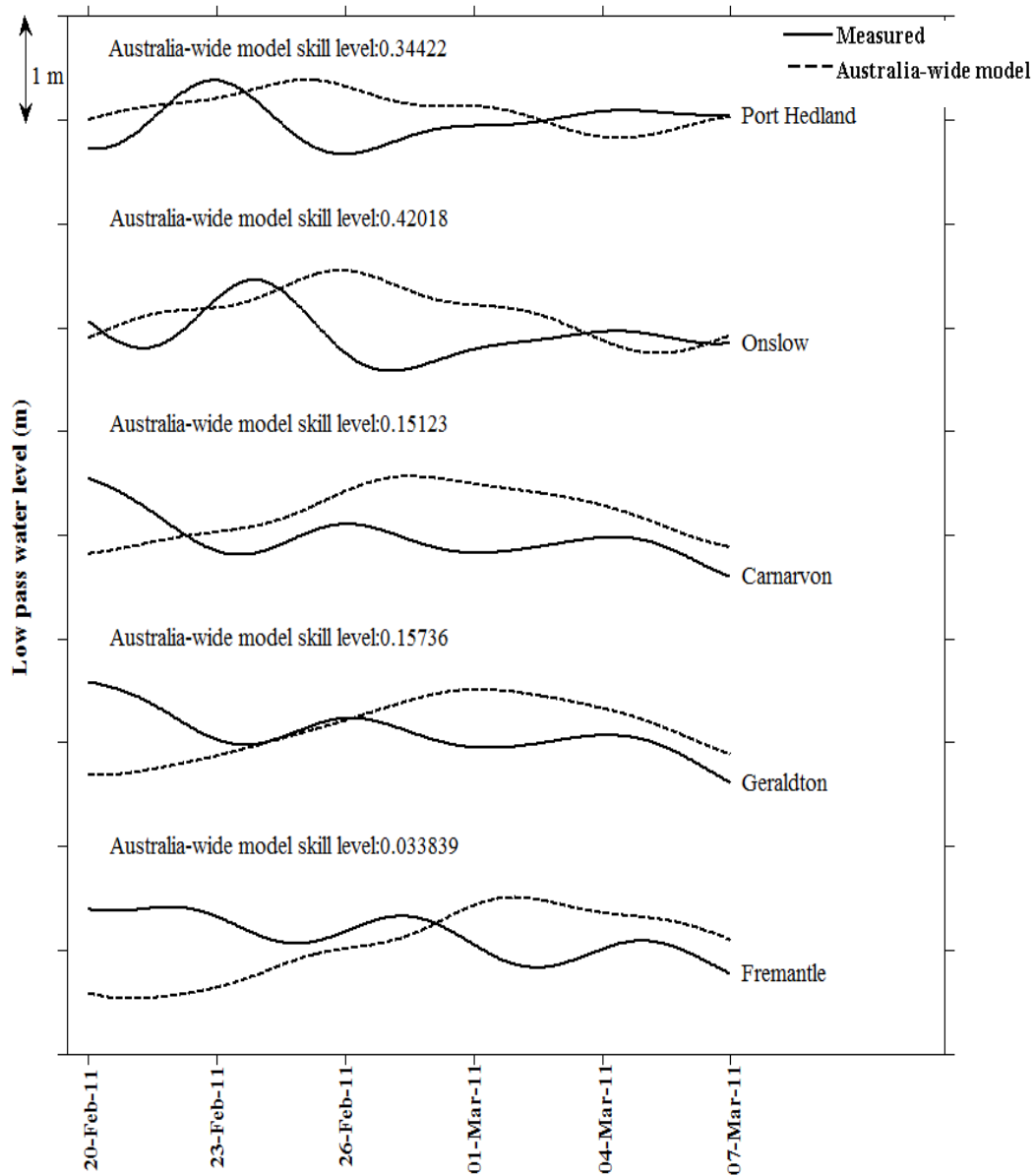


FIGURE 35 - AUSTRALIA-WIDE MODEL AND MEASURED DATA RESULTS OF THE CSW GENERATED BY TROPICAL CYCLONE CARLOS.



A comparison of the CSW's height from the Australia-wide model with the measured data generated by Tropical Cyclone Carlos shows that the model wave heights do not change very much at the different locations. The Australia-wide model predicts the CSW to be approximately 0.25 m in wave height at all locations, whereas the CSW heights in the measured data ranged between 0.13 to 0.33 m at the different locations. The calculated linear trendline showed that the Australia-wide model does not predict the CSW very well when compared with the measured data.

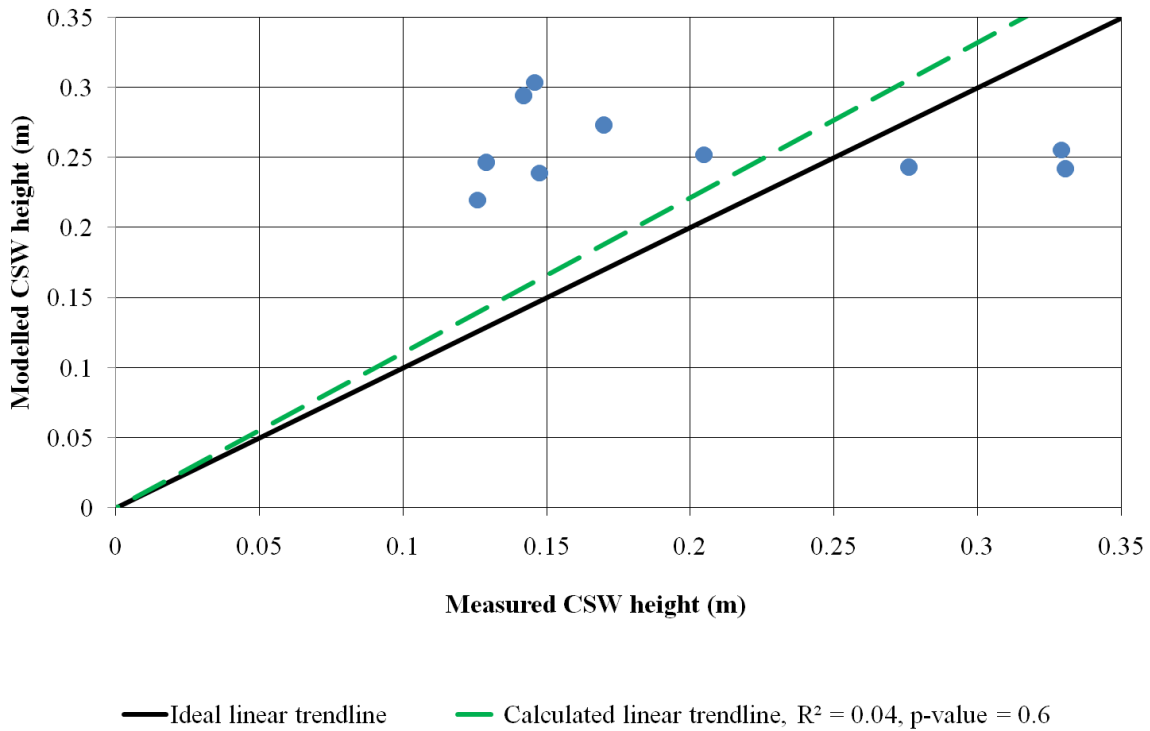


FIGURE 36 - MODELLED CSW HEIGHT AGAINST MEASURED CSW HEIGHT GENERATED BY TROPICAL CYCLONE CARLOS.

A lag correlation plot of both the measured and the Australia-wide model results show that the CSW travels much more quickly in the model (Figure 37). Table 4 summarises the average speed of the wave between two locations and the comparison with the measured and modelled data. Although the modelled data and measured data did not have the same CSW propagation speed, the two data sets both show similar trends. For example, between Port Hedland and Onslow, the wave travelled 6.6 ms⁻¹ in the measured data and 7 ms⁻¹ in the modelled data. Between Exmouth and Carnarvon, the CSW speed decreased to 3 ms⁻¹ in the measured data and 4 ms⁻¹ in the modelled data. The CSW then increased in speed between Carnarvon and Geraldton. Between Geraldton and Jurien Bay the CSW decreased in speed before increasing between Jurien Bay and Port Geographe.

A linear trendline of the CSW distance with arrival of maximum peak was also calculated for both the modelled and measured results for Tropical Cyclone Carlos from the lag correlation plot to calculate the average CSW propagation speed. The linear trendline generated for Tropical Cyclone Carlos from the measured data produced an R² value of 0.963 (p-value < 0.01) and a CSW



propagation speed of 5.8 ms⁻¹. The linear trendline for Tropical Cyclone Carlos from the modelled data produced an R² value of 0.963 (p-value < 0.01) and a CSW propagation speed also of 5.8 ms⁻¹.

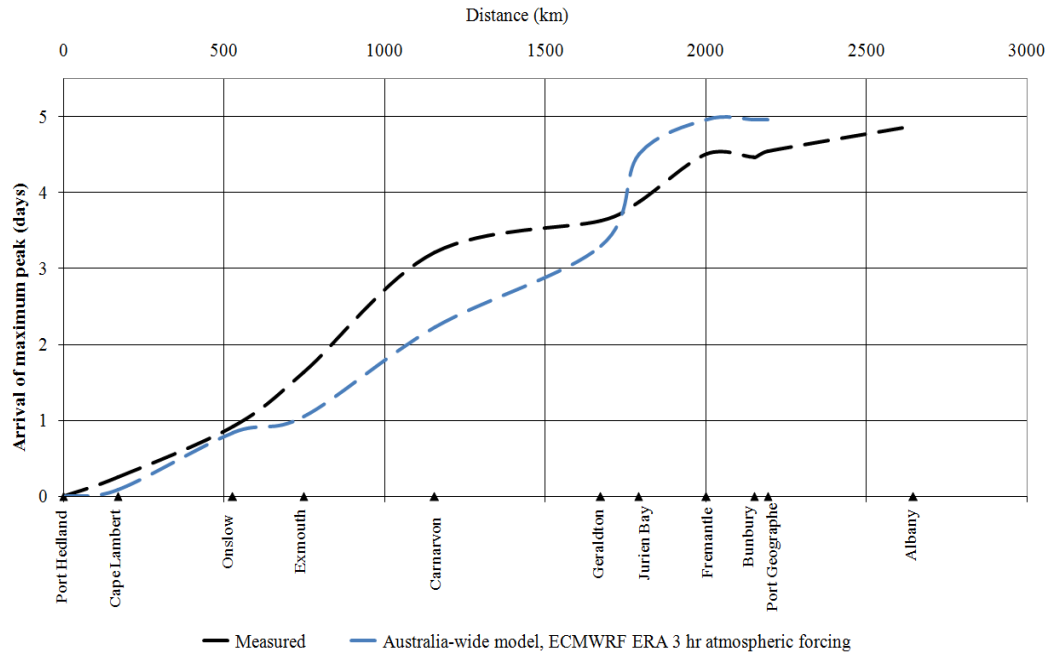


FIGURE 37 - LAG CORRELATION PLOT OF THE ARRIVAL OF THE MAXIMUM PEAK FOR THE CSW GENERATED BY TROPICAL CYCLONE CARLOS.

TABLE 4 - AVERAGE PROPAGATION SPEEDS BETWEEN SELECTED LOCATIONS OF THE CSW GENERATED BY TROPICAL CYCLONE CARLOS.

Locations	Measured speed (ms ⁻¹)	Australia-wide model speed (ms ⁻¹)
Port Hedland to Onslow	6.6	7.3
Exmouth to Carnarvon	3	4
Carnarvon to Geraldton	14.4	5.6
Geraldton and Jurien Bay	5.5	1.1
Jurien Bay to Port Geographe	7	10.1

The maximum CSW height at each of the measured data locations shows that the CSW height decreases by 0.055 m between Port Hedland and Cape Lambert in the measured data (Figure 38). The CSW height then returned to the same height of 0.3 m when it at Port Hedland,. Between Onslow and Geraldton the CSW then gradually decreased in height to 0.13 m. The CSW height continued to decrease but there was an increase in CSW height at Fremantle. In the Australia-wide model results, the CSW height remained around 0.25 m for all locations, between Port Hedland and Geraldton. The wave did not seem to decrease in height except at Jurien Bay (Figure 38). The CSW then increased in height between Fremantle and Port Geographe. It is difficult to identify the CSW in the modelled data at Albany.

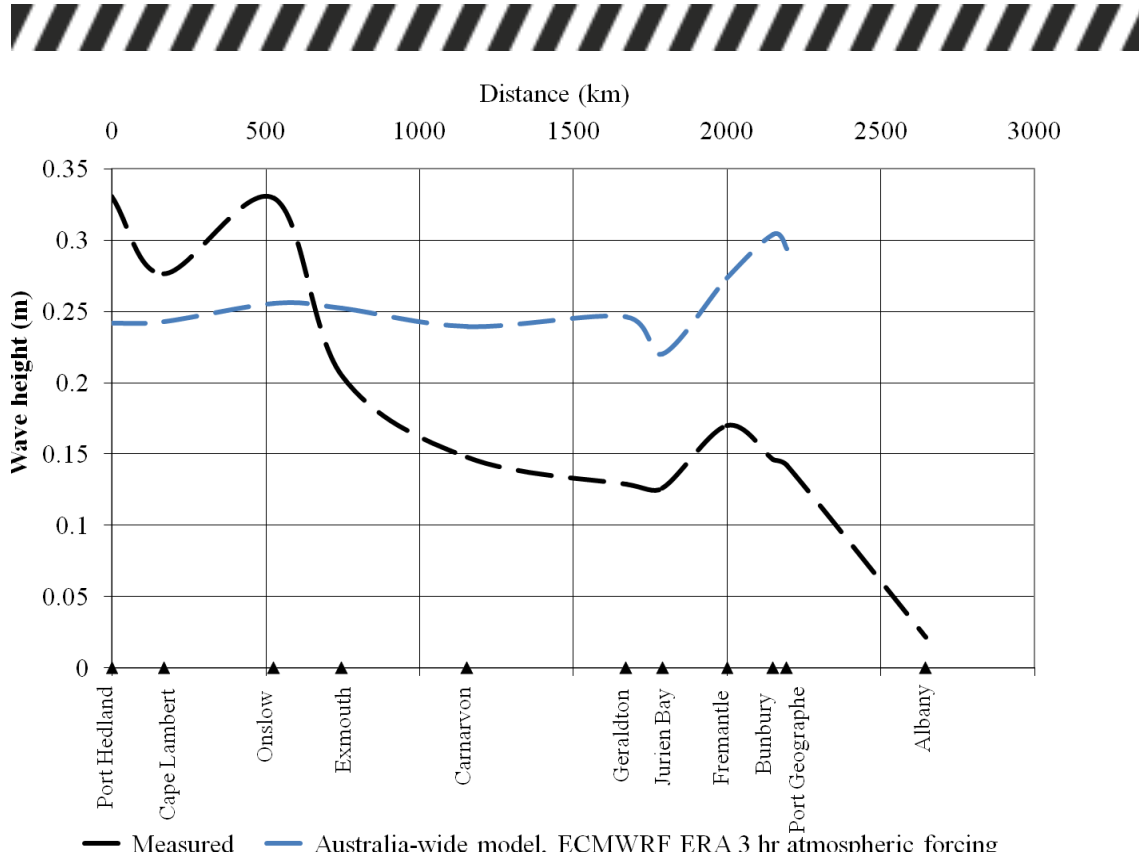


FIGURE 38 - MAXIMUM CSW HEIGHT GENERATED BY TROPICAL CYCLONE CARLOS IN 2011.

Spatial plots of the model results of the CSW generated by Tropical Carlos confirmed that the CSW only maintained wave heights greater than 0.1 m above the latitude of 34°S (Figure 39 and Figure 40). The CSW was generated on the NWS where the maximum amplitude of the wave occurred along the coastline. Waters from the CSW become trapped in Exmouth Gulf but then travelled around the Gulf, between the coastline and the 200 m depth contour. The CSW moved into Shark Bay, where this whole region of WA experienced water levels greater than 0.1 m. The CSW moved further south all the way to Port Geographe. Water levels greater than 0.2 m did not occur around the Capes Region and it was difficult to identify the CSW in both the measured and modelled data in southern WA locations such as Albany, Bremer Bay and Esperance.

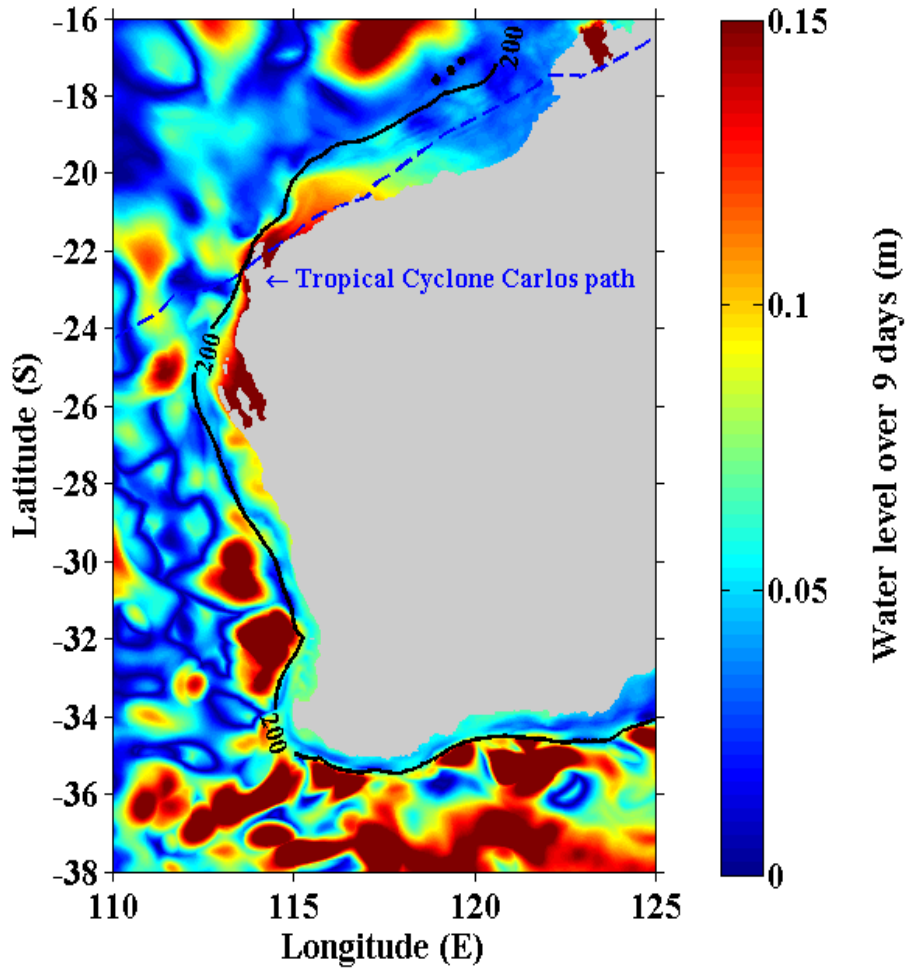


FIGURE 39 - SPATIAL PLOT OVER 9 DAYS OF MAXIMUM WATER LEVELS FROM THE AUSTRALIA-WIDE MODEL. THE FIGURE SHOWS THE CSW GENERATED BY TROPICAL CYCLONE CARLOS, WHICH TRAVELS WITHIN THE 200 M DEPTH CONTOUR.

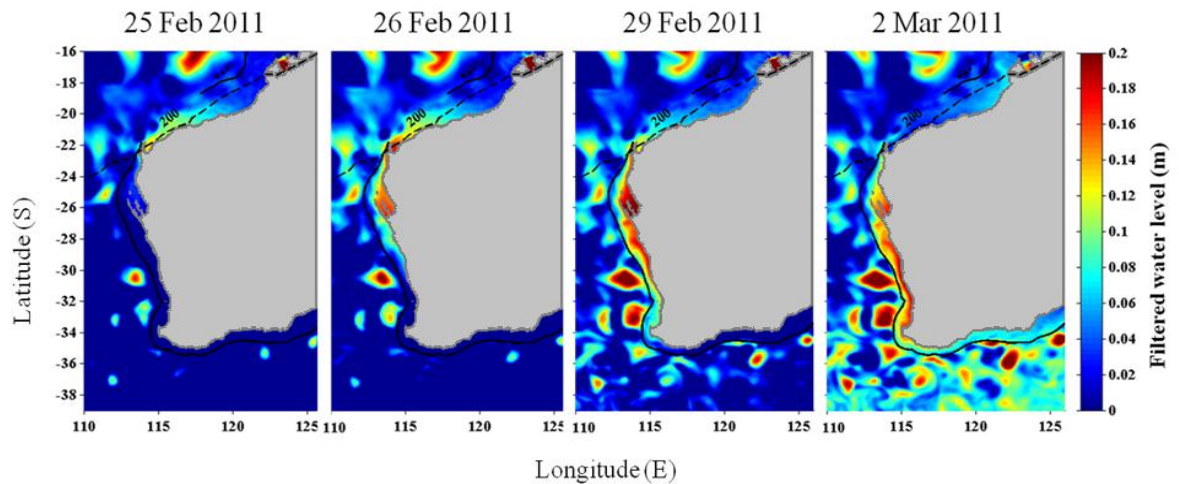


FIGURE 40 - SPATIAL PLOT OF THE CSW GENERATED BY TROPICAL CYCLONE CARLOS OVER FOUR DIFFERENT DAYS.

DISCUSSION AND CONCLUSIONS

Influence of cyclone incident parameters

The relationship between cyclone parameters (i.e. direction, speed and category) and the generation of CSWs has been explored in this study using an idealised model of the NWS. The NWS idealised model, using a very simple, cyclone-like, wind and pressure field was able to create CSWs, which is one of the common generating mechanisms (Tang & Grimshaw 1995). The CSW heights generated in the model were similar to observed CSW heights found in the literature, ranging in the order of centimetres (e.g. Ding, Bao & Shi 2012; Eliot & Pattiaratchi 2010; Martínez & Allen 2004). Cyclone path, speed and category were found to influence both the CSW height and propagation speed.

Perpendicular cyclones

Perpendicular moving cyclones that generated CSWs in the model were identified as an initial low moving body of water, which occurred ahead of the tropical cyclone path, followed by a westward moving body of water along the coastline. The maximum amplitude of the CSW occurred after the cyclone reached the continental shelf and then made landfall, by causing a convergence of high water along the coastline. The CSW then moved to the west in the model grid, as a "free wave" not affected by the presence of the cyclone.

Simulations also showed the generation of a wave that travelled in the opposite direction to the CSW. This wave had a propagation speed of 23 ms^{-1} and small amplitude ($< 0.06 \text{ m}$) when the tropical cyclone travelled slower ($1.4 \text{ ms}^{-1} - 5.6 \text{ ms}^{-1}$). When the cyclone forward speed was faster (i.e. $\geq 7.46 \text{ ms}^{-1}$) the wave speed increased to 42 ms^{-1} and heights ranged between 0.07 m and 0.16 m . Wave heights greater than 0.13 m occurred with cyclones travelling greater or equal to 10 ms^{-1} and this also occurred when the CSW, travelling in the opposite direction, had the lowest heights of 0.2 m . As the cyclone forward speed increased, the height of this wave also increased and can be representative of an edge wave. This is because the speed of the wave is fast, has relatively quick decay and the greater heights occurred with faster cyclone forward speed because Coriolis force played less of a role. This implies that edge waves may be an important component in the ocean's response to a perpendicular moving cyclone with fast speeds. Slower moving cyclones will generate a greater build-up of water at the coast, whereas faster moving cyclones have less exposure time in the ocean basin. This greater build-up of water at the coast means that there is more time for the Coriolis force to become dominant so the generation of edge waves are diminished as they depend more on refraction and gravity and dominate over the Coriolis force (Yankovsky 2009).

CSWs in the simulations had propagation speeds that ranged between 5.1 ms^{-1} and 23.5 ms^{-1} and did not specifically show a correlation between cyclone forward speed and CSW propagation speed. CSWs, have been identified as having phase speeds (c) that scale with $c \sim fL$ and with mode 1 speeds in the range of $2 \text{ ms}^{-1} - 20 \text{ ms}^{-1}$ (Eliot & Pattiaratchi 2010; Merrifield 1992; Thiebaut & Vennell 2010). Taking typical values of the Coriolis parameter and cross shelf characteristic length scale for the NWS idealised model, gives CSW phase speeds of:

$$c = fL = 2 \times 7.2921 \times 10^{-5} \times \sin 23 \times 252 \text{ km} \times 10^3 = 14.4 \text{ ms}^{-1} \approx O(10) \text{ ms}^{-1}$$

In the idealised model the propagation speeds of the CSW were near to the CSW phase speed of 14.4 ms^{-1} and similar to the range found in literature.

Model simulations showed that CSW height decreased with increasing cyclone forward speed. This result can be explained by the fact that slower perpendicular cyclones have more time to input more energy into the CSW. There may also reach a point when a perpendicular cyclone travels too fast to generate a CSW.

Parallel cyclones

Parallel moving cyclones that generated CSWs were identified as an initial low moving body of water, which occurred ahead of the tropical cyclone path, followed by a westward moving body of high water along the coastline. Two different parallel cyclone paths were simulated:

- Parallel cyclones that moved over the whole model domain at 19°S , travelling at different speeds; and
- Parallel cyclones that moved over a quarter of the model domain at 19°S , travelling at different speeds.

Parallel cyclones that moved over the *whole* model domain generated CSWs that displayed properties which depended on the presence of the cyclone. These CSWs propagated as "forced waves". For example, CSW height increased with increased wave speed because by increasing the cyclone forward speed, the cyclone travelled more alongside the CSW. When the tropical cyclone travelled directly parallel to the CSW (i.e. forward speeds of 7.64 ms^{-1} or 10 ms^{-1}) the CSW had the greatest wave heights ($\sim 1 \text{ m}$). Parallel cyclones that travelled too fast (i.e. forward speeds 14.4 ms^{-1} and 20 ms^{-1}) generated CSWs with the lowest wave height as these CSWs trailed behind the cyclone.

As these types of CSWs move as "forced waves" they have the greatest wave heights than any of the the CSWs generated by perpendicular, 45° cyclones or the same cyclones that moved parallel but only a quarter of the way through the model domain. The greater wave height in these parallel cyclones can be explained by the phenomenon of Greenspan Resonance (Greenspan 1956). Greenspan Resonance results in amplification of the CSW because the forward speed of the cyclone is near to the CSW mode speeds (Greenspan 1956). A condition to this is that the CSW must travel less than the shallow water wave speed (Vennell 2010). A simple calculation of the shallow water wave speed gives:

$$c = (gh)^{0.5} = (9.81 \text{ ms}^{-1} \times 5.5 \text{ m})^{0.5} = 7.4 \text{ ms}^{-1}$$

where h in the idealised model approximates to an average of 5.5 m water depth along the coast. The model simulations do show that by increasing the cyclone forward speed, the CSW height also increased, but only up to cyclone forward speeds of 7.64 ms^{-1} , which is near to the calculated shallow water wave speed at the coast, before that CSW height actually decreased with increased cyclone forward speed. Other research completed shows that parallel cyclones can amplify the height of the CSW. For example, Eliot & Pattiaratchi (2010) found that cyclones in WA that travelled parallel to the coastline generated CSWs with the highest wave amplitudes. Tang & Grimshaw




(1995) and Fandry, Leslie & Steedman (1984) also confirm this result in their studies. Hence from this study and other literature, a parallel moving cyclone to the coast can play a role in amplifying a CSW height.

While Greenspan Resonance (Greenspan 1956) influences CSW height, the CSW propagation speed was also influenced by the speed of a parallel moving cyclone. Cyclones that travelled parallel over the model domain generated CSWs that were slower (i.e. 6 ms^{-1}) when the cyclone also had slower forward speeds (i.e. 1.4 ms^{-1}). CSW propagation speeds were faster (i.e. 9.2 ms^{-1}), with faster moving cyclones (i.e. 5.6 ms^{-1}) but decreased when the cyclone forward speed was 20 ms^{-1} . Yankovsky (2009) discusses how forced CSW propagation speeds relate to a parallel tropical cyclone's forward speed. He explains that CSWs do not travel at the phase velocity (i.e. 14.4 ms^{-1} for this study), but travel much slower, even though the CSW can occupy the whole shelf width. This is because a slower moving CSW fits the structure of a moving cyclone much better (Yankovsky 2009). The result from his study is confirmed in this study. The CSWs that moved faster than the tropical cyclones (i.e. 1.4 ms^{-1} - 5.6 ms^{-1} forward speeds) all travelled less than the phase velocity of 14.4 ms^{-1} . When the tropical cyclone travelled 7.64 ms^{-1} the CSW propagation speed was near to the phase velocity. Tropical cyclones that travelled faster than this ($\geq 10 \text{ ms}^{-1}$) generated waves that had propagation speeds greater than the phase velocity. This may be explained by the fact that these CSWs, once generated, trailed behind the cyclone so behaved less as a "forced wave" and more as a "free wave".

Tropical cyclones that moved over only a *quarter* of the model domain also allowed for the generation of CSWs. However, the behaviour of the wave, in terms of its propagation speed and height were studied as free waves, because the parallel cyclone ceased forcing the ocean. The results show that a CSW that was generated by a parallel moving cyclone but moved as a "free wave", developed similar propagation speed and wave height characteristics as a CSW generated by a perpendicular moving cyclone. That is, when the cyclone forward speed increased, the CSW height decreased. This result implies that the slower moving cyclones had more time to input more energy into the ocean for the generation of CSWs so there was a greater potential for the cyclone to influence water levels and generate CSWs with greater wave heights. The CSW propagation speed was 15 ms^{-1} or 23.5 ms^{-1} which was near to the calculated phase speed. As the CSW moved as a "free wave" the CSW was able to occupy the whole shelf width because there was no presence of the tropical cyclone. The result from these simulations of "free" CSWs generated by parallel cyclones provide an insight into the behaviour of a CSW that may be generated by a cyclone that travels parallel but then may change course to be perpendicular in direction.

Freely generated CSWs by parallel cyclones with different forward speeds showed similar properties to the CSWs generated by perpendicular cyclones. Altering a parallel cyclone's *distance from the coast* also influenced the properties of the CSW. The results show that CSW height increased, the further the cyclone was from the shore but decreased when the cyclone was far from the continental shelf. For example, the cyclone that travelled at 22°S , which was near to the coast, generated a CSW height of 0.35 m . A majority of this wave height comprised low water because part of the cyclone was over land, preventing the convergence of high water at the coast. In the study by Fandry & Steedman (1994), they identified a depression of water which occurred




ahead of the cyclone and a surge of water behind the cyclone, which is similar to the simulation in this study. They explain that due to the cyclone being partly over land, the low water ahead of the cyclone is caused by the prevailing offshore winds on the cyclone's west side and the onshore winds on the cyclone's east side, because of the cyclone's clockwise motion (Fandry & Steedman 1994). The CSW has a slower propagation speed (11.5 ms^{-1}) in this instance because the CSW is not able to occupy the whole shelf width due to the cyclone being partially over land. Cyclones that were further from the coast but near to the continental shelf break (20.5°S and 19°S) travelled at speeds close to the phase speed because the latitude of the cyclone allowed for the CSW to occupy the whole shelf width. The latitude of the cyclone also allowed for the generation of the greatest amplitude CSW because the prevailing onshore winds onto the continental shelf had full affect. CSWs were also generated by tropical cyclones at distances far from the continental shelf (16.5°S and 14°S). These CSWs had a propagation speed of 23 ms^{-1} because the distance between the cyclone and the coast increased. The wave heights were small (0.2 m) due to the cyclones' distance from the coast. While CSW heights generated by offshore cyclones in this study were small, Eliot & Pattiaratchi (2010) found that offshore cyclones that move parallel to the NWS were able to generate quite a large CSW signal. They attribute this to the extended fetch from the offshore cyclones which allowed more energy transfer and hence created a larger amplitude CSW. Tang, Holloway & Grimshaw (1997) also identify the presence of a CSW generated by Tropical Cyclone Jane in two offshore moorings.

Distance offshore played an important role on a free CSW's height and speed. However, altering the cyclone *category* of a parallel cyclone moving only a quarter of the model domain, influenced only the free CSW's height. CSW height increased with increased cyclone category. The alongshore component of wind stress and pressure gradient play an important role in the generation of these waves. By having greater wind velocities and greater pressure gradient, there is more energy placed into the CSW. As a result, a greater amplitude CSW is generated when the cyclone category is higher. Because the cyclone's path or distance from the coast did not change, the CSW propagation speed did not change.

While grid spacing did not seem to have a great impact on CSW properties, CSW generation could be dependent on the number of vertical sigma coordinates. In both test cases of grid resolution, 30 sigma layers were used. However, research has found that CSWs could not be generated when using a z-coordinate model (Maiwa, Masumoto & Yamagata 2010). Using less sigma layers or a z-coordinate system may alter the CSW characteristics because bathymetry and bottom friction is less represented in model these models. Bathymetry and bottom friction can play important roles in CSW generation and propagation and under-representing these components in any model may jeopardise the model's simulation results.

45° cyclones

45° moving cyclones that generated CSWs in the model were identified as initially a low moving water body of water, which occurred ahead of the tropical cyclone path, followed by high water that moved west along the coastline. The CSWs generated by a 45° cyclone travelled as a "free wave", similar to a CSW generated by a perpendicular cyclone. The CSW had similar



propagation speed and wave height properties as the CSW generated by a perpendicular moving cyclone. CSW propagation speeds ranged between 11 ms^{-1} and 23.5 ms^{-1} , which are near the calculated phase speed of 14.42 ms^{-1} . The CSW propagated with a speed representative of a free wave response that scales to the calculation $c \sim fL$. CSW height also decreased with increased cyclone forward speed which means that slower cyclones had more time to input more energy into the CSW and hence the greater CSW height. However the CSW height was greater when generated by a 45° moving cyclone. This can be explained by the cyclone having an alongshore component when moving through the model domain. When the cyclone crosses the shelf, the alongshore component allows for more energy to be transferred to the CSW and Greenspan Resonance may be occurring. In a study by Jelesnianski (1966) the maximum surge occurred for a cyclone travelling 65° . These CSW simulations and other studies show that cyclone approach angle and speed can play an important role in CSW generation. The inclusion of an along shore component with appropriate cyclone time scales can influence CSW height.


Regional scale modelling of CSWs

CSW heights and propagation speeds were analysed from measured tide gauge data and model results for Tropical Cyclones Bianca and Carlos in 2011. The measured and modelled CSW heights and propagation speeds of the two CSWs generated by Tropical Cyclones Bianca and Carlos are consistent with other studies of CSWs generated in WA and other locations around the globe (e.g. Ding, Bao & Shi 2012; Eliot & Pattiaratchi 2010; Fandry, Leslie & Steedman 1984). The measured data and modelled data produced a CSW that travelled at an average speed of 5.8 ms^{-1} for both CSWs generated by the two tropical cyclones. The CSWs also travelled long distances south of their generating region, and in particular, the CSW generated by Tropical Cyclone Bianca as it is likely to be a low mode CSW (Eliot & Pattiaratchi 2010; Tang & Grimshaw 1995). The following analysis highlights important features that affect CSW generation and propagation in WA.

Cyclone path

Tropical Cyclones Bianca and Carlos both travelled parallel to the NWS coastline. Tropical Cyclone Bianca then continued to move approximately parallel to the WA coastline whereas Tropical Cyclone Carlos, after making landfall at Exmouth continued moving offshore in a southwards direction. The two differences between the cyclones' paths can explain the extent of influence of the CSW in southern WA. The CSW generated by Tropical Cyclone Bianca was present in the data as far as Thevenard. The CSW generated by Tropical Cyclone Carlos was not identified in water level data or measured data in Albany. As Tropical Cyclone Carlos moved more offshore, the CSW became significantly weak as it moved further south. This is because the Tropical Cyclone Carlos was not present near to the coast to reinforce the signal the signal (Eliot & Pattiaratchi 2010; Fandry, Leslie & Steedman 1984). The CSW generated by Tropical Cyclone Bianca travelled as far as Thevenard because Tropical Cyclone Bianca was a southward travelling, coast parallel cyclone which was able to reinforce the wave signal (Eliot & Pattiaratchi 2010).

The path of the cyclone may also explain why some locations along the WA coast experienced a greater CSW height. For example, the CSW generated by Tropical Cyclone Carlos showed an increase in CSW height at Onslow. Tropical



Cyclone Carlos' path was very near to Onslow so some of the CSW height component may also include the locally generated surge from the cyclone. The CSW height also increased at Fremantle. As Tropical Cyclone Carlos was well offshore, other influences on water levels near Fremantle are likely to be the cause of increased CSW height. This means that the CSW, although it is influenced by the cyclone path, locally generated surges and other water level oscillations are also present which can amplify the wave signal.

Continental shelf bathymetry

The behaviour of a CSW and its characteristics can be influenced by the *shelf width* (Church & Freeland 1987). The two CSWs in both the measured and modelled results had propagation speeds range between 6.6 ms^{-1} and 7.7 ms^{-1} in the generating region of the NWS. The CSWs then both decreased in propagation speed between Exmouth and Carnarvon and then increased in speed between Carnarvon and Geraldton. The decrease in propagation speed between Exmouth and Carnarvon also corresponded to a decrease in CSW height, which is a similar result found by Tang, Holloway & Grimshaw (1997). The decrease in CSW speed between Exmouth and Carnarvon can be explained by the significant decrease in continental shelf width between these two locations. The continental shelf then widens between Carnarvon and Geraldton where the CSW increases in speed. The decrease in continental shelf width may result in the scattering of the CSW into a number of modes, which suggests the CSW energy is also scattered (Wilkin & Chapman 1990). Maiwa, Masumoto & Yamagata (2010) and Church & Freeland (1987) also identify this in their studies. As the characteristic length scale of the shelf (L) decreases, then the calculated phase speed $c \sim fL$ will decrease. This is why the propagation speed of the CSW decreases between Exmouth and Carnarvon. Because the continental shelf widens between Carnarvon and Geraldton, the results are showing the opposite, where the CSW speed increases with increasing shelf width. This result is also suggested in Eliot & Pattiaratchi (2010).

Shelf width has been shown to influence CSW propagation speed and height but also *coastline features* have also been identified in literature. In WA, both Exmouth Gulf and Shark Bay are important topographic features that have affected the CSWs generated by Tropical Cyclones Bianca and Carlos. Model simulations showed Exmouth Gulf and Shark Bay experienced a high build-up of water from the CSW which remained high over a longer time period than other straighter sections of the coastline. As these two features are large variations in the coastline, the CSW may experience strong scattering (Allen 1979; Ding, Bao & Shi 2012; Dorr & Grimshaw 1990; Fuller 1975; Wilkin & Chapman 1990). Further south of Shark Bay, the continental shelf width between Geraldton and Port Geographe is quite constant and there are not huge irregularities in the coastline. Between Geraldton and Port Geographe, if other water level oscillation and locally induced surges are excluded, the CSWs show a decreasing trend in wave height between these two locations. The decay in the CSW height between these locations can be attributed to bottom friction (Brink 1991, 2006; Csanady 1987; Church & Freeland 1987; Schulz, Mied & Snow 2012; Webster 1985). CSW propagation speed generated by Tropical Cyclone Bianca between these two locations was the same (6.6 ms^{-1}) for both the measured and modelled data, but much slower for the CSW generated by Tropical Cyclone Carlos.



While the CSW generated by Tropical Cyclone Carlos did not travel beyond Cape Leeuwin, the CSW generated by Tropical Cyclone Bianca travelled as far as Thevenard. The CSW between Port Geographe and Albany showed a decrease in wave height and propagation speed in both the measured and modelled data. The curvature around the southwest Capes region, another *coastline feature* is likely to have also affected the dynamics of the CSW by causing scattering and hence decay of the CSW signal (Eliot & Pattiaratchi 2010). This is because the coastline curves abruptly from south to east. In the modelled results, the CSW as it curves around the coastline also shows a component of this high water being pushed offshore of the Capes Region.

The continuation of the CSW generated by Tropical Cyclone Bianca, further east, demonstrates the affect at the regional scale that CSWs can have on water levels. The CSW maintains a similar wave height of ~ 0.24 m as it travels east. It is likely that in this region the CSW experiences affects from other water variability. It is this region that studies have identified the generation of CSWs by mid-latitude cyclones (Church & Freeland 1987; Griffin & Middleton 1991). Hence the behaviour of CSWs in this southern region may be strongly influenced by the meteorology and ocean dynamics of the southern ocean; however the extent of this influence requires further investigation.

Another important coastal feature in WA, although not a topographic feature, is the *Leeuwin Current System*. CSW properties may be influenced by the presence of the Leeuwin Current. This is because of current shear (Baines, Boyer & Xie 2005). However, the extent of this influence is still unknown. The Leeuwin Current is weakest during the occurrence of tropical cyclones in WA and further investigation is required to understand the influence of currents on CSWs.

CONCLUSIONS

Measured tide gauge data and the ROMS numerical model were used to investigate the generation and propagation of Continental shelf waves (CSWs) in Australia. An idealised model of the Australian Northwest Shelf (NWS) was created to test the influence of various tropical cyclone parameters (i.e. path, forward speed and category) on CSW height and propagation speeds. An Australia-wide model predicted water levels and was used to investigate the behaviour of the CSWs generated by Tropical Cyclones Bianca and Carlos in 2011, along the coastline of WA.

The results from the NWS idealised model showed that a tropical cyclone's path, forward speed and category influence both CSW generation and propagation. Cyclones that travel *parallel* to the coastline, near to the continental shelf, generate the greatest amplitude waves because of Greenspan Resonance. As cyclone forward speed increases, the CSW height also increases. A cyclone travelling 7.94 ms^{-1} generated the greatest amplitude wave. Cyclones that travel too fast generate CSWs with much smaller wave heights. This is characteristic of a forced wave response. These cyclones are likely to have the greatest impact on water levels far from the generation region as they are able to form CSWs with the greatest wave heights. A higher cyclone category is further able to increase CSW height because of the greater alongshore component of wind stress and pressure gradient.

Cyclones that travel *perpendicular* or at 45° , eventually making landfall, generate CSWs that travel as "free waves" which had lower wave heights than the CSWs generated by parallel cyclones. Slower moving perpendicular and 45° cyclones generate CSWs with higher wave heights than faster moving cyclones because there is more time to transfer energy into the CSW. Perpendicular cyclones that travel very fast ($\geq 10 \text{ ms}^{-1}$) are able to generate edge waves, which are unidirectional, because the influence of Coriolis is much less. 45° cyclones generate CSWs with greater heights than perpendicular cyclones because there is an alongshore component included in the cyclones path. The greatest impact of CSWs on water levels generated by these cyclones occurs near or to the cyclone prone regions. In general, the propagation speed of a "free" CSW scales to $c \sim fL$. Differences found in the free moving CSW propagation speed was caused by the methods used to filter the water levels, which could not remove all shelf oscillations and resonances not related to the CSW and thus influencing the CSW speed.

The importance of a cyclone's path and speed on CSWs is further demonstrated from the two simulations and analysis of measured data of the CSWs generated by Tropical Cyclones Bianca and Carlos. The CSW generated by Tropical Cyclone Bianca travelled as far as Thevenard, in South Australia, because Tropical Cyclone Bianca travelled approximately parallel and near to the coast, reinforcing the CSW signal. Tropical Cyclone Carlos moved further offshore so this CSW was not able to travel around the Capes Region. The changes in continental shelf bathymetry (i.e. width and coastline features) is also able to influence the CSW speed and height. The long stretch of WA coastline allows the CSW to travel long distances, which is able to affect water levels in southern WA, a micro-tidal region. Studies have identified that with climate change, cyclones are expected to increase in intensity (Walsh & Ryan 2000) but decrease in frequency (Oouchi *et al.* 2006). Water levels in southern WA will be more affected if cyclones on the NWS move parallel to the coast



with a high category as these cyclones are likely to generate the greatest amplitude CSWs.



REFERENCES

- Aguado, E & Burt, JE 2013, *Understanding weather and climate*, 6th edn, Pearson Education Inc, Boston.
- Allen, JS 1975, 'Coastal trapped waves in a stratified ocean', *Journal of Physical Oceanography*, vol. 5, pp. 300-325.
- Allen, JS 1976, 'Continental shelf waves and alongshore variations in bottom topography and coastline', *Journal of Physical Oceanography*, vol. 6, pp. 864-878.
- Allen, JS 1980, 'Model's of wind-driven currents on the continental shelf', *Annual Review of Fluid Mechanics*, vol. 12, pp. 389-433.
- Anthes, RA 1982, *Tropical cyclones, their evolution, structure and effects*, Meteorological Monographs, vol. 19, no. 41, American Meteorological Society, Boston.
- Arakawa, A & Lamb, VR 1977, *Methods of computational physics*, vol. 17, pp. 174-265, Academic Press.
- Baines, PG, Boyer, DL & Xie, B 2005, 'Laboratory simulations of coastally trapped waves with rotation, topography and stratification', *Dynamics of Atmospheres and Oceans*, vol. 39, pp. 153-173.
- Baker, C, Potter, A, Tran, M, Heap, AD 2008, *Geomorphology and sedimentology of the northwest marine region of Australia, record 2008/07*, Geoscience Australia, Canberra.
- Bakun, A, McLain, DR, & Mayo, FY 1974, 'The mean annual cycle of coastal upwelling off western North America as observed from surface measurements', *Fisheries Bulletin*, vol. 72, pp. 843-844.
- Battisti, DS & Hickey, BM 1984, 'Application of remote wind-forced coastal trapped wave theory to the Oregon and Washington coasts', *Journal of Physical Oceanography*, vol. 14, no. 5, pp. 887-903.
- Beardsley, RC, Mofjeld, H, Wimbush, M, Flagg, CN & Vermersch, JA 1977, 'Ocean tides and weather-induced bottom pressure fluctuations in the Middle-Atlantic Bight', *Journal of Geophysical Research*, vol. 82, pp. 3175-3182.
- Brink, KH 1991, 'Coastal-trapped waves and wind driven currents over the continental shelf', *Annual Review of Fluid Mechanics*, vol. 23, pp. 389-412.
- Brink, KH 2006, 'Coastal-trapped waves with finite bottom friction', *Dynamics of Atmospheres and Oceans*, vol. 41, pp. 172-190.
- Bryant, EA 1990, 'Sea level change and greenhouse: implications for wetlands', *Wetlands (Australia)*, vol. 10, no. 12, pp. 7-14.
- Buchan, SJ, Black, PG & Cohen, RL 1999, 'The impact of Tropical Cyclone Olivia on Australia's Northwest Shelf'. Paper presented at the *Offshore Technology Conference*, Houston, Texas.
- Buchwald, VT & Adams, JK 1968, 'The propagation of continental shelf waves', *Proceedings of the Royal Society of London*, vol. A305, pp. 235-250.
- Bureau of Meteorology 2013a, *Tropical cyclones – frequently asked questions*. Available from: <http://www.bom.gov.au/cyclone/faq/> [3 August 2013].



Bureau of Meteorology 2013b, *Climatology of Tropical Cyclones in Western Australia*. Available from:

<http://www.bom.gov.au/cyclone/climatology/wa.shtml>. [19 January 2013].

Bureau of Meteorology 2011a, *Severe Tropical Cyclone Bianca*. Available from:

<http://www.bom.gov.au/announcements/sevwx/wa/watc20110121.shtml> [4 August 2013].

Bureau of Meteorology 2011b, *Severe Tropical Cyclone Carlos*. Available from:

<http://www.bom.gov.au/announcements/sevwx/wa/watc20110213.shtml> [4 August 2013].

Cartwright, DE 1969, 'Extraordinary tidal currents near St Kilda', *Nature*, vol. 223, pp. 928-932.

Chassignet, EP, Arango, HG, Dietrich, D, Ezer, T, Ghil, M, Haidvogel, DB, Ma, CC, Mehra, A, Paiva, AM & Sirkes, Z 2000, 'DAMEE-NAB: the base experiments', *Dynamics of Atmospheres and Oceans*, vol. 32, pp. 155-183.

Christensen, N, de la Paz, R & Gutiérrez, G 1983, 'A study of sub-inertial waves off the west coast of Mexico', *Deep Sea Research*, vol. 30, pp. 835-850.

Church, AJ & Freeland, HJ 1987, 'The energy source for the coastal trapped waves in the Australian coastal experiment region', *Journal of Physical Oceanography*, vol. 17, pp. 289-300.

Church, AJ, Freeland, HJ & Smith, RL 1986, 'Coastal trapped waves on the east Australian continental shelf Part I: Propagation of modes', *Journal of Physical Oceanography*, vol. 16, pp. 1929-1943.

Church, AJ, White, NJ, Clarke, AJ, Freeland, HJ & Smith, RL 1986, 'Coastal trapped waves on the east Australian continental shelf Part II: Modal verification', *Journal of Physical Oceanography*, vol. 16, pp. 1945-1957.

Clarke, AJ 1977, 'Observational and numerical evidence for wind-forced coastal trapped long waves', *Journal of Physical Oceanography*, vol. 7, pp. 231-247.

Codiga, DL, Renouard, DP & Fincham, AM 1999, 'Experiments on waves trapped over the continental slope and shelf in a continuously stratified rotating ocean, and their incidence on a canyon', *Journal of Marine Research*, vol. 57, pp. 585-612.

Cresswell, GR, Boland, FM, Peterson, JL & Wells, GS 1989, 'Continental shelf currents near the Abrolhos Islands, Western Australia', *Australian Journal of Marine and Freshwater Research*, vol. 40, pp. 113-128.

Cresswell, GR & Golding, TJ 1980, 'Observations of a south-flowing current in the south-eastern Indian Ocean', *Deep Sea Research Part A Oceanographic Research Papers*, vol. 27, no. 6, pp. 449-466.

Cry, GW 1965, *Tropical cyclones of the North Atlantic Ocean, tracks and frequencies of hurricanes and tropical storms 1871 - 1963*, Weather Bureau technical paper no. 55, US Department of Commerce.

Csanady, G 1978, 'The arrested topographic wave', *Journal of Physical Oceanography*, vol. 8, pp. 47-62.



Cutchin, DL & Smith, RL 1973, 'Continental shelf waves: low frequency variations in sea level and currents over the Oregon continental shelf', *Journal of Physical Oceanography*, vol. 3, pp. 73-82.

Davis, AMJ 1981, 'The scattering by a headland of the dominant continental shelf wave', *Philosophical Transactions of the Royal Society of London*, vol. A303, pp. 383-431.

Ding, Y, Bao, X & Shi, M 2012, 'Characteristics of coastal trapped waves along the northern coast of the South China Sea during year 1990', *Ocean Dynamics*, vol. 62, pp. 1259-1285.

Dorr, A & Grimshaw, R 1983, 'Barotropic continental shelf waves on a β -plane', *Journal of Physical Oceanography*, vol. 16, pp. 1345-1357.

Dorr, A & Grimshaw, R 1990, 'Continental shelf wave scattering by a rigid barrier normal to the coast', *Journal of Physical Oceanography*, vol. 20, pp. 1849-1866.

Dukhovskoy, DS, Morey, SL & O'Brien, JJ 2009, 'Generation of baroclinic topographic waves by a tropical cyclone impacting a low-latitude continental shelf', *Continental Shelf Research*, vol. 29, pp. 333-351.

Egbert, GD, Bennett, AF & Foreman, MGG 1994, 'Topex/Poseidon tides estimated using a global inverse model', *Journal of Geophysical Research*, vol. 99, pp. 24821-24852.

Eliot, M & Pattiaratchi, C 2010, 'Remote forcing of water levels by tropical cyclones in southwest Australia', *Continental Shelf Research*, vol. 30, pp. 1549-1561.

Emanuel, K 2005, *Divine wind: the history and science of hurricanes*, Oxford University Press, Oxford.

Emery, WJ & Thomson, RE 1998, *Data analysis methods in physical oceanography*, Pergamon Press, Oxford.

Enfield, DB & Allen, JS 1983, 'The generation and propagation of sea level variability along the Pacific coast of Mexico', *Journal of Physical Oceanography*, vol. 13, pp. 1012-1033.

Fandry, CB, Leslie, LM & Steedman, RK 1984, 'Kelvin type coastal surges generated by tropical cyclones', *Journal of Physical Oceanography*, vol. 14, pp. 582-593.

Fandry, CB & Steedman, RK 1989, 'An investigation of tropical cyclone generated circulation on the North West Shelf of Australia using a three dimensional model', *Deutsche Hydrografische Zeitschrift*, vol. 42, no. 306, pp. 307-341.

Fandry, CB & Steedman, RK 1994, 'Modelling the dynamics of the transient, barotropic response of continental shelf waters to tropical cyclones', *Continental Shelf Research I*, vol. 14, pp. 1723-1750.

Freeland, HJ, Boland, FM, Church, AJ, Forbes, AMG, Huyer, RL, Smith, RL, Thompson, RORY & White, NJ 1986, 'The Australian coastal experiment: a search for coastal-trapped waves', *Journal of Physical Oceanography*, vol. 16, pp. 1230-1249.

Fuller, JD 1973, *Edge waves in the presence of an irregular coastline*. MSc. thesis, The University of British Columbia.



- Geng, Q & Sugi, M 2001, 'Variability of the North Atlantic cyclone activity in winter analyzed from NCEP-NCAR Reanalysis Data', *Journal of Climate*, vol. 14, pp. 3863-3873.
- Gill, AE & Clarke, AJ 1974, 'Wind-induced upwelling, coastal currents and sea-level changes', *Deep-Sea Research*, vol. 21, pp. 325-345.
- Gill, AE & Schumann, EH 1974, 'The generation of long shelf waves by the wind', *Journal of Physical Oceanography*, vol. 4, pp. 83-90.
- Gill, AE & Schumann, EH 1979, 'Topographically induced changes in the structure of an inertial coastal jet: application to the Agulhas Current', *Journal of Physical Oceanography*, vol. 9, pp. 975-991.
- Greatbatch, RJ 1984, 'On the response of the ocean to a moving storm: parameters and scales', *Journal of Physical Oceanography*, vol. 14, pp. 59-78.
- Greenspan, HP 1956, 'The generation of edge waves by moving pressure distributions', *Journal of Fluid Mechanics*, vol. 1, no. 6, pp. 574-592.
- Griffin, DA & Middleton, JA 1986, 'Coastal-trapped waves behind a large continental shelf island, southern Great Barrier Reef', *Journal of Physical Oceanography*, vol. 16, pp. 1651-1664.
- Griffin, DA & Middleton, JA 1991, 'Local and remote wind forcing of New South Wales inner shelf currents and sea level', *Journal of Physical Oceanography*, vol. 21, no. 2, pp. 304-322.
- Grimshaw, R 1977, 'The effects of a variable Coriolis parameter, coastline curvature and variable bottom topography on continental shelf waves', *Journal of Physical Oceanography*, vol. 7, pp. 547-554.
- Grimshaw, R 1988, 'Large-scale, low frequency response on the continental shelf due to localised atmospheric forcing systems', *Journal of Physical Oceanography*, vol. 18, pp. 1906-1919.
- Haidvogel, DB, Arango, HG, Hedstrom, K, Beckmann, A, Malanotte-Rizzoli, P & Shchepetkin, AF 2000, 'Model evaluation experiments in the North Atlantic Basin: simulations in nonlinear terrain-following coordinates', *Dynamics of Atmospheres and Oceans*, vol. 32, pp. 239-281.
- Haidvogel, D.B., Arango, H., Budgell, W.P., Cornuelle, B.D., Curchitser, E., Di Lorenzo, E., Fennel, K., Geyer, W.R., Hermann, A.J., Lanerolle, L., Levin, J., McWilliams, J.C., Miller, A.J., Moore, A.M., Powell, T.M., Shchepetkin, A.F., Sherwood, C.R., Signell, R.P., Warner, J.C., Wilkin, J., 2008. Ocean forecasting in terrain-following coordinates: Formulation and skill assessment of the Regional Ocean Modeling System. *Journal of Computational Physics* 227, 3595-3624.
- Hamilton, P & Lugo-Fernandez, A 2001, 'Observations of high speed deep currents in the northern Gulf of Mexico', *Geophysical Research Letters*, vol. 28, pp. 2867-2870.
- Hamon, BV 1962, 'The spectrums of mean sea level at Sydney, Coff's Harbour and Lord Howe Island', *Journal of Geophysical Research*, vol. 67, pp. 5147-5155.
- Hamon, BV 1966, 'Continental shelf waves and the effects of atmospheric pressure and wind stress on sea level', *Journal of Geophysical Research*, vol. 71, pp. 2883-2893.



- Hatcher, BG & Larkum, WD 1983, 'An experimental analysis of factors controlling the standing crop of the epilithic algal community on a coral reef', *Journal of Experimental Marine Biology and Ecology*, vol. 69, pp.61-84.
- Hearn, C & Holloway, P 1990, 'A three-dimensional barotropic model of the response of the Australian North West Shelf to tropical cyclones', *Journal of Physical Oceanography*, vol. 20, pp. 60-80.
- Heffner, DM, Subrahmanyam, B & Shriver, JF 2008, 'Indian Ocean Rossby waves detected in HYCOM sea surface salinity', *Geophysical Research Letters*, vol. 35, No. L03065.
- Holland, GJ 1980, 'An analytic model of the wind and pressure profiles in hurricanes', *Monthly Weather Review*, vol. 108, pp. 1212-1218.
- Holland, GJ & Gray, PIW 1983, 'Tropical cyclones in the Australia/Southwest Pacific region', *Atmospheric Science Paper*, no. 363.
- Holloway, PE 1983, 'Tides on the Australian North-west Shelf', *Australian Journal of Marine and Freshwater Research*, vol. 34, pp. 213-230.
- Hosseini, S & Willis, M 2009, 'Analysis of long-term cyclone track records for estimation of extreme design conditions'. Paper presented at the 5th Western Australian State Coastal Conference 2009: *Whose coast is it? Adapting for the future*, Perth.
- Hu, K, Chen, Q & Kimball, SK 2012, 'Consistency in hurricane surface wind forecasting: an improved parametric model', *Natural Hazards*, vol. 61, pp. 1029-1050.
- Huthnance, JM 1977, 'On coastal trapped waves: analysis and numerical calculation by inverse iteration', *Journal of Physical Oceanography*, vol. 8, pp. 74-92.
- Huthnance, JM, Mysak, LA & Wang, DP 1986, 'Coastal trapped waves', in *Baroclinic Processes on Continental Shelves, Coastal Estuarine Science, Vol. 3*, ed. CNK Mooers, AGU, Washington DC, pp. 1-18.
- Igeta, Y, Kitade, Y & Matsuyama, M 2007, 'Characteristics of coastal-trapped waves induced by typhoon along the southeast coast of Honshu, Japan', *Journal of Oceanography*, vol. 63, pp. 745-760.
- Jayawardena, AW 2011, 'Dynamics of hydro-meteorological and environmental hazards', in *Environmental Hazards: Fluid dynamics and geophysics of extreme events*, eds HK Moffatt & E Shuckburgh, World Scientific Publishing Co. Pte. Ltd., Singapore, pp. 229-267.
- Jelesnianski, CP 1966, 'Numerical computations of storm surges without bottom stress', *Monthly Westher Review*, vol. 94, no. 6, pp. 379-394.
- Kantha, LH & Clayson, C 2000, *Small scale processes in geophysical fluid flows*, Academic Press, San Diego.
- Kishi, MJ & Sugiharara, N 1975, 'Effects of longshore variation of coastline geometry and bottom topography on coastal upwelling in a two-layer model', *Journal of the Oceanographical Society of Japan*, vol. 31, pp. 48-50.
- Kitade, Y & Matsuyama, M 2000, 'Coastal-trapped waves with several-day period caused by wind along the southeast coast of Honshu, Japan', *Journal of Oceanography*, vol. 56, pp. 727-744.



- Kubota, M, Nakata, K & Nakamura, Y 1981, 'Continental shelf waves off the Fukushima coast, part 1: observations', *Journal of the Oceanographical Society of Japan*, vol. 37, pp. 267-278.
- LeBlond, P & Mysak, L 1978, *Waves in the ocean*, Oceanography Series, vol. 20, Elsevier Science, New York.
- Li, M, Zhong, L, Boicourt, WC, Zhang, S & Zhang, DL 2006, 'Hurricane-induced storm surges, currents and destratification in a semi-enclosed bay', *Geophysical Research Letters*, vol. 33, no. L02604.
- Lynett, PJ, Borrero, JC, Weiss, R, Son, S, Geer, D & Renteria, W 2012, 'Observations and modeling of tsunami-induced currents in ports and harbours', *Earth and Planetary Science Letters*, vol. 327-328, pp. 68-74.
- Macdonald, H, Roughan, M, Baird, M & Wilkin, J 2012, 'A numerical modelling study of the East Australian Current encircling and over-washing a warm-core eddy', *Journal of Geophysical Research*, doi:10.1029/2012JC008386, in press.
- Magaard, L & Mysak, LA 1986, 'Ocean waves: classification and basic features', in *Landolt-Boernstein, New Series, Vol. V/3c: Oceanography*, ed. J Suendermann, Springer-Verlag, Berlin, pp. 1-16.
- Maiwa, K, Masumoto, Y & Yamagata, T 2010, 'Characteristics of coastal trapped waves along the southern and eastern coasts of Australia', *Journal of Oceanography*, vol. 66, pp. 243-258.
- Martínez, JA & Allen, JS 2004, 'A modelling study of coastal-trapped wave propagation in the Gulf of California. Part I: Response to remote forcing', *Journal of Physical Oceanography*, vol. 34, pp. 1313-1331.
- Masselink, G & Pattiaratchi CB 1998 'The effects of sea breeze on beach morphology, surf zone hydrodynamics and sediment resuspension', *Marine Geology*, vol. 146, pp. 115-135.
- McBride, JL 2012, *The estimated cost of tropical cyclone impacts in Western Australia*, A technical report for the Indian Ocean Climate Initiative Stage 3, Project 2.2: Tropical Cyclones in the North West, Bureau of Meteorology.
- Merrifield, MA 1992, 'A comparison of long coastal-trapped wave theory with remote storm-generated wave events in the Gulf of California', *Journal of Physical Oceanography*, vol. 22, pp. 5-18.
- Merrifield, AM & Middleton, JH 1994, 'The influence of strongly varying topography on coastal-trapped waves at the southern Great Barrier Reef', *Journal of Geophysical Research*, vol. 99, pp. 10193-10205.
- Meuleners, MJ, Pattiaratchi, CB & Ivey, GN 2007, 'Numerical modelling of the mean flow characteristics of the Leeuwin Current System', *Deep Sea Research Part II: Tropical Studies in Oceanography*, vol. 54, no.8-10, pp. 837-858.
- Middleton, JF 1991, 'Coastal-trapped wave scattering into and out of straits and bays', *Journal of Physical Oceanography*, vol. 21, pp. 681-694.
- Mihanovic, H & Pattiaratchi, C 2012, 'Interaction between the Leeuwin Current and continental shelf along the Rottneest shelf and Perth Canyon'. Poster presentation at the *Australian Coastal and Oceans Modelling and Observations Workshop*, ACOMO, Canberra.



Mitchum, GT & Clarke, AJ 1986, 'The frictional nearshore response to forcing by synoptic scale winds', *Journal of Physical Oceanography*, vol. 16, no. 5, pp. 934-946.

Mooers, CNK & Smith, RL 1968, 'Continental shelf waves off Oregon', *Journal of Geophysical Research*, vol. 73, no. 2, pp. 549-557.

Munk, W, Snodgrass, F & Carrier, G 1956, 'Edge waves on the continental shelf', *Science*, vol. 123, pp. 127-132.

Mysak, LA 1967, 'On the theory of continental shelf waves', *Journal of Marine Research*, vol. 25, pp. 205-227.

Mysak, LA 1980, 'Topographically trapped waves', *Annual Review of Fluid Mechanics*, vol. 12, pp.45-76.

NASA 2011, 'Tropical Cyclone Carlos (15S) off Western Australia', *NASA earth observing system data and information system*, Available from: <http://rapidfire.sci.gsfc.nasa.gov/cgi-bin/imagery/single.cgi?image=Carlos.A2011055.0615.2km.jpg> [19 October 2013].

Niiler, PP & Mysak, LA 1971, 'Barotropic waves along an eastern continental shelf', *Geophysical Fluid Dynamics*, vol. 2, pp. 273-288.

Nott, J 2006, *Extreme events: a physical reconstruction and risk assessment*, Cambridge University Press, Cambridge.

O'Callaghan, J, Pattiaratchi, C & Hamilton, D 2007, 'The response of circulation and salinity in a micro-tidal estuary to sub-tidal oscillations in coastal sea surface elevation', *Continental Shelf Research*, vol. 27, no. 14, pp. 1947-1965.

Oouchi, K, Yoshimura, J, Yoshimura, H, Mizuta, R, Kusunoki, S & Noda, A 2006, 'Tropical Cyclone Climatology in a Global-Warming Climate as Simulated in a 20 km-Mesh Global Atmospheric Model: Frequency and Wind Intensity Analyses', *Journal of the Meteorological Society of Japan. Ser. II*, vol. 84, no. 2, pp. 259-276.

Partricola, CM, Change, P, Saravanan, R & Montuoro, R 2012, 'The effect of atmosphere-ocean-wave interactions and model resolution on Hurricane Katrina in a coupled regional climate model', *Geophysical Research Abstracts, EGU General Assembly*, vol. 14, no. 11855.

Pattiaratchi, CB 2006, 'Surface and sub-surface circulation and water masses off Western Australia', *Bulletin of the Australian Meteorological and Oceanographic Society*, vol. 19, pp. 95-104.

Pattiaratchi, CB & Wijeratne, EMS 2009, 'Tide gauge observations of 2004–2007 Indian Ocean tsunamis from Sri Lanka and Western Australia', *Pure and Applied Geophysics*, vol. 166, pp. 233-258.

Pearce, A, Buchan, S, Chiffings, T, D'Adamo, N, Fandry, C, Fearn, P, Mills, D, Phillips, R & Simpson, C 2003, 'A review of the oceanography of the Dampier Archipelago, Western Australia', in *The marine flora and fauna of Dampier, Western Australia*, eds FE Wells, DI Walker & DS Jones. Western Australian Museum, Perth, Available from: <http://wamuseum.com.au/dampier/documents/pdf/pearce%20et%20al.pdf> [21 April 2013].



Pearce, SM 2011, Coastal trapped waves generated by Hurricane Andrew on the Texas-Louisiana Shelf, MSc. thesis, Texas A&M University.

Pearman, GI (ed.) 1988, *Greenhouse: planning for climate change*, CSIRO Publications, East Melbourne.

Peffley, MB & O'Brien, JJ 1976, 'A three-dimensional simulation of coastal upwelling off Oregon', *Journal of Physical Oceanography*, vol. 6, pp. 164-180.

Pilke, RA & Lardsea, CW 1998, 'Normalized hurricane damage in the United States', *Weather and Forecasting*, vol. 13, pp. 621-631.

Porter-Smith, R, Harris, PT, Anderson, OB, Coleman, R, Greenslade, D & Jenkins, CJ 2004, 'Classification of the Australian continental shelf based on predicted sediment threshold exceedance from tidal currents and swell waves', *Marine Geology*, vol. 211, no. 102, pp. 1-20.

Price, JF 1981, 'Upper ocean response to a hurricane', *Journal of Physical Oceanography*, vol. 11, pp. 153-175.

Provis, DG & Radok, R 1970, 'Sea-level oscillations along the Australian coast', *Australian Journal of Marine and Freshwater Research*, vol. 30, pp. 295-301.

Pugh, DT 1987, *Tides, Surges and Mean Sea-level: A Handbook for Engineers and Scientists*, Wiley, Chichester.

Rayson, M, Ivey, GN, Meuleners, M & Wake, GW 2011, 'Internal tide dynamics in a topographically complex region: Browse Basin, Australian North West Shelf', *Journal of Geophysical Research: Oceans*, vol. 116, no. C01016.

Rego, JL 2009, Storm surge dynamics over wide continental shelves: numerical experiments using the finite-volume coastal ocean model, Ph.D thesis, Louisiana State University.

Rhines, PB 1970, 'Edge-, bottom-, and Rossby waves in a rotating stratified fluid', *Geophysical Fluid Dynamics*, vol. 1, pp. 273-302.

Robinson, AR 1964, 'Continental shelf waves and the response of sea level to weather systems', *Journal of Geophysical Research*, vol. 69, pp. 367-368.

Romea, RD & Smith, RL 1983, 'Further evidence for coastal trapped waves along the Peru coast', *Journal of Physical Oceanography*, vol. 13, pp. 1341-1356.


Schumann, EH & Brink, KH 1990, 'Coastal-trapped waves off the coast of South Africa: generation, propagation and current structures', *Journal of Physical Oceanography*, vol. 20, pp. 1206-1218.

Shchepetkin, AF & McWilliams, JC 2005, 'The regional oceanic modelling system (ROMS): a split-explicit free-surface, topography-following-coordinate oceanic model', *Ocean Modelling*, vol. 9, no. 4, pp. 347-404.

Schulz, WJ, Mied, RP & Snow, CM 2012, 'Continental shelf wave propagation in the Mid-Atlantic Bight: A general dispersion relation', *Journal of Physical Oceanography*, vol. 42, pp. 558-568.

Schwartz, M (ed.) 2006, *Encyclopaedia of coastal science*, Springer, Berlin.

Smith, RL 1978, 'Poleward propagating perturbations in currents and sea level along the Peru coast', *Journal of Geophysical Research*, vol. 83, pp. 6083-6092.

- 
- Song, Y & Haidvogel, DB 1994, 'A semi-implicit ocean circulation model using a generalised topography-following coordinate system', *Journal of Computational Physics*, vol. 115, no.1, pp. 228-244.
- Suginohara, H 1974, 'Onset of coastal upwelling in a two-layer ocean by wind stress with longshore variation', *Journal of the Oceanographical Society of Japan*, vol. 30, pp. 23-33.
- Tang, YM 1994, *Numerical studies of the coastal ocean*, Ph.D. thesis, Monash University.
- Tang, YM & Grimshaw, R 1995, 'A modal analysis of the coastally trapped waves generated by tropical cyclones on continental shelves', *Journal of Physical Oceanography*, vol. 25, pp. 1577-1598.
- Tang, YM, Holloway, P & Grimshaw, R 1997, 'A numerical study of the storm surge generated by Tropical Cyclone Jane', *Journal of Physical Oceanography*, vol. 27, pp. 963-976.
- Thiebaud, S & Vennell, R 2010, 'Observation of a fast continental shelf wave generated by a storm impacting Newfoundland using wavelet and cross-wavelet analysis', *Journal of Physical Oceanography*, vol. 40, pp. 417-428.
- Valle-Levinson, A 1995, 'Observation of barotropic exchanges in the mowar Chesapeake Bay', *Continental Shelf Research*, vol. 15, pp. 1631-1647.
- Van Gastel, P Ivey, GN, Meuleners, M, Antenucci, J & Fringer, O 2009, 'The variability of the large-amplitude internal wave field on the Australian North West Shelf', *Continental Shelf Research*, vol. 29, pp. 1373-1393.
- Vennell, R 2010, 'Resonance and trapping of topographic transient ocean waves generated by a moving atmospheric disturbance', *Journal of Fluid Mechanics*, vol. 650, pp. 427-442.
- Walsh, KJE & Ryan, FR 2000, 'Tropical cyclone intensity increase near Australia as a result of climate change', *Journal of Climate*, vol. 13, no. 16, pp. 3029-3036.
- Walters, RA 1982, 'Low frequency variations in sea level and currents in south San Francisco Bay', *Journal of Physical Oceanography*, vol. 12, pp. 658-668.
- Wang, DP 1980, 'Diffraction of continental shelf waves by irregular alongshore geometry', *Journal of Physical Oceanography*, vol. 10, pp. 1187-1199.
- Warner, JC, Sherwood, CR, Signell, RP, Harris, CK & Arango, HG 2008, 'Development of a three-dimensional, regional, coupled wave, current, and sediment-transport model', *Computers & Geosciences*, vol. 34, pp. 1284-1306.
- Weaver, AJ 1987, 'Bass Strait as a reverse estuary source for coastally trapped waves', *Australian Journal of Marine and Freshwater Research*, vol. 38, pp. 685-699.
- Webb, DJ 2013, *On the impact of a radiational open boundary condition on continental shelf resonances*, National Oceanography Centre Internal Document No. 06, unpublished, National Oceanography Centre, Southampton.
- Webster, I 1983, *Wind-driven circulation on the North West Shelf of Australia*, Ph.D. thesis, University of Western Australia.
- Webster, I 1985, 'Frictional continental shelf waters and the circulation response of a continental shelf to wind forcing', *Journal of Physical Oceanography*, vol. 15, pp. 855-964.



Wilkin, JL & Chapman, DC 1990, 'Scattering of coastal-trapped waves by irregularities in coastline and topography', *Journal of Physical Oceanography*, vol. 20, pp. 396-421.

Willmott, CJ 1984, 'On the evaluation of model performance in physical geography' in *Spatial Statistics and Models*, eds GL Gaile & CJ Willmott, Reidel, Dordrecht, Netherlands, pp. 443-460.

Wilson, BR 2013, *The biogeography of the Australian North West Shelf: environmental change and life's response*, Elsevier, Burlington.

Wong, KC 2002, 'On the wind-induced exchange between Indian River Bay, Delaware and the adjacent continental shelf', *Continental Shelf Research*, vol. 22, pp. 1651-1668.

Woo, M & Pattiaratchi, C 2008, 'Hydrography and water masses off the Western Australia coast', *Deep – Sea Research I*, vol. 55, pp. 1090-1104.

Xu, J, Lowe, RJ, Ivey, G, Pattiaratchi, C, Jones, N, Brinkman, R 2013, 'Dynamics of the summer shelf circulation and transient upwelling off Ningaloo Reef, Western Australia', *Journal of Geophysical Research: Oceans*, vol. 118, no. 3, pp. 1099-1125.

Yankovsky, AE 2009, 'Large-scale edge waves generated by hurricane landfall', *Journal of Geophysical Research*, vol. 114, no. C03014, doi:10.1029/2008JC005113.

Zamudio, L, Hurlburt, HE, Metzger, EJ & Smedstad, OM 2002, 'On the evolution of coastally trapped waves generated by Hurricane Juliette along the Mexican west Coast', *Geophysical Research Letters*, vol. 29, no. 23, pp. 561-564.

Zed, M 2007, *Modelling of tropical cyclones on the North West Shelf*. Honours thesis, University of Western Australia. Available from: http://www.uwa.edu.au/__data/assets/pdf_file/0010/1637479/Zed_final_2008.pdf [21 April 2007].

Zhang, C 2012, *Effect of hurricane forward speed and approach angle on coastal storm surge*, MSc. thesis, Louisiana State University.

Zheng, L, Weisberg, RH, Huang, Y, Luettich, RA, Westerink, JJ, Kerr, PC, Donahue, A, Crane, G & Acli, L 2013, 'Implications from the comparisons between two- and three-dimensional model simulations of the Hurricane Ike storm surge', *Journal of Geophysical Research*, doi: 10.1002/jgrc.20248.

APPENDIX A - TROPICAL CYCLONE BIANCA DETAILED DESCRIPTION

Tropical Cyclone Bianca formed as a tropical low over land, at the most northern part of WA on the 21 January 2011. This low moved south west, over land, until the 25 January 2011, when it moved out onto open waters to the north of Broome. Tropical Cyclone Bianca moved parallel to the Pilbara coastline, along the NWS and was classified as a Category 3 on the 27 January 2011 (see Figure 41). Tropical Cyclone Bianca continued to move south west, but further offshore, intensifying as a Category 4 on 28 January. The cyclone then moved southwards, decreasing in intensity to a Category 3, before moving southeast towards Perth. However, Tropical Cyclone Bianca did not reach the southwest of WA as it became below cyclone intensity by 30 January 2011 (Bureau of Meteorology 2011a). Tropical Cyclone Bianca's lowest central pressure was 945 hPa. The cyclone's minimum eye radius reached 15 km with cyclone winds spanning a radius of 444 km around 28 January 2011. Maximum sustained wind speeds were 49 ms⁻¹ with maximum wind gusts reaching 70 ms⁻¹ (Bureau of Meteorology 2013b).

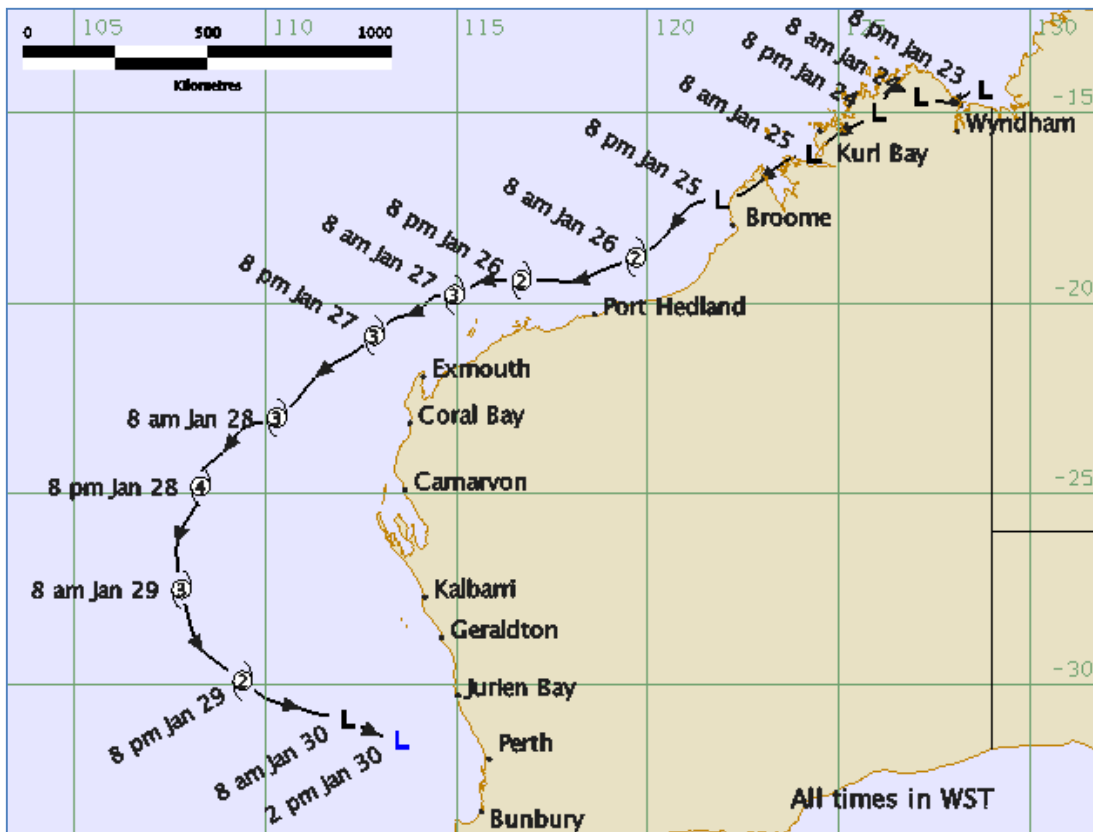


FIGURE 41 – PASSAGE AND INTENSITY OF TROPICAL CYCLONE BIANCA (BUREAU OF METEOROLOGY 2011A).

APPENDIX B - TROPICAL CYCLONE CARLOS DETAILED DESCRIPTION

Tropical Cyclone Carlos formed as a tropical low over the northern part of Australia on 13 February 2011 (see Figure 42). It intensified as it moved towards Darwin and was classified as a Category 1 cyclone on 16 February 2011. However, as it moved south west over land, it weakened and became a tropical low. Tropical Cyclone Carlos moved offshore near Broome on 21 February 2011. It moved parallel to the coastline where it intensified to become a Category 2 cyclone on 22 February 2011. The cyclone moved over land and continued to travel south west, remaining as a Category 2 and briefly became a Category 3. Tropical Cyclone Carlos continued to travel south west but moved further offshore where it weakened and became a tropical low by 26 February 2011 (Bureau of Meteorology 2011b). Tropical Cyclone Carlos' lowest central pressure was 969 hPa. The cyclone's winds spanned a radius of 444 km around 24 February 2011. Maximum sustained wind speeds were 33 ms⁻¹ with maximum wind gusts reaching 47 ms⁻¹ (Bureau of Meteorology 2013b).



FIGURE 42 – PASSAGE AND INTENSITY OF TROPICAL CYCLONE CARLOS (BUREAU OF METEOROLOGY 2011B).

APPENDIX C- IDEALISED CYCLONE WIND FORCING MATLAB CODE

```

%% Cyclone wind and air pressure field
%
% Script that generates a simple vortex-like cyclone wind field for a
% parallel cyclone moving at -19 degree south when placed on the NWS
% idealised model grid.
% Prepared by Sarath Wijeratne
% Updated by Elizabeth Joseph

%% Assign grid size and location of cyclone path
yyb = -24.9298:0.0368:-10.2306; % Cyclone region latitude
xxb = 129.9329:-0.0372:115.0576; % Cyclone region longitude
y = -19; % Latitude for the path of the cyclone
numbd = 10; % Radial resolution, change to any resolution
timestep = 1;

lon = [];
for jj = 1:length(yyb);
    lon = [lon xxb];
end

lat = [];
for ii = 1:length(yyb);
    lat = [lat; yyb(ii)*ones(length(xxb),1)];
end

%% Create cyclone wind and pressure field
for x = min(xxb)-2:0.335:max(xxb) % cyclone movement per 3 hours

    uu = [];
    vv = [];
    xx1 = [];
    yy1 = [];
    xx1p = [];
    yy1p = [];
    app = [];

    rr = [.1:.01:3]; % Cyclone radius

    for r = rr;

        th = 0:pi/numbd:2*pi;
        xunit = r*cos(th)+x;
        yunit = r * sin(th)+y;
        uwind = []; vwind = [];
        ap = 905-3.1+ones(length(xunit),1)*32.2*r; %Cyclone pressure
        field by radius

        for i = 1:length(xunit)-1 % Cyclone wind by radius

            xx = xunit(i+1)-xunit(i);
            yy = yunit(i+1)-yunit(i);
            if r < mean(rr)
                uwind = [uwind; xx*81.67];
                vwind = [vwind; yy*81.67];
            end
            if (r >= mean(rr) & r < (max(rr)+mean(rr))/2)

```



```

        uwind = [uwind; xx*59.72];
        vwind = [vwind; yy*59.72];
    end

    if r >= (max(rr)+mean(rr))/2
        uwind = [uwind; xx*30];
        vwind= [vwind; yy*30];
    end

end

uu = [uu; uwind];
vv = [vv; vwind];
xx1 = [xx1; (xunit(1:length(uwind)))'];
yy1 = [yy1; (yunit(1:length(vwind)))'];
xx1p = [xx1p; xunit'];
yy1p = [yy1p; yunit'];

app = [app; ap];

end

uux = griddata(xx1,yy1,uu,lon,lat');
vvx = griddata(xx1,yy1,vv,lon,lat');
slp = griddata(xx1p,yy1p,app,lon,lat');
slpp = [];
xxyz =1:length(xxb):length(slp)+1;

for mm=1:length(xxyz)-1;
    slpp=[slpp; slp(xxyz(mm):xxyz(mm+1)-1)];
end

xzx = find(isnan(slpp)==1);
slpp(xzx)= max(max(slpp));
ltxx = lat(1:length(xxb):length(lat));
lnxx = lon(1:length(xxb));
slpp_timestep(:,:,timestep) = slpp(:,:,); % create matrix of
pressure
xzy = find(isnan(uux)==1);
uux(xzy) = -5; % All other values are assigned as 5 m/s
xzy2 = find(isnan(vvx)==1);
vvx(xzy2) = 0;
uux_timestep(:,:,timestep) = -uux(:,:,); % create matrix of u-
velocity
vvx_timestep(:,:,timestep) = vvz(:,:,); % create matrix of v-
veocity

    timestep = timestep + 1;
end

[rr cc tt] = size(slpp_timestep);
uux_timestep = reshape(uux_timestep, rr, cc, tt);
vvx_timestep = reshape(vvx_timestep, rr, cc, tt);

% Keep only the required variables
clearvars -except uux_timestep vvz_timestep slpp_timestep

```